Nonlinear Dynamics of Self-excitation
in
Autoparametric Systems

Nietlineaire Dynamica van Zelf-excitatie in Autoparametrische Systemen

(met een samenvatting in het Nederlands)

Proefschrift

ter verkrijging van de graad van doctor aan de Universiteit Utrecht op gezag van de Rector Magnificus, Prof. dr. W.H. Gispen, ingevolge het besluit van het College voor Promoties in het openbaar te verdedigen op maandag 6 oktober 2003 des middags te 16.15 uur

door

Abadi

geboren op 30 augustus 1965 te Surabaya, Indonesië

Promotor: Prof. dr. F. Verhulst
Faculteit der Wiskunde en Informatica,
Universiteit Utrecht

Cover illustration: The ruin of The Tacoma Narrows Bridge (1940).

To:
my wife, Atik
and
our sons, Levi and Dhani

Contents

CHAPTER 1

Introduction

Coupled oscillators containing self-excitation are extensively explored in this thesis. These studies are mainly focused on mechanical models of vibrating systems. The models presented in this thesis are basic in the sense that they were not proposed to model real-life problems, but to provide information about the underlying dynamics with the hope that the information obtained can be used to study more complicated systems.

To understand the discussion in this thesis, we provide some background knowledge.

1.1. Self-excited Oscillations

The study of self-excited oscillations has increasingly become one of the main interests in electrical and mechanical engineering since the beginning of the twentieth century.

Rayleigh was the first to study such phenomena in acoustical problems. Later, it was van der Pol who pioneered the study of self-excitation in connection with an electrical system involving vacuum tubes.

In mechanics, basically self-excited oscillations are due to nonlinearity of the exciting force. This particular exciting force has the property that it tends to increase the energy for small velocities, but to decrease it for large velocities. With such a property an oscillation will be built up even in the absence of external forces. It turned out that the existence (and uniqueness) of an orbitally stable periodic solution (limit cycle) is typical for such an oscillation. See Andronow[**4**], Stoker [**48**] for the literature.

In applications, i.e. in solid or fluid mechanics and mathematical physics, systems of this kind are very common. They occur always through absorption of energy from a constant flow of energy producing a periodic motion.

There are some sources of constant flow of energy that can induce self-excited oscillations. In his experiment, van der Pol used a direct electrical current as a source of the energy. Rayleigh pointed out that a continuous bowing on a violin string also induces self-excited oscillations of the string.

In real life, such as a flowing medium (wind or fluid) with constant velocity can be considered as a source of self-excited oscillations. Another well-known source of self-excited oscillations in mechanical systems is relative dry friction. A mechanical model for such a dry friction oscillator is that of a mass resting on a conveyor belt and held in the equilibrium position by a spring. If the velocity of the belt, which is set
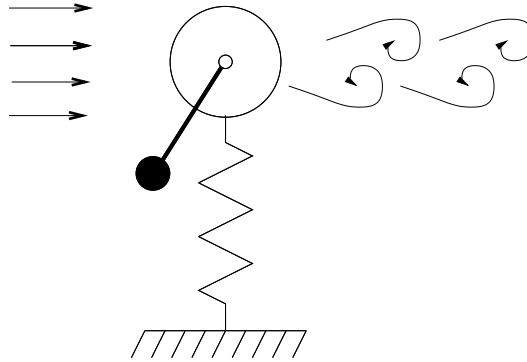
FIGURE 1. The spring-pendulum model.

to be constant, is properly chosen, then the mass will oscillate jerky but periodically. This kind of oscillator is used in the system considered in chapter 3.

Another type of self-excited oscillation is relaxation oscillation. Such an oscillation is characterised by intervals of time in which very little happens, followed by short intervals of time in which notable changes take place. A nice description of the relaxation oscillation can be found in Grimshaw [**24**] and Verhulst [**60**]. The standard reference is Grasman [**23**]. In chapter 4 we use this kind of oscillator in the system considered.

Sometimes self-excited oscillations have unfavourable effects in practical situations. The failure of the Tacoma bridge in the year of 1940 is generally ascribed to a particularly heavy self-excited oscillation in which the constant energy source was the wind. A similar situation occurred in airplane wings in which the engines are mounted under the wings by elastic suspenders. See Tondl et al.[**59**] and Stoker[**48**] for some more examples.

1.2. Autoparametric resonance

Such disastrous phenomena mentioned above can happen in a class of systems called *autoparametric systems*. Autoparametric systems are vibrating systems which consist of at least two subsystems. The secondary subsystem is coupled to the primary subsystem nonlinearly, but in such a way that the secondary subsystem can be at rest while the primary one is vibrating. This is called a *semitrivial solution* or *normal mode*.

A simple model of an autoparametric system is a spring-pendulum system in cross flow, as described in Figure 1. The system is excited by cross flow with a constant flow velocity. As the flow hits the primary subsystem, the normal mode motion is unstable and energy is transferred gradually to the swinging of the secondary subsystem. This is called *autoparametric instability* or *autoparametric resonance*. See Tondl et al. [**59**] for other types of autoparametric system.

In relation with the undesirable behaviour mentioned above, what really happened is so-called saturation effects; putting more energy in the primary system

results in a strong increase of the deflections of the secondary subsystem, whereas the increase of the vibration amplitudes of the primary subsystem is much smaller.

The study of autoparametric resonance is important, especially if we want to avoid some unfavourable effects or to get a desired oscillation motion due to self-excited oscillations. For that purpose, the secondary subsystem, which is supposed to act as a tuned absorber, has to be chosen appropriately. Thus, we are dealing with the problem of quenching, while at the same time we investigate the stability region of the semitrivial solution (normal mode) [**53**]. There are several ways for the purpose of quenching self-excited oscillations. The use of a pendulum-like absorber with viscous damping is a common one. Another way which is less common and has extensively been studied recently is the use of parametric excitation, for example an attached spring with periodically variable stiffness. We consider this kind of absorber in chapter 5. See the references therein for more details on such a coupling.

Moreover, the study of bifurcations from the semitrivial solution due to the autoparametric resonance can also show some interesting phenomena, such as torus bifurcations, periodic doubling leading to chaos [**43, 13**].

1.3. Methods and numerical tools

Periodic solutions or limit cycles are typical in systems containing a self-excited oscillator. Very often we consider the vibration problems in this thesis as a small perturbation of a known problem. Thus, we may apply a perturbation method in order to compute the corresponding approximation of the periodic solution of the system. Throughout the chapters of this thesis we mostly apply the averaging method [**46, 60**] in determining the approximate periodic solutions of the systems. We specifically use the Lagrange's variation of constants method [**62**] in the discussion in chapter 3. We compute normal forms [**25, 34**] of the systems through averaging in order to perform bifurcation analysis of the solutions.

We evaluate the analytical results by performing numerical analysis. In chapter 2 and chapter 5, we use the software package CONTENT [**35**], a continuation programme which, basically, uses a path-following technique to analyse the bifurcations of a periodic solution numerically.

In chapter 3 we use the software package SLIDECONT [**10**], a continuation programme which is designed for analysing the bifurcations of a periodic solution containing a sliding segment due to discontinuity

In chapter 4, as well as in chapter 2 and chapter 3, we perform numerical simulations using a well-known Runge-Kutta integrator programme to provide more information about the solutions of the systems.

We present short descriptions of the softwares used in this thesis for those who are not familiar with the softwares.

1.3.1. About CONTENT**.** CONTENT is a multi-platform interactive environment to study dynamical systems. It is designed to perform simulation, continuation, and normal form analysis of dynamical systems appearing in research and engineering.

CONTENT provides the following: online specification and updating of the dynamical systems, symbolic generation of derivatives of the right-hand side of the systems, visualisation of the solution in multiple 2-dimensional and 3-dimensional graphic windows, as well as in the numerical form, PostScript hardcopy, storage, import and export of computed curves in a platform-independent format, online hypertext help with figures. For more about the software package, see [**35**].

1.3.2. About SLIDECONT. SLIDECONT is an AUTO97 driver for sliding bifurcation analysis of discontinuous piecewise-smooth autonomous systems. The software allows for the detection and continuation of co-dimension 1 sliding bifurcations, as well as the detection of some co-dimension 2 singularities, with special attention to planar systems ($n = 2$). Some bifurcations are considered also for n-dimensional systems.

The general idea is that SLIDECONT sets up the proper defining equations of the user-selected problem in AUTO97 format, so that the computation can be performed by means of standard AUTO97 routines. See [**11**] for the documentation of AUTO97. As in AUTO97, the user must provide three files: an equations file (`<filename>.f`, where `<filename>` is a user-specified name), a constants file (`sc.<filename>`), and possibly, a data file (`<filename>.dat`). The equations file contains a set of Fortran subroutines specifying the discontinuous system presented in two vector fields and the scalar function representing the discontinuity boundary of the two smooth vector fields. The file also contains the starting solution, either analytically or numerically, and possible state and parameter user functions to be monitored during continuation. Analytical derivatives of the vector fields and the scalar function are required by some problems. The constants file specifies all parameter qualifying the AUTO97 continuation algorithms plus some SLIDECONT specific constants, including the problem type, namely a constant indicating the problem to be solved. The data files is required to numerically specify the starting solution of boundary value problems. For more about SLIDECONT, see [**10**].

1.4. Outline of this thesis

This thesis is a collection of research papers on systems containing self-excited oscillators. In particular, most of them are on self-excited autoparametric systems. Various types of self-excited oscillators are implemented and the study of the solutions, stabilities and bifurcations, shows very different results. These are presented in separate chapters of this thesis, summarised as follows:

This chapter is an introductory chapter which consists of some background knowledge for understanding the content of the thesis. We briefly present the concepts of self-excited oscillation and autoparametric systems.

In chapter 2, we consider a self-excited autoparametric system containing a Rayleigh type oscillator. We study the semitrivial solution and its domain of instability where nontrivial solutions are initiated. We are interested in the existence and stability of the nontrivial solutions and we analyse the behaviour of the solutions by examining it for various values of the parameters. We divide the discussion on the nontrivial solutions in exact resonance and near resonance cases. In the analysis

we use both normal forms (or averaging) and numerical bifurcation path-following techniques by using CONTENT. The system displays a rich pattern of different bifurcations, a robust heteroclinic cycle and instability behaviour.

In chapter 3, we consider an autoparametric system containing a dry-friction oscillator characterised by a small parameter. One interesting aspect of the analysis of the semitrivial (planar) solution is the possibility of calculating the boundary value of parameters for the existence of a non-smooth periodic solution. Moreover, the application of the software package SLIDECONT shows the phenomenon of the *sliding* bifurcation of the periodic solution of the system. The study of the 4-dimensional system is treated qualitatively by asymptotic analysis, enhanced with numerical simulations.

In chapter 4, we consider an autoparametric system containing a relaxation oscillator of van der Pol type. The possibility of destabilising the undesirable vibrations due to the stable normal mode of the system is studied by choosing a suitable tuning and coupling parameters. In the case of normal mode vibration derived from a relaxation oscillation, we need low-frequency tuning of the attached oscillator. An additional feature is that to make the quenching effective we also have to deform the slow manifold by choosing appropriate coupling.

In chapter 5, we consider vibrating systems containing self-excitation and parametric excitation. The purpose of the study is to analyse how the excitations in the systems interact. Especially, we study conditions for suppression or quenching (partly suppression) the self-excitation by using parametric excitation. We first look for the so-called parametric combination anti-resonance, condition where full suppression of self-excitation can be achieved. Then, we provide the boundaries and regions of stability of the trivial solution. We show that outside the stability regions, where nontrivial solutions occur, a condition for suppression can still be applied. This study considers the case of two-mass and three-mass systems. Surprisingly, the normal form for three masses in $1 : 2 : 3$-resonance produces partial decoupling of the system.

We conclude that nonlinear dynamics obtained from embedding a self-excited oscillator in a higher dimensional system is of practical interest and at the same time it is a rich source of interesting phenomena.

The results presented in this thesis are based on the following papers:

Abadi, On Self-excited Autoparametric Systems, *Nonlinear Dynamics*, **24**: 147-166, 2001.

Abadi, A Self-excited Autoparametric System with Dry Friction, [Submitted], 2003.

F. Verhulst and Abadi, Autoparametric Resonance of Relaxation Oscillations, [Submitted], 2003.

Abadi, Interaction Between Self-excitation and Parametric Excitation [Work in Progress].

On Self-excited Autoparametric Systems

2.1. Introduction

An autoparametric system is a vibrating system which consists of at least two subsystems; an oscillator which generally be in a vibrating state and the excited system which is excited indirectly and is coupled to the oscillator in a nonlinear way such that the excited system can be at rest while the oscillator is vibrating (this state is called *semitrivial solution*).

Autoparametric systems form a subclass of nonlinearly coupled systems. The semitrivial solution is one typical characteristic of the systems which do not belong to other nonlinearly coupled systems. (See Tondl [**54**] for examples of such a system).

A self-excited autoparametric system is a special type of autoparametric system with a self-excited oscillator in its vibrating state. There are many mechanical systems which are considered to have the characteristics of self-excited autoparametric systems, for instance systems with flow-induced vibrations; see for instance the books by Tondl, Nabergoj, Verhulst, and Ruijgrok ([**43**], [**57**], or [**59**]) and other references there. For a discussion of the applications in mechanics, the reader may refer to [**47**], [**53**], or [**59**].

This paper discusses a Rayleigh type self-excited autoparametric system. We study the solutions of the system, semitrivial and nontrivial solutions, and analyse their behaviour. By using the response-oriented approach we study the instability domain of the solutions. And we focus on varying the damping coefficient κ of the excited system (and fixing the other parameters) to see the behaviour of the solutions (stabilities and bifurcations). See the monographs by Guckenheimer and Holmes [**25**] or Wiggins [**63**] for the references on the bifurcation theory.

2.2. Formulation of a Rayleigh type self-excited autoparametric system

We consider a self-excited auto-parametric system of Rayleigh type in the non-dimensional form:

$$\begin{array}{rcl} x'' - \beta(1 - x'^2)x' + x + \gamma_1 y^2 & = & 0 \\ y'' + \kappa y' + q^2 y + \gamma_2 xy & = & 0 \end{array} \qquad (2.1)$$

where $\beta > 0$, is the self-excitation coefficient, $\kappa > 0$ is the damping coefficient of the excited system, γ_1 and γ_2 are the nonlinear coupling coefficients; q is the tuning

coefficient expressing the ratio of natural frequencies of the undamped linearised subsystems, where the frequency of the x-mode is normalised to 1. We restrict our discussion in this paper by considering the important resonance $q = \frac{1}{2}$ and nearby (detuned) values. The prime indicates the derivative with respect to the non-dimensional time variable. The first equation of (2.1) refers to the motion of the oscillator whereas the second one refers to the excited subsystem. We have chosen nonlinear coupling terms which are important for the instability of the semitrivial solution and the occurence of autoparametric resonance; see also the discussion at the end of this paper.

To study the system above we divide our discussion into two parts. That is, the semitrivial solution and the nontrivial solution.

First, we assume that all the parameters in system (2.1) are small and in order to apply the averaging method (see [**46**]), we rescale the parameters as follows. Let $\beta = \varepsilon\bar{\beta}$, $\kappa = \varepsilon\bar{\kappa}$, $\gamma_1 = \varepsilon\bar{\gamma_1}$, $\gamma_2 = \varepsilon\bar{\gamma_2}$, and take $q^2 = \frac{1}{4} + \varepsilon\sigma$. Then, substituting these into equation (2.1), after dropping the bars, we have the following standard form

$$
\begin{aligned}
x'' + x &= \varepsilon(\beta(1 - x'^2)x' - \gamma_1 y^2) \\
y'' + \frac{1}{4}y &= -\varepsilon(\kappa y' + \sigma y + \gamma_2 xy).
\end{aligned}
\tag{2.2}
$$

Further analysis of system (2.2), as we shall see in the subsequent section, leads us to the conclusion that periodic solutions exist.

2.3. The semitrivial solution and its stability

The semitrivial solution is defined as the solution of the system (2.2) by putting $y = 0$. Thus, we have the well-known Rayleigh equation

$$
x'' + x = \varepsilon\beta(1 - x'^2)x', \; y = 0.
\tag{2.3}
$$

We put $x(\tau) = R\cos(\tau + \psi)$ with $x'(\tau) = -R\sin(\tau + \psi)$ to obtain slowly varying equations for R and ψ; after averaging over τ, we obtain:

$$
\begin{aligned}
R' &= \varepsilon\frac{1}{2}\beta R(1 - \frac{3}{4}R^2) \\
\psi' &= 0.
\end{aligned}
\tag{2.4}
$$

For this standard procedure in averaging theory see [**46**] or [**60**]. Finding the non-trivial equilibrium for R, we have $R = R_0 = \sqrt{\frac{4}{3}}$. And, because of the translation property for autonomous systems we may take $\psi = \psi_0 = 0$. Therefore, $x_0(\tau) = R_0\cos(\tau + \psi_0) = \sqrt{\frac{4}{3}}\cos\tau$ is an approximation to the periodic solution of (2.3) up to $\mathcal{O}(\varepsilon)$. By a simple calculation we conclude that the semitrivial solution is a periodic stable solution with period near to 2π (stable in equation (2.3)).

For the stability investigation of the semitrivial solution $x_0(\tau)$ in the full system (2.2), we apply a small perturbation to the solution, i.e., we consider the perturbations:

$$x = x_0(\tau) + u, \text{ and } y = 0 + v. \tag{2.5}$$

Then, we substitute (2.5) into system (2.2). Thus, after performing linearisation, we obtain the following uncoupled equations.

$$
\begin{aligned}
u'' + u &= \varepsilon\beta(1 - 3x_0'(\tau)^2)u', \\
v'' + \frac{1}{4}v &= -\varepsilon(\kappa v' + \sigma v + \gamma_2 x_0(\tau)v).
\end{aligned} \tag{2.6}
$$

By the averaging method (putting $u(\tau) = r\cos(\tau + \varphi)$, $u'(\tau) = -r\sin(\tau + \varphi)$ for the first equation of (2.6)), we can show that the differential equation for r gives asymptotic stability of the trivial solution $u = 0$. Thus, the semitrivial solution is stable in the x-direction. Therefore it remains to analyse the second equation of (2.6) in order to investigate the stability of the semitrivial solution in the full system.

The second equation of (2.6) is of Mathieu type and its main instability domain is found for values of q near $\frac{1}{2}$. (See [60] Appendix 2, for a description of the Mathieu type equation). Then, the solution of the equation can be analysed by putting

$$v(\tau) = R\cos(\frac{1}{2}\tau + \psi), \text{with } v'(\tau) = -\frac{1}{2}R\sin(\frac{1}{2}\tau + \psi). \tag{2.7}$$

By substituting the relations in (2.7) into equation (2.6) for v, then applying the averaging over τ and after absorbing the rescaling factor ε into τ, we obtain:

$$
\begin{aligned}
R' &= -\frac{1}{4}\kappa R + \frac{1}{4}R\gamma_2 R_0 \sin 2\psi, \\
\psi' &= \frac{1}{2}\sigma + \frac{1}{4}\gamma_2 R_0 \cos 2\psi,
\end{aligned} \tag{2.8}
$$

where R_0 is the amplitude of the semitrivial solution we obtained earlier.

From the right-hand sides of (2.8), we can eliminate the variable ψ and after applying the response-oriented approach (see [57] or [59]), we have the following relation for the boundary of the stability domain:

$$R_c^2 = R_0^2 = \frac{1}{\gamma_2^2}(\kappa^2 + 4\sigma^2), \tag{2.9}$$

where R_c stands for R-critical. Thus, for $q^2 = \frac{1}{4} + \varepsilon\sigma$, we have the stability boundary values in terms of q and κ as follows:

$$q^2 = \frac{1}{4} + \varepsilon\sqrt{\frac{\gamma_2^2 R_0^2 - \kappa^2}{4}}, \tag{2.10}$$

which exists for $\kappa \leq \gamma_2\sqrt{\frac{4}{3}}$. As an illustration, we take $\gamma_2 = 2$, $\kappa = 1$, and we have a stability boundary curve, as shown by the R_c-curve in Figure 1 below.
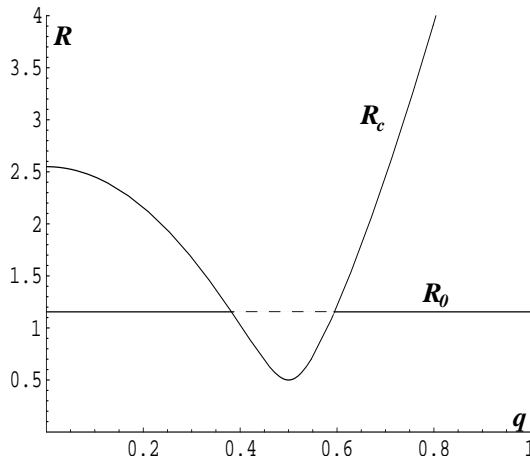
FIGURE 1. R_0 corresponds to the semitrivial solution and R_c corresponds to the stability boundary curve as a function of tuning ratio q for $\gamma_2 = 2$, $\kappa = 1, \varepsilon = 0.1$. Values of $R_0 > R_c$ correspond with instability.

The value $\kappa = \gamma_2 \sqrt{\frac{4}{3}}$ is a *bifurcation value* where the semitrivial solution changes its property and a nontrivial solution is initiated. We will see this phenomenon in the subsequent section.

2.4. Analysis of nontrivial solutions

The nontrivial solutions of (2.2) for $\varepsilon = 0$ can be written in the following form:

$$x = R_1 \cos(\tau + \psi_1) \text{ and } y = R_2 \cos(\frac{1}{2}\tau + \psi_2). \tag{2.11}$$

We substitute (2.11) into (2.2), then we apply the averaging method. Thus, we obtain the following averaged system (after absorbing the rescaling factor ε into τ).

$$
\begin{aligned}
R_1' &= \frac{1}{2}\beta R_1 - \frac{3}{8}\beta R_1^3 + \frac{1}{4}\gamma_1 R_2^2 \sin(\psi_1 - 2\psi_2) \\
\psi_1' &= \frac{1}{4}\gamma_1 \frac{R_2^2}{R_1} \cos(\psi_1 - 2\psi_2) \\
R_2' &= -\frac{1}{2}\kappa R_2 - \frac{1}{2}\gamma_2 R_1 R_2 \sin(\psi_1 - 2\psi_2) \\
\psi_2' &= \sigma + \frac{1}{2}\gamma_2 R_1 \cos(\psi_1 - 2\psi_2).
\end{aligned}
\tag{2.12}
$$

Note that the combination angle $\phi = \psi_1 - 2\psi_2$ figures in system (2.12) and we may reduce the system to:

10

$$R_1' = \frac{1}{2}\beta R_1 - \frac{3}{8}\beta R_1^3 + \frac{1}{4}\gamma_1 R_2^2 \sin\phi$$

$$R_2' = -\frac{1}{2}\kappa R_2 - \frac{1}{2}\gamma_2 R_1 R_2 \sin\phi \qquad (2.13)$$

$$\phi' = -2\sigma + (\frac{1}{4}\gamma_1 \frac{R_2^2}{R_1} - \gamma_2 R_1) \cos\phi.$$

To remove the singularity of the vector field in system (2.13) (see the equation for ϕ') we define

$$\rho = R_2^2, \; u = R_1 \cos\phi, \; v = R_1 \sin\phi, \qquad (2.14)$$

and the transformed system reads

$$\rho' = -\kappa\rho - \gamma_2\rho v$$

$$u' = \frac{1}{2}\beta(1 - \frac{3}{4}R_1^2)u + \gamma_2 uv + 2\sigma v \qquad (2.15)$$

$$v' = \frac{1}{2}\beta(1 - \frac{3}{4}R_1^2)v + \frac{1}{4}\gamma_1\rho - \gamma_2 u^2 - 2\sigma u,$$

where $R_1^2 = u^2 + v^2$.

To study system (2.15), we consider exact resonance ($\sigma = 0$), which is simpler, and near-resonance ($\sigma \neq 0$).

The fixed points of system (2.15) correspond to periodic solutions of system (2.12). First, we find the fixed points by assuming that ρ, u, and v are constants. Then by fixing the values of the parameters β, γ_1, and γ_2 and letting the value of κ vary, we study the bifurcations of the fixed points.

2.5. Exact resonance

Putting $\sigma = 0$ and assuming that $\beta > 0$, $\gamma_1 > 0$, and $\gamma_2 > 0$, system (2.15) becomes

$$\rho' = -\kappa\rho - \gamma_2\rho v$$

$$u' = \frac{1}{2}\beta(1 - \frac{3}{4}(u^2 + v^2))u + \gamma_2 uv \qquad (2.16)$$

$$v' = \frac{1}{2}\beta(1 - \frac{3}{4}(u^2 + v^2))v + \frac{1}{4}\gamma_1\rho - \gamma_2 u^2.$$

Note that system (2.16) is invariant under $(\rho, u, v) \rightarrow (\rho, -u, v)$. $\rho = 0$ is an invariant manifold of the system. This is obvious since taking $\rho = 0$ is related to our previous analysis of the semitrivial solution. In addition, $u = 0$ is also an invariant manifold of system (2.16).

2.5.1. Fixed points and their bifurcations.
To analyse the fixed points of system (2.16), we will make use of the existence of the invariant manifolds $\rho = 0$ and $u = 0$.

Solving $f_1(\rho, u, v) = 0, f_2(\rho, u, v) = 0, f_3(\rho, u, v) = 0$, where f_1, f_2, f_3 are the right-hand sides of (2.16), we obtain the following fixed points. $\mathbf{x_{00}} = (\rho_0, u_0, v_0) =$

$(0,0,0)$ (the trivial solution), $\mathbf{x_{10}} = (0,0,\sqrt{\frac{4}{3}})$, and $\mathbf{x_{20}} = (0,0,-\sqrt{\frac{4}{3}})$ (the semitrivial solution) and the following fixed points corresponding with nontrivial periodic solutions

$$\mathbf{X_1} = \left(\frac{2\beta\kappa}{\gamma_1\gamma_2}(1 - \frac{3}{4}\frac{\kappa^2}{\gamma_2^2}), 0, -\frac{\kappa}{\gamma_2} \right), \tag{2.17}$$

and

$$\mathbf{X_2} = \left(\frac{16}{3}\frac{\gamma_2}{\gamma_1}(1 - 2\frac{\kappa}{\beta}), \pm\sqrt{\frac{4}{3}(1 - \frac{3}{4}\frac{\kappa^2}{\gamma_2^2}) - \frac{8}{3}\frac{\kappa}{\beta}}, -\frac{\kappa}{\gamma_2} \right). \tag{2.18}$$

Note that the points $\mathbf{x_{00}}$, $\mathbf{x_{10}}$, and $\mathbf{x_{20}}$ are in the invariant manifold $\rho = 0$, the points $\mathbf{x_{00}}$, $\mathbf{x_{10}}$, $\mathbf{x_{20}}$ and $\mathbf{X_1}$ are in the invariant manifold $u = 0$. Thus, we may begin the analysis of the fixed points from the manifolds where they are in, while we need to analyse the point $\mathbf{X_2}$ separately.

We apply linear analysis by, first, finding the Jacobian matrix of system (2.16). Then we find the eigenvalues of the corresponding fixed points whose stability properties are to be determined. The Jacobian matrix of system (2.16) is as follows

$$J = \begin{pmatrix} -\kappa - \gamma_2 v & 0 & -\gamma_2\rho \\ 0 & \frac{1}{2}\beta - \frac{9}{8}\beta u^2 - \frac{3}{8}\beta v^2 + \gamma_2 v & -\frac{3}{4}\beta uv + \gamma_2 u \\ \frac{1}{4}\gamma_1 & -\frac{3}{4}\beta uv - 2\gamma_2 u & \frac{1}{2}\beta - \frac{3}{8}\beta u^2 - \frac{9}{8}\beta v^2 \end{pmatrix}. \tag{2.19}$$

In the invariant manifold $\rho = 0$, where the points $\mathbf{x_{00}}$, $\mathbf{x_{10}}$, and $\mathbf{x_{20}}$ are located, the corresponding 2×2 Jacobian matrix is as follows.

$$J_1 = \begin{pmatrix} \frac{1}{2}\beta - \frac{9}{8}\beta u^2 - \frac{3}{8}\beta v^2 + \gamma_2 v & -\frac{3}{4}\beta uv + \gamma_2 u \\ -\frac{3}{4}\beta uv - 2\gamma_2 u & \frac{1}{2}\beta - \frac{3}{8}\beta u^2 - \frac{9}{8}\beta v^2 \end{pmatrix} \tag{2.20}$$

Linear analysis yields that $(0,0)$ which has eigenvalues $\lambda_1 = \lambda_2 = \frac{1}{2}\beta$ is an unstable node with lines phase flows pointing outward. In $(0,\sqrt{\frac{4}{3}})$ the eigenvalues are $\gamma_2\sqrt{\frac{4}{3}}$ and $-\beta$. This corresponds with a saddle point with its stable manifold on the v axis. In $(0,-\sqrt{\frac{4}{3}})$ the eigenvalues are $-\gamma_2\sqrt{\frac{4}{3}}$ and $-\beta$. This corresponds with a stable node with parabolic phase curves pointing inward. By some algebraic manipulation on the equations in (2.16) for $\rho = 0$ we obtain a separatrix curve $u^2 + v^2 = \frac{4}{3}$ connecting the points $(0,\sqrt{\frac{4}{3}})$ and $(0,-\sqrt{\frac{4}{3}})$; An orbit which starts from a point outside the curve will never cross the separatrix curve and it will go either to the stable manifold of $(0,\sqrt{\frac{4}{3}})$ or to the stable manifold of $(0,-\sqrt{\frac{4}{3}})$. Some authors call such a separatrix curve a *saddle-sink connection*. This saddle-sink connection actually corresponds with the semitrivial solution obtained previously as we can check it by using transformation (2.14). For the illustration of the dynamics on the $u-v$ plane see Figure 2.

In the invariant manifold $u = 0$, where the points $\mathbf{x_{00}}$, $\mathbf{x_{10}}$, $\mathbf{x_{20}}$, and $\mathbf{X_1}$ are located, the corresponding 2×2 Jacobian matrix is as follows.

$$J_2 = \begin{pmatrix} -\kappa - \gamma_2 v & -\gamma_2\rho \\ \frac{1}{4}\gamma_1 & \frac{1}{2}\beta - \frac{3}{8}\beta u^2 - \frac{9}{8}\beta v^2 \end{pmatrix} \tag{2.21}$$
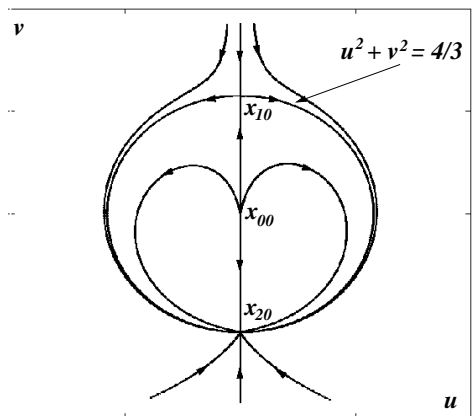
FIGURE 2. The dynamics in the $u-v$ plane.

Using a similar analysis as above, we find that at $(0,0)$ the eigenvalues are $-\kappa$ and $\frac{1}{2}\beta$. This corresponds with a saddle point with its unstable manifold on the v axis. In $(0, \sqrt{\frac{4}{3}})$ the eigenvalues are $-\kappa - \gamma_2\sqrt{\frac{4}{3}}$ and $-\beta$ which correspond with a stable node. An interesting phenomenon happens at $(0, -\sqrt{\frac{4}{3}})$. The eigenvalues are $-\kappa + \gamma_2\sqrt{\frac{4}{3}}$ and $-\beta$, as can be seen from the following matrix which is obtained by substituting $(0, -\sqrt{\frac{4}{3}})$ into J_2.

$$J_p = \begin{pmatrix} -\kappa + \gamma_2\sqrt{\frac{4}{3}} & 0 \\ \frac{1}{4}\gamma_1 & -\beta \end{pmatrix} \tag{2.22}$$

Focusing on the change of values of the parameter κ, we see that $\kappa = \gamma_2\sqrt{\frac{4}{3}}$ is a critical value where the corresponding fixed point changes its property (recall the bifurcation value we mentioned in section 2.3). We can check easily that $\kappa > \gamma_2\sqrt{\frac{4}{3}}$ results in the point $(0, -\sqrt{\frac{4}{3}})$ to be a stable node, while $\kappa < \gamma_2\sqrt{\frac{4}{3}}$ results in the point $(0, -\sqrt{\frac{4}{3}})$ to be a saddle. To see what happens at $\kappa = \gamma_2\sqrt{\frac{4}{3}}$ we apply the centre manifold approach (see [8] for details).

We consider the equations (2.16)(i) and (2.16)(iii) for ρ and v, respectively, by taking $u = 0$. For the sake of simplicity, we fix the values of $\beta = 2$, $\gamma_1 = 1$, $\gamma_2 = 2$. Thus, the system we consider is as follows.

$$\begin{aligned} \rho' &= -\kappa\rho - 2\rho v \\ v' &= v - \frac{3}{4}v^3 + \frac{1}{4}\rho. \end{aligned} \tag{2.23}$$

We translate the point $(0, -\sqrt{\frac{4}{3}})$ to $(0,0)$, the bifurcation value to 0, and take $h(\bar{\rho}, \bar{\kappa}) = a_1\bar{\rho}^2 + a_2\bar{\rho}\bar{\kappa} + a_3\bar{\kappa}^2$+h.o.t. as an approximation for the centre manifold, where the bars indicate the new coordinate after translation. After some calculations, we obtain the values $a_1 = 1 + \frac{3}{4}\sqrt{3}, a_2 = 0$, and $a_3 = 0$ so that $h(\bar{\rho}, \bar{\kappa}) = (1 + \frac{3}{4}\sqrt{3})\bar{\rho}^2$. The following equation gives the flow on the centre manifold.

$$\begin{aligned}
\bar{\rho}' &= -\bar{\rho}(\bar{\kappa} + 2\bar{\rho} + 2(1 + \frac{3}{4}\sqrt{3})\bar{\rho}^2) \\
\bar{\kappa}' &= 0.
\end{aligned} \quad (2.24)$$

We see from the flow (2.24) that we have a super-critical pitchfork bifurcation around $(0,0)$. At $\bar{\kappa} = 0$, the point $(0,0)$ which corresponds with the semitrivial solution $\mathbf{x_{20}}$ branches off; The semitrivial solution loses its stability while a stable nontrivial solution is initiated. The nontrivial solution which occurs corresponds with the point $(\frac{2\beta\kappa}{\gamma_1\gamma_2}(1 - \frac{3}{4}\frac{\kappa^2}{\gamma_2^2}), -\frac{\kappa}{\gamma_2})$ (or $\mathbf{X_1}$ in $\rho-u-v$ space).

Now we investigate the stability of the nontrivial solution. After substituting $(\frac{2\beta\kappa}{\gamma_1\gamma_2}(1 - \frac{3}{4}\frac{\kappa^2}{\gamma_2^2}), -\frac{\kappa}{\gamma_2})$ into matrix J_2, we obtain the corresponding 2×2 Jacobian matrix

$$J_h = \begin{pmatrix} 0 & -\frac{2\beta\kappa}{\gamma_1}(1 - \frac{3}{4}\frac{\kappa^2}{\gamma_2^2}) \\ \frac{1}{4}\gamma_1 & \frac{1}{2}\beta(1 - \frac{9}{4}\frac{\kappa^2}{\gamma_2^2}) \end{pmatrix}. \quad (2.25)$$

We see from (2.25) that $\kappa = \frac{2}{3}\gamma_2$ is another bifurcation value where the fixed point changes its properties as κ varies. We can check that for $\kappa > \frac{2}{3}\gamma_2$ the corresponding fixed point is a stable focus while for $\kappa < \frac{2}{3}\gamma_2$ the corresponding fixed point is an unstable focus. At the critical value we have a Hopf bifurcation with a pair of purely imaginary eigenvalues. In analysing the bifurcation, using the centre manifold method, we will look for the approximation for the centre manifold, the flow in the centre manifold, and determine the stability of the limit cycle associated with Hopf bifurcation. First we translate the point $(\frac{2\beta\kappa}{\gamma_1\gamma_2}(1 - \frac{3}{4}\frac{\kappa^2}{\gamma_2^2}), -\frac{\kappa}{\gamma_2})$ to $(\hat{\rho}, \hat{v}) = (0,0)$ and $\kappa = \frac{2}{3}\gamma_2$ to $\hat{\kappa} = 0$, where the hats indicate the corresponding new coordinate after translation. We take the same values of $\beta = 2$, $\gamma_1 = 1$, $\gamma_2 = 2$ as before. To avoid the algebraic complexity due to the presence of the parameter $\hat{\kappa}$, we take $\hat{\kappa} = 0$ from the beginning. Thus, we have the Jacobian matrix of the form

$$A = \begin{pmatrix} 0 & -\frac{32}{9} \\ \frac{1}{4} & 0 \end{pmatrix} \quad (2.26)$$

After normalisation and applying the centre manifold approach, we obtain the centre manifold where the corresponding flow is given by

$$\begin{aligned}
\hat{\rho}' &= -\frac{2}{3}\sqrt{2}\hat{v} - 2\hat{\rho}\hat{v} \\
\hat{v}' &= \frac{2}{3}\sqrt{2}\hat{\rho} + \frac{3}{2}\hat{v}^2 - \frac{3}{4}\hat{v}^3.
\end{aligned} \quad (2.27)$$

The stability of the limit cycle which occurs can be determined by calculating the

following quantity. (See [**25**] for a formal presentation of the formula).

$$a = \frac{1}{16}[f_{xxx} + f_{xyy} + g_{xxy} + g_{yyy}] + \frac{1}{16\omega_0}[f_{xy}(f_{xx} + f_{yy})$$
$$- g_{xy}(g_{xx} + g_{yy}) - f_{xx}g_{xx} + f_{yy}g_{yy}],$$

(2.28)

where $\omega_0 = \frac{2}{3}\sqrt{2}$, f, g are, respectively, the right-hand sides of $\hat{\rho}'$, $\hat{v}'$ of (2.27), and the subscripts 'x' and 'y' denote derivation with respect to $\hat{\rho}$ and $\hat{v}$, respectively. We obtain $a = -\frac{9}{32}$, which is negative. Thus, we have a super-critical Hopf bifurcation; a stable limit cycle occurs while the periodic solution changes its stability. To illustrate this phenomenon, we implement the numerical software packages CONTENT and DsTool, on the basis of the analytical results above. (See [**35**] and [**26**] for more about the packages).
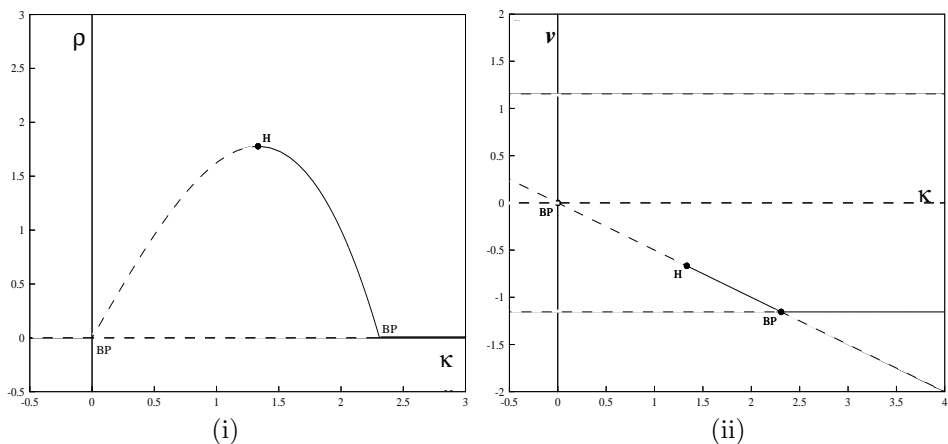

FIGURE 3. **Exact resonance**. Bifurcation diagram of system (2.23) on (i) the $\kappa-\rho$ plane and (ii) the $\kappa-v$ plane, for $\beta = 2$, $\gamma_1 = 1$, $\gamma_2 = 2$. BP stands for branching point and H stands for Hopf point. Solid and dashed lines/curves indicate a stable and an unstable solution, respectively.

Figure 3 gives the corresponding bifurcation diagram which describes the fixed points by giving ρ and v as a function of κ and their stabilities and bifurcations. As commonly used, in bifurcation diagrams displayed in this paper stable solutions are indicated by solid lines/curves and unstable ones by dashed lines/curves. To illustrate the dynamics in the $\rho-v$ plane, especially near the bifurcation point, we refer to Figure 4.
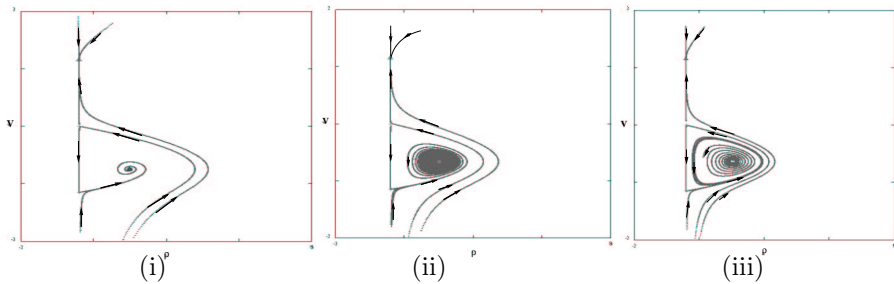
FIGURE 4. **Hopf bifurcation**. The dynamics in the $\rho-v$ plane for $\beta = 2$, $\gamma_1 = 1$, $\gamma_2 = 2$. (i) at $\kappa = 1.5$, (ii) at $\kappa = \frac{4}{3}$ (the Hopf point), (iii) at $\kappa = 1.28$.

Figure 4 (ii) shows the starting point where the stable limit cycle occurs while the nontrivial solution changes its stability (from a stable focus (in Figure 4 (i)) to an unstable focus (in Figure 4 (iii))).

Continuation with respect to the value of κ on the limit cycle produced by the Hopf bifurcation, results in the stable limit cycle breaking down into a heteroclinic cycle which takes place at $\kappa \approx 1.243761$; The orbit connects the saddle points $(0,0)$ and $(0, -\sqrt{\frac{4}{3}})$ which correspond with the points $\mathbf{x_{00}}$ and $\mathbf{x_{20}}$, respectively. Moreover, perturbing the value of κ by decreasing it, the heteroclinic cycle breaks up. Thus, we have a heteroclinic bifurcation as shown in Figure 5. Figure 5 (i) shows that the stable limit cycle is getting closer to the heteroclinic cycle connecting the saddle points $(0,0)$ and $(0, -\sqrt{\frac{4}{3}})$. Figure 5 (ii) shows that the limit cycle breaks down into a heteroclinic cycle. Finally, in Figure 5 (iii) the heteroclinic cycle breaks up and we have another saddle-sink connection connecting the saddle point $(0, -\sqrt{\frac{4}{3}})$ and the stable node $(0, \sqrt{\frac{4}{3}})$.
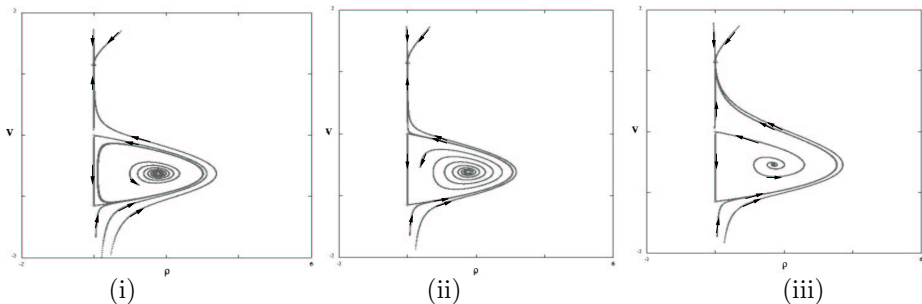

FIGURE 5. **Heteroclinic bifurcation**. The dynamics in the $\rho-v$ plane for $\beta = 2$, $\gamma_1 = 1$, $\gamma_2 = 2$. (i) at $\kappa = 1.26$, (ii) at $\kappa \approx 1.243761$ (the heteroclinic cycle bifurcation), (iii) at $\kappa = 1.1$.

Continuing to vary the value of κ we find the persistence of the saddle-sink connection.

Now, we analyse the point $\mathbf{X_2}$ which is neither in the $u-v$ plane nor in the $\rho-v$ plane. To apply linear analysis, we substitute the nontrivial solution $\mathbf{X_2}$ (we take the plus sign) into the Jacobian matrix J to obtain the following matrix.

$$\begin{pmatrix} 0 & 0 & -\frac{16}{3}\gamma_1\gamma_2^2(1-2\frac{\kappa}{\beta}) \\ 0 & -\frac{1}{12}\beta\mathcal{C}_2 & (\frac{1}{4}\frac{\beta\kappa}{\gamma_2}+\frac{1}{3}\gamma_2)\sqrt{\mathcal{C}_2} \\ \frac{1}{4}\gamma_1 & (\frac{1}{4}\frac{\beta\kappa}{\gamma_2}-\frac{2}{3}\gamma_2)\sqrt{\mathcal{C}_2} & -\frac{3}{4}\frac{\beta\kappa^2}{\gamma_2^2}+\kappa \end{pmatrix} \quad (2.29)$$

where $\mathcal{C}_2 = 12 - 9\frac{\kappa^2}{\gamma_2^2} - 24\frac{\kappa}{\beta}$. Because of the complexity of the expressions in (2.29) we perform a numerical calculation, fixing the parameters β, γ_1, and γ_2, to obtain the eigenvalues.

(i)

(ii)

(iii)
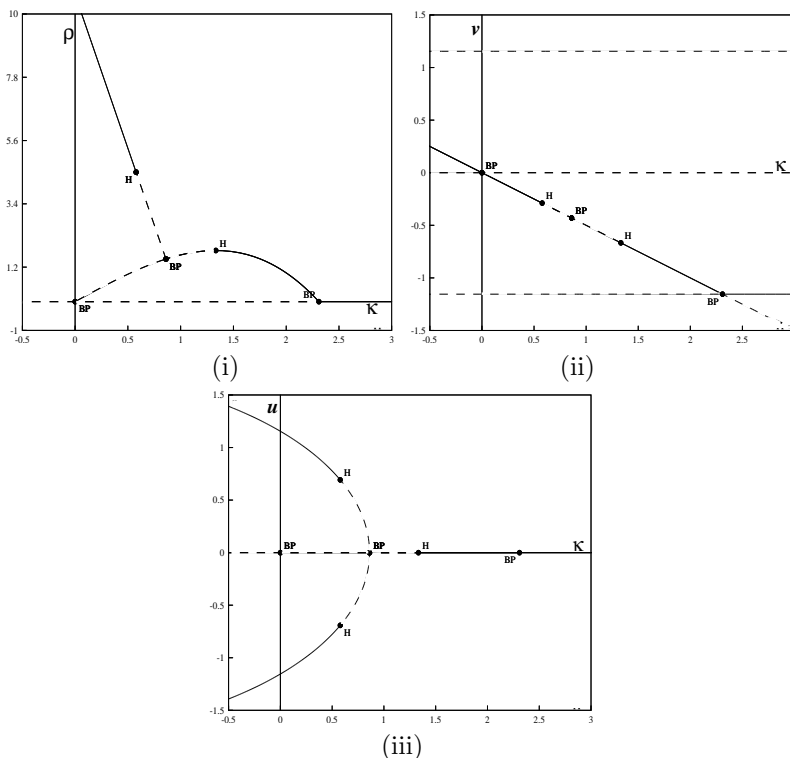
FIGURE 6. **Exact resonance**. Bifurcation diagram of system (2.16) (i) projected on the $\kappa-\rho$ plane, (ii) projected on the $\kappa-v$ plane, (iii) projected on $\kappa-u$ plane, for $\beta = 2$, $\gamma_1 = 1$, $\gamma_2 = 2$. BP stands for branching point and H stands for Hopf point.

By taking $\beta = 2$, $\gamma_1 = 1$, $\gamma_2 = 2$, and assuming $\kappa > 0$, the eigenvalues of the Jacobian matrix (2.29) are one real and two complex conjugate which are of the form

c and **d** ± i**e**, where **c**, **d** and **e** are functions of κ. Taking **c** = 0, which corresponds with taking $\kappa \approx 0.861002$, the Jacobian has one zero eigenvalue and two complex conjugate eigenvalues. This corresponds with a branching point where the curve of $\mathbf{X_2}$ points parameterised by κ tangents to the curve of $\mathbf{X_1}$ points. Moreover, taking **d** = 0 which corresponds with $\kappa \approx 0.578051$ (for $\gamma_1 = 1$, $\gamma_2 = 2$, $\beta = 2$), the Jacobian has one real eigenvalue and two purely imaginary eigenvalues. This implies the presence of a sub-critical Hopf bifurcation; an unstable limit cycle occurs while the fixed point changes its stability. Now we have a complete bifurcation diagram for system (2.16). We describe the fixed points by giving ρ, u, and v as a function of κ as shown in Figure 6.

Figure 6(i) and Figure 6(ii) are similar to Figure 3(i) and Figure 3(ii), respectively, except that we have new branches of nontrivial solutions which correspond with $\mathbf{X_2}$. These solutions are shown clearly in Figure 6(iii).

2.5.2. The heteroclinic cycle. By combining the dynamics in the $u-v$ plane (see Figure 2) and Figure 5 (iii) we obtain a *robust heteroclinic cycle*; a cycle which is formed by two saddle-sink connections of the invariant manifolds $u-v$ plane and $\rho-v$ plane. (See [**30**] for the definition). This, actually, also follows from system (2.16) when we integrate a point nearby the unstable nontrivial solution for $\kappa < 1.243761$. Figure 7 gives a clear illustration of the cycle in the 3-dimensional phase-space $\rho-u-v$.
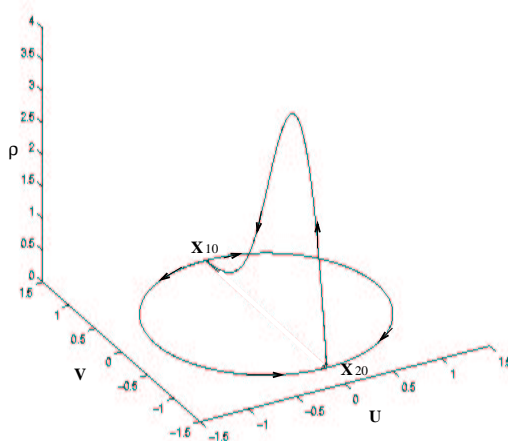

FIGURE 7. The robust heteroclinic cycle connecting the saddle points $\mathbf{x_{10}}$ and $\mathbf{x_{20}}$.

In the original system (2.13), $\mathbf{x_{10}}$ and $\mathbf{x_{20}}$ should be identified and correspond with the semitrivial periodic solution. In system (2.13) the part of the heteroclinic cycle for $\rho > 0$ corresponds with a solution homoclinic to the semitrivial periodic solution.

Note that since the heteroclinic cycle persists in the interval of κ where no stable solution exists (see the bifurcation diagram of Figure 3), we may further the analysis by studying the stability of the heteroclinic cycle.

Studies on the stability of robust heteroclinic cycles have been done by several authors. (See, for example, [**30**], [**31**], and the references there). In [**31**] Krupa and Melbourne develop a general sufficient and necessary condition for investigating the asymptotic stability of such cycles. They use the fact that a trajectory following the robust heteroclinic cycle (see Figure 7) will spend large amounts of time near the fixed points ($\mathbf{x_{10}}$ and $\mathbf{x_{20}}$) while the passages outside fixed points will be relatively short. Hence the relative size of the eigenvalues of the linearisations at the fixed points will be the factor determining stability. The discussion below will follow this idea.

First, we take the same fixed values of the parameters $\beta = 2$, $\gamma_1 = 1$, $\gamma_2 = 2$ as before and assume that we are in the interval of κ where we have unstable solutions only. So, we may take $\kappa = 1$. Recall that the point $\mathbf{x_{10}}$ is a saddle point with its stable eigenvalues $\lambda_{s_1} = -1 - 2\sqrt{\frac{4}{3}}$ and $\lambda_{s_2} = -2$ are in the $\rho - v$ plane, while the unstable one $\lambda_u = 2\sqrt{\frac{4}{3}}$ is in the $u - v$ plane. The point $\mathbf{x_{20}}$ is a saddle point with its stable eigenvalues $\nu_{s_1} = -2\sqrt{\frac{4}{3}}$ and $\nu_{s_2} = -2$ are in the $u - v$ plane while its unstable eigenvalue $\nu_u = -1 + 2\sqrt{\frac{4}{3}}$ is in the $\rho - v$ plane. Thus, our heteroclinic cycle is formed by two saddle-sink connections as obtained earlier. This is clear from Figure 7 above. Then we implement the result in [**31**] saying that if S is a robust heteroclinic cycle then S is asymptotically stable provided the condition

$$\prod_{j=1}^{m} \min(c_j, e_j - t_j) > \prod_{j=1}^{m} e_j, \qquad (2.30)$$

is satisfied, where

- c_j is the magnitude of the maximal real part of the eigenvalue of $Df(\xi_j)$, linearised vector field near fixed point, restricted to $P_{j-1} \backslash P_j$,
- e_j is the magnitude of the maximal real part of the eigenvalue of $Df(\xi_j)$ restricted to $P_j \backslash P_{j-1}$,
- t_j is the maximal real part of the eigenvalues whose eigenvectors are normal to $P_{j-1} + P_j$,

with P_{j-1}, P_j the corresponding invariant subspaces. (See Theorem 2.7 of [**31**] for more detail in the formulation). We change the condition (2.30) slightly since in our case, we do not have t_j. Therefore condition (2.30) reduces to the standard condition that

$$\prod_{j=1}^{m} c_j > \prod_{j=1}^{m} e_j. \qquad (2.31)$$

From the eigenvalues of $\mathbf{x_{10}}$ and $\mathbf{x_{20}}$ mentioned above we obtain that $\frac{\lambda_{s_1} \nu_{s_1}}{\lambda_u \nu_u} \approx 1.322781 > 1$. Thus, by (2.31) we conclude that our heteroclinic cycle is asymptotically stable. Therefore, this gives the boundedness of the solution in the interval of the parameter κ where no stable periodic solution takes place.

We find that the stable heteroclinic cycle persists as we vary the value of κ. This is due to the persistence of the corresponding saddle-sink connections mentioned

earlier. Thus, in the interval $0 < \kappa < 0.578051$ we have two attractors; the stable heteroclinic cycles and the stable fixed points produced by the sub-critical Hopf bifurcation (see the analysis of the point $\mathbf{X_2}$ mentioned earlier). Therefore, the dynamics in that region is attracted either to the fixed point $\mathbf{X_2}$ or to the heteroclinic cycle.

2.6. Near-resonance

In this section we analyse the full averaged system (2.15) by considering $\sigma \neq 0$. In system (2.15) the symmetry $(\rho, u, v) \rightarrow (\rho, -u, v)$ which takes place in the exact resonance case no longer exists while we keep the invariance of $\rho = 0$. In the following we discuss this symmetry breaking property when σ is perturbed from 0 as it reflects on the solutions, stabilities and bifurcations, as κ varies.

We follow similar lines for determining fixed points as in the previous section, and obtain the following fixed points. $\mathbf{y_{00}} = (\rho_1, u_1, v_1) = (0, 0, 0)$ (the trivial solution), $\mathbf{y_{10}} = (0, -\frac{2\sigma}{\gamma_2}, \sqrt{\frac{4}{3} - \frac{4\sigma^2}{\gamma_2^2}})$, and $\mathbf{y_{20}} = (0, -\frac{2\sigma}{\gamma_2}, -\sqrt{\frac{4}{3} - \frac{4\sigma^2}{\gamma_2^2}})$ (the semitrivial solution), and the nontrivial solutions

$$\mathbf{Y_1} = (\rho_1(u_1), u_1, -\frac{\kappa}{\gamma_2}), \tag{2.32}$$

where u_1 will be determined from the following cubic polynomial equation in u_1.

$$u_1^3 + (\frac{3\beta\kappa^2 + 8\kappa\gamma_2^2 - 4\beta\gamma_2^2}{3\beta\gamma_2^2})u_1 + \frac{16}{3}\frac{\kappa\sigma}{\beta\gamma_2} = 0 \tag{2.33}$$

Using Cardano's formula for solving a cubic equation, we determine the quantity $\mathcal{D} = \frac{q^2}{4} + \frac{p^3}{27}$, where $p = \frac{16}{3}\frac{\kappa\sigma}{\beta\gamma_2}$, $q = \frac{3\beta\kappa^2 + 8\kappa\gamma_2^2 - 4\beta\gamma_2^2}{3\beta\gamma_2^2}$. After a rather lengthy calculation we arrive to the following expression for $\mathcal{D}$.

$$\mathcal{D} = \frac{1}{729\beta^3\gamma_2^6}((\beta - \beta_0)^3 + 5184\beta\gamma_2^4\kappa^2\sigma^2), \tag{2.34}$$

where

$$\beta_0 = \frac{8\gamma_2^2\kappa}{4\gamma_2^2 - 3\kappa^2}. \tag{2.35}$$

From (2.35) we restrict the value of κ into $0 < \kappa < \gamma_2\sqrt{\frac{4}{3}}$. Then, Cardano's formula guarantees the existence of at least one real solution for u_1 in (2.33) which unfortunately has a quite complicated expression.

Next, we analyse the stability of the fixed points by using the same method as before. We consider the Jacobian matrix of system (2.15) as follows.

$$J_s = \begin{pmatrix} -\kappa - \gamma_2 v & 0 & -\gamma_2\rho \\ 0 & \frac{1}{2}\beta - \frac{9}{8}\beta u^2 - \frac{3}{8}\beta v^2 + \gamma_2 v & -\frac{3}{4}\beta uv + \gamma_2 u + 2\sigma \\ \frac{1}{4}\gamma_1 & -\frac{3}{4}\beta uv - 2\gamma_2 u - 2\sigma & \frac{1}{2}\beta - \frac{3}{8}\beta u^2 - \frac{9}{8}\beta v^2 \end{pmatrix} \tag{2.36}$$

Since the plane $\rho = 0$ is an invariant manifold we start the analysis from the points in that plane, i.e. $(0,0)$, $(-\frac{2\sigma}{\gamma_2}, \sqrt{\frac{4}{3} - \frac{4\sigma^2}{\gamma_2^2}})$, and $(-\frac{2\sigma}{\gamma_2}, -\sqrt{\frac{4}{3} - \frac{4\sigma^2}{\gamma_2^2}})$ which correspond to $\mathbf{y_{00}}$, $\mathbf{y_{10}}$, and $\mathbf{y_{20}}$, respectively. Linear analysis gives the results that the point

$(0,0)$ is an unstable focus, $(-\frac{2\sigma}{\gamma_2}, \sqrt{\frac{4}{3} - \frac{4\sigma^2}{\gamma_2^2}})$ is a saddle, and $(-\frac{2\sigma}{\gamma_2}, -\sqrt{\frac{4}{3} - \frac{4\sigma^2}{\gamma_2^2}})$ is a stable node as shown in the following figure.
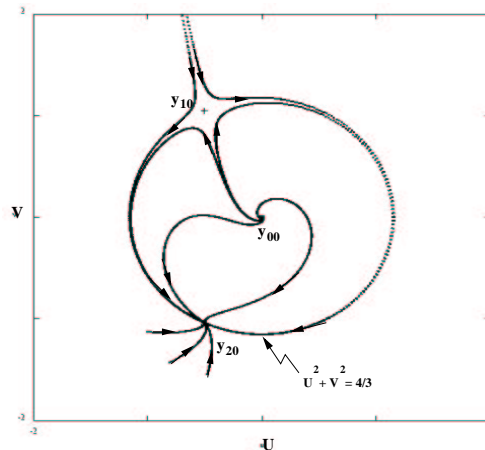

FIGURE 8. The dynamics in the $u-v$ plane for $\sigma = 0.5$

If we compare Figure 8 with Figure 2, points $\mathbf{y_{00}}$, $\mathbf{y_{10}}$, and $\mathbf{y_{20}}$ actually correspond with points $\mathbf{x_{00}}$, $\mathbf{x_{10}}$, and $\mathbf{x_{20}}$, respectively. Those Figures show that the σ perturbation does not change qualitatively the dynamics in the $u-v$ plane. Also, in the $u-v$ plane we have a separatrix $u^2 + v^2 = \frac{4}{3}$ which corresponds with the semitrivial solution. Then, the semitrivial solution will bifurcate for a certain value of κ where the nontrivial solution $\mathbf{Y_1}$ is initiated.

Due to the complexity of the expression of $\mathbf{Y_1}$ we perform numerical approaches to determine its stability. Solving Det $J_s\big|_{\mathbf{Y_1}} = 0$, we obtain a parameter space $\kappa-\sigma$ showing the stability boundary for the solutions where the stable semitrivial solution passing through the boundary branches off in a pitchfork bifurcation. This is shown by curve P in Figure 9. Furthermore, continuation by using CONTENT we obtain a Hopf curve H in Figure 9 where the nontrivial solutions have Hopf bifurcations and a saddle-node curve SN in Figure 9 where the nontrivial solutions have saddle-node bifurcations. Note that the boundedness of the range of σ is clear from the existence of the above mentioned semitrivial solution, $\mathbf{y_{10}}$ and $\mathbf{y_{20}}$. Figure 10 and Figure 11 are the corresponding bifurcation diagrams which describe the number of solutions and their stabilities and bifurcations by giving ρ and u as a function of κ. Figure 10 (i) and (ii) clearly illustrate the behaviour of the nontrivial periodic solutions of system (2.15) for $\sigma = 0.5$ (line l_2 of Figure 9). We start from the stable semitrivial solution in the outer part of curve P. As the solution passes through curve P, a pitchfork bifurcation takes place (shown by the BP point on the right); the semitrivial solution loses its stability while a stable nontrivial solution is initiated. On the other hand, continuation on the unstable trivial solution $\mathbf{y_{00}}$, from the BP point on the left, we obtain an unstable nontrivial solution which undergoes a
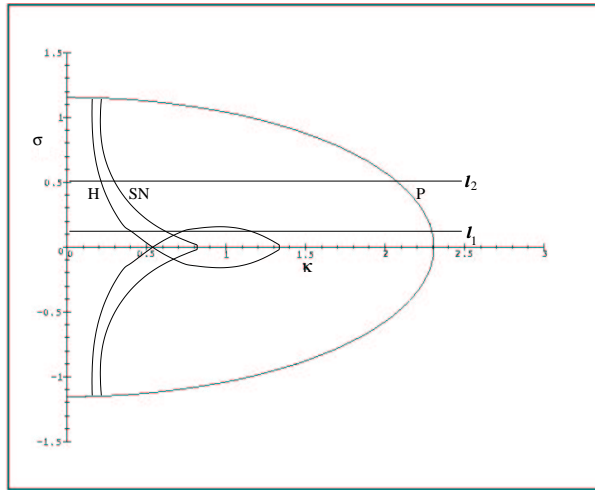
FIGURE 9. **Near resonance**. The parameter space $\kappa - \sigma$ showing Curves P, H, and SN for $\beta = 2$, $\gamma_1 = 1$, $\gamma_2 = 2$.
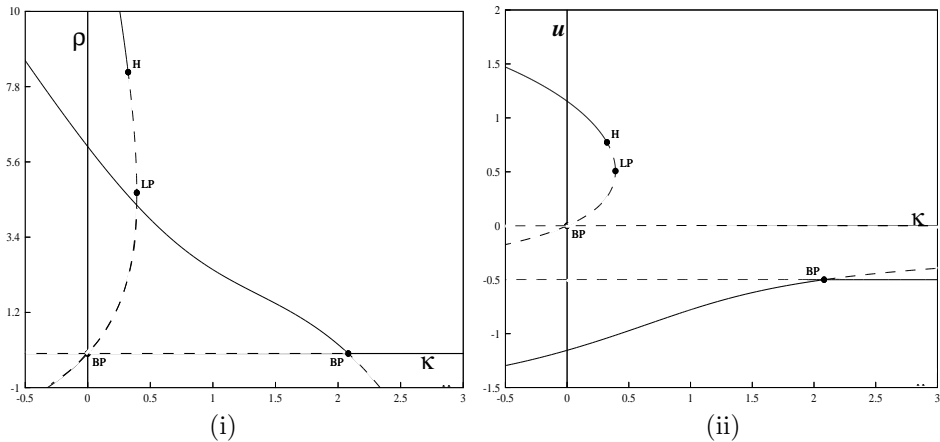

FIGURE 10. **Near resonance**. Bifurcation diagram of system (2.15) (i) projected on the $\kappa - \rho$ plane and (ii) projected on the $\kappa - u$ plane, for $\beta = 2$, $\gamma_1 = 1$, $\gamma_2 = 2$, $\sigma = 0.5$ (line l_2). BP stands for pitchfork point, H for Hopf point, and LP for saddle-node point.

saddle-node bifurcation (at the LP point) when hitting curve SN. Then, the unstable nontrivial solution undergoes a sub-critical Hopf bifurcation (at the H point) when passing through curve H.

It is interesting to see what happens to the nontrivial solution if we take σ closer to 0. Taking $\sigma = 0.1$ (line l_1 of Figure 9) we have the bifurcation diagram as shown in Figure 11.
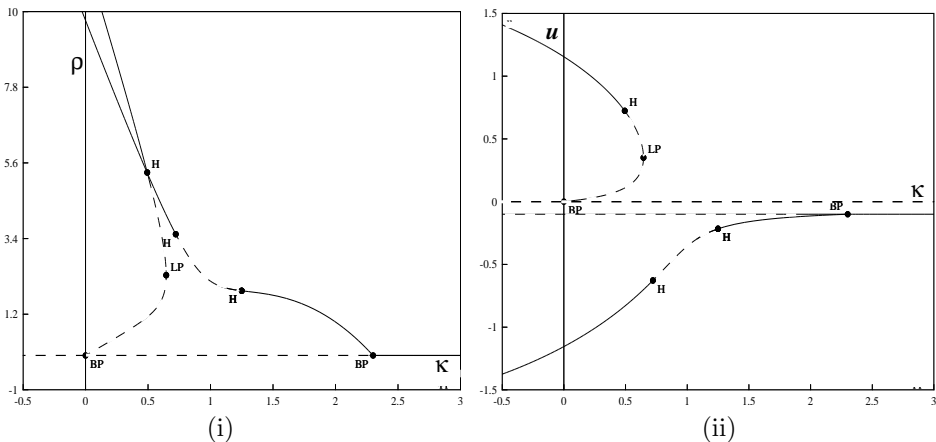
FIGURE 11. **Near resonance**. Bifurcation diagram of system (2.15) (i) projected on the $\kappa - \rho$ plane and (ii) projected on the $\kappa - u$ plane, for $\beta = 2$, $\gamma_1 = 1$, $\gamma_2 = 2$, $\sigma = 0.1$ (line l_1). BP stands for pitchfork point, H for Hopf point, and LP for saddle-node point.

Figure 11 shows more complicated dynamics than Figure 10. Obviously, Figure 11 (i) and (ii) tend to, respectively, Figure 6 (i) and (iii) of the exact resonance case if we take σ closer to 0. However, taking $\sigma \neq 0$ means we slightly perturb equation (2.16) such that the symmetry under $u = 0$ is broken; a *forced symmetry breaking* takes place. (See Krupa [**30**]). Thus, destruction of the stable robust heteroclinic orbit obtained earlier will take place. In [**49**] Swift shows that forced symmetry breaking for such an attracting orbit leads to the occurrence of a long-periodic orbit. We perform a numerical exploration to demonstrate the phenomenon in our system.

Taking an initial point nearby the robust heteroclinic orbit, it will go to a "one-half" orbit which has a long-period as shown in Figure 12 (i) and (ii) depending on the sign of σ. And Figure 12 (iii) gives a clear illustration of the forced symmetry breaking phenomenon if we compare it with Figure 7 of the exact resonance case.

2.7. Concluding remarks

The study of stability and bifurcation of the solutions of system (2.1) produces rich results as we have shown in the previous sections. Our results on the stability of the semitrivial solution of such a system plays an important role in mechanical engineering. The exact resonance analysis gives interesting phenomena, especially the boundedness of the solution shown by the attracting robust heteroclinic orbit. More interesting and important results are obtained from the near resonance analysis. We have shown numerically what happens with the solutions of our system if we apply the detuning coefficient.

A study of self-excited autoparametric systems of different type (e.g. van der Pol type) is also of interest. In our future work we will explore that type of system (see the work of Nabergoj and Tondl in [**39**] or Tondl et al. in [**59**]) and we will

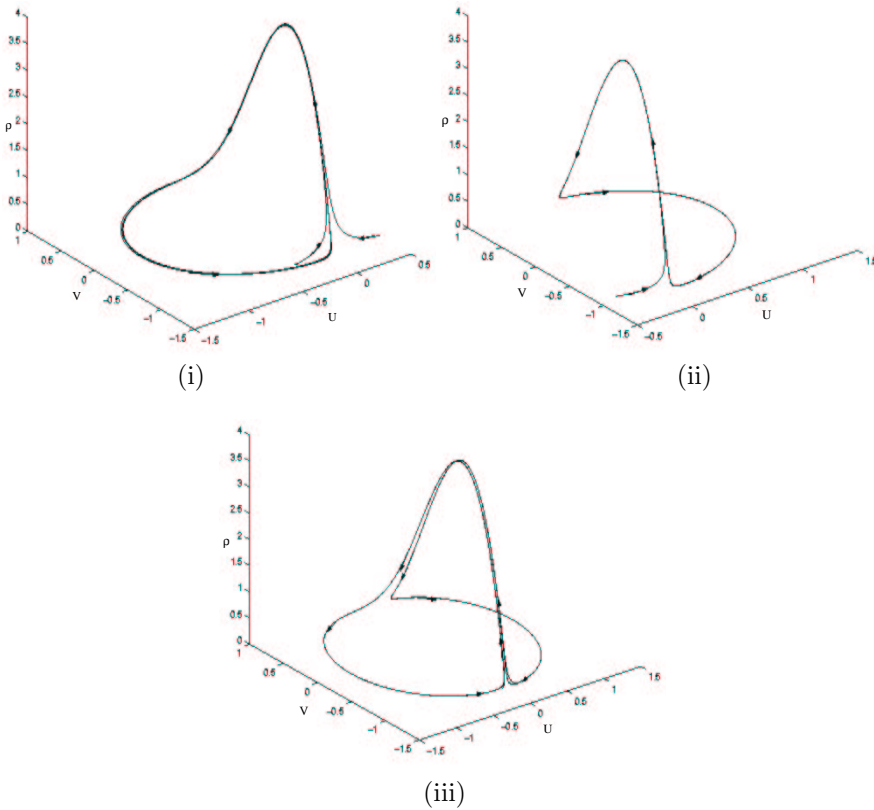FIGURE 12. **Forced symmetry breaking**. (i) a long-periodic orbit for $\sigma = 0.01$, (ii) a long-periodic orbit for $\sigma = -0.01$, (iii) the combination of (i) and (ii).

compare the results to those of this paper. Of course we can generalise system (2.1), for instance by generalising the coupling term. The result of this have to be studied but we expect to recover the fundamental bifurcations discussed in this paper.

A Self-excited Autoparametric System with Dry Friction

Has been submitted to journal.

3.1. Introduction

In mechanics, the van der Pol-type or Rayleigh-type oscillators are commonly used to model systems with self-excited vibrations induced by flow. The presence of self-excited vibrations itself can be highly detrimental to the performance of mechanical systems. One of the characteristics of self-excitation is the possibility of the appearance of a closed orbit, in the phase space of the mechanical system constructed, corresponding with a periodic solution of the system. (See [**50**] and [**59**] for some examples).

Another cause for the onset of self-excited vibrations in mechanical systems is dry friction. A classical example of such a system is an oscillator with Coulomb friction that can be described by a differential equation with a discontinuous right-hand side. This kind of system belongs to a class of discontinuous systems which is called the Filippov type of system.(See [**20**] for more details about the theoretical results).

Due to the discontinuity, there is a significant difference between the self-excitation in systems with dry friction and in systems with the other types of oscillators mentioned previously. In systems with dry friction, the periodic solution obtained is continuous but non-smooth. This requires more theoretical knowledge and methods to analyse than by simply using the available methods which are only applicable to smooth dynamical systems.

During the past few decades, there has been a tremendous amount of studies on dynamical systems containing a discontinuity. They are mainly devoted to the theoretical mathematics viewpoint (e.g. the works of Aizerman and Gantmakher [**3**], Filippov [**20**], Aubin and Cellina [**5**], Kunze [**32**], Kunze and Küpper [**33**], Kuznetsov et.al [**36**]) and to the mechanical engineering viewpoint (e.g. the works of Tondl [**50**], Popp and Stelter [**42**], Bothe [**7**], Babitsky and Krupenin [**6**]). These studies clearly point out that dry friction in dynamical systems is an important topic in both mathematical and engineering research.

Recently, in [**1**] the author applied the Rayleigh-type oscillator to an autoparametric system. The system is commonly used to model a mechanical construction

that undergoes self-excited vibrations induced by flow. The stability of the solutions of the system is studied by using the averaging method (see [**60**]) and numerical bifurcation path-following techniques. The result showed that the system displays a rich pattern of different bifurcations and instability behaviour. For more references on autoparametric systems the reader may see [**51**], or [**14**] for a more recent one.

We start with some observations regarding discontinuous systems with a small parameter. In particular we consider the possibilities of using the concept of differential inclusion, Lagrange's variation of constants and averaging to approximate the solution of the systems.

Then, we study the existence and the stability behaviour of solutions of an autoparametric system containing a dry friction oscillator. Especially, we investigate non-smooth solutions of the system like periodic solutions and other invariant sets.

3.2. Asymptotic analysis of systems with discontinuities

There are many results dealing with systems containing discontinuities by using asymptotic methods. One of the most common method that has been used to analyse such a problem is the averaging method. In the following, we mention results by Matveev et al. [**38**], Plotnikov [**40, 41**], Samoilenko and Pere'styuk [**45, 44**], Fidlin [**19**] and the references therein. We also make some observations on some asymptotic methods for analysing systems with discontinuity, as we will present shortly.

3.2.1. The use of differential inclusion. We consider a system with a discontinuous right-hand side as follows:

$$\dot{\mathbf{x}} = \mathbf{f}(t, \mathbf{x}, \varepsilon), \tag{3.1}$$

with $\mathbf{x} \in \mathfrak{D} \subset \mathbb{R}^n$ and ε is a small positive parameter. Suppose that $\mathbf{f}$ can be expanded to some order in a power series with respect to ε. More precisely, we have a system in the following form

$$\dot{\mathbf{x}} = \mathbf{f_0}(t, \mathbf{x}) + \varepsilon \mathbf{f_1}(t, \mathbf{x}) + \mathcal{O}(\varepsilon^2) \tag{3.2}$$

for $0 < t < h$, $\mathbf{x}$ is in a compact set $\mathfrak{D} \subset \mathbb{R}^n$, $0 \le \varepsilon \le \varepsilon_0$. $\mathbf{f_0}$ is a continuous function in t, continuously differentiable vector function in $\mathbf{x}$. $\mathbf{f_1}$ is a continuous function in t, a piecewise differentiable vector function in $\mathbf{x}$, with a finite number of discontinuities. For the sake of simplicity, we assume in the sequel that $\mathbf{f_1}$ has a single surface of discontinuity, Σ_1 in $\mathbb{R}^n$. A natural way to deal with such an equation is by considering the set

$$\mathbf{F_1}(t, \mathbf{x}) = \overline{\mathrm{co}}\{\mathbf{h} \in \mathfrak{D} \subset \mathbb{R}^n \mid \mathbf{h} = \lim_{\mathbf{k}^* \to \mathbf{x}} \mathbf{f_1}(t, \mathbf{k}^*), \ \mathbf{k}^* \in \mathfrak{D} \backslash \Sigma_1\},$$

where $\overline{\mathrm{co}}\, A$ denotes the smallest closed convex set containing A. It is clear that $\forall \mathbf{x}, f_1(t, \mathbf{x}) \in \mathbf{F_1}(t, \mathbf{x})$ and whenever f_1 is continuous at $\mathbf{x}$, $\mathbf{F_1}(t, \mathbf{x}) = \{f_1(t, \mathbf{x})\}$. Thus, any solution of (3.2) is a solution to the differential inclusion

$$\dot{\mathbf{x}} \in \mathbf{f_0}(t, \mathbf{x}) + \varepsilon \mathbf{F_1}(t, \mathbf{x}) + \mathcal{O}(\varepsilon^2). \tag{3.3}$$

(See [**20**] or [**5**] for the theory of differential inclusion.)

In [**5**] p. 120, a theory is developed which based on the assumption that $\mathbf{F}_1$ satisfies a Lipschitz condition with respect to $\mathbf{x}$ as follows

$$\mathfrak{d}(\mathbf{F_1}(t, \mathbf{x_a}) - \mathbf{F_1}(t, \mathbf{x_b})) \leq \lambda \|\mathbf{x_a} - \mathbf{x_b}\|, \ \forall \ \mathbf{x_a}, \mathbf{x_b} \in \mathfrak{D} \subset \mathbb{R}^n, \tag{3.4}$$

where λ is a Lipschitz constant and $\mathfrak{d}(P, Q)$ is the Hausdorff distance between the set P and Q, i.e.,

$$\mathfrak{d}(P, Q) = \min \{d \mid P \subset \mathcal{N}_d(Q), \ Q \subset \mathcal{N}_d(P)\},$$

where $\mathcal{N}_d(A)$ is the d-neighbourhood of the set $A \subset \mathbb{R}^n$. The condition is sufficient for the construction of an asymptotic approximate solution.
Unfortunately, if f_1 has jumps at Σ_1, the set-valued function $\mathbf{F}_1$ is not even continuous as a function of $\mathbf{x}$, and therefore cannot satisfy (3.4).

3.2.2. Lagrange's variation of constants. Now we show how the classical method by Lagrange might be applied to systems containing a discontinuity in Σ_1. Again, we consider equation (3.2). The unperturbed system in $\mathfrak{D}$ is given by

$$\dot{\mathbf{x}} = f_0(t, \mathbf{x}), \tag{3.5}$$

where f_0 is assumed as before.
Assuming that there exists $\varphi(t, \mathbf{z})$ such that

$$\frac{\partial \varphi(t, \mathbf{z})}{\partial t} = f_0(t, \varphi(t, \mathbf{z})). \tag{3.6}$$

Therefore, $\varphi(t, \mathbf{z})$ is a family of solutions of (3.5) parameterised by $\mathbf{z} \in \mathbb{R}^n$. Assume also that $\varphi(t, \mathbf{z})$ depends smoothly on $\mathbf{z}$, and that $\frac{\partial \varphi}{\partial \mathbf{z}}$ is an invertible matrix.
A variation of constants by taking

$$\mathbf{x}(t) = \varphi(t, \mathbf{z}(t)) \tag{3.7}$$

and then we derive the differential equation for $\mathbf{z}$ with the exclusion of Σ_1 by first substituting (3.7) into (3.1) to have

$$\frac{\partial \varphi(t, \mathbf{z})}{\partial t}\bigg|_{\mathbf{z}=\mathbf{z}(t)} + \frac{\partial \varphi(t, \mathbf{z})}{\partial \mathbf{z}}\bigg|_{\mathbf{z}=\mathbf{z}(t)} \frac{\partial \mathbf{z}(t)}{\partial t} = f(t, \varphi(t, \mathbf{z}(t)), \varepsilon).$$

Making use of (3.6) for the first summand, the equality in (3.2) (ignoring the higher order terms) and the invertibility of the matrix $\frac{\partial \varphi}{\partial \mathbf{z}}$ we obtain in $\mathfrak{D}$

$$\frac{\partial \mathbf{z}(t)}{\partial t} \in \left(\frac{\partial \varphi(t, \mathbf{z})}{\partial \mathbf{z}}\bigg|_{\mathbf{z}=\mathbf{z}(t)} \right)^{-1} (\varepsilon \mathbf{F}_1(t, \varphi(t, \mathbf{z}(t)), \varepsilon)), \tag{3.8}$$

where $\mathbf{F}_1$ is as defined earlier.
Applying an initial value by letting $\mathbf{z}(0) = \eta$ (implying that $\mathbf{x}(0) = \varphi(0, \eta)$), we solve for $\mathbf{z}$

$$\mathbf{z}(t) \in \eta + \varepsilon \int_0^t \left(\frac{\partial \varphi(s, \mathbf{z})}{\partial \mathbf{z}}\bigg|_{\mathbf{z}=\mathbf{z}(s)} \right)^{-1} \mathbf{F}_1(s, \varphi(s, \mathbf{z}(s)), \varepsilon) ds.$$

This implies that $\mathbf{z}(t) = \eta + \mathcal{O}(\varepsilon)$, when $\mathbf{F}_1$ is bounded.

Now the difficulty remains to check the asymptotic validity of the formal approximation obtained from this integral equation. The only obstruction to prove the

asymptotic validity of the approximate solution is the assumption on f_1 appearing in the integral. If f_1 is continuously differentiable with respect to φ, the substitution of $\mathbf{z}(s) = \eta + \mathcal{O}(\varepsilon)$ leads to an expansion

$$\mathbf{z}(t) = \eta + \varepsilon \int_0^t \left(\left. \frac{\partial \varphi(s, \mathbf{z})}{\partial \mathbf{z}} \right|_{\mathbf{z}=\eta} \right)^{-1} f_1(s, \varphi(s, \eta), 0) ds + \mathcal{O}(\varepsilon^2).$$

Then, substitute $\mathbf{z}(t)$ into (3.7) to have an approximate solution for $\mathbf{x}(t)$ of the system. However, as assumed earlier that f_1 is discontinuous for some values of φ, an intensive study must be done to obtain an asymptotic expansion with a remainder term of smaller order than $\mathcal{O}(\varepsilon)$.

Example 1:
Consider a differential equation with a discontinuous right-hand side of the following form:

$$\dot{x} = -\varepsilon \text{ sgn } (x), \tag{3.9}$$

where sgn is the signum function with sgn $(0) = 0$. As t increases, each solution initially started at $x(0) \neq 0$, sooner or later will arrive at the line $x = 0$, and cannot leave the line. Thus, we have non-smooth solutions with sliding along the line $x = 0$ as time increases. This is the delicate situation explained in the previous subsections when we want to approximate the solution, to describe the jump due to the discontinuity. After some time the solution is represented by the sliding solution which stays forever on the t-axis as time increases.

A classical example, which is often used in mechanical engineering, is the following example.

Example 2:
Consider the system of the following form:

$$\ddot{x} + x = \varepsilon \text{ sgn } (v - \dot{x}), \tag{3.10}$$

where sgn is the signum function and v is a positive constant. Thus, we have

$$\ddot{x} + x = \begin{cases} \varepsilon, & v > \dot{x} \\ -\varepsilon, & v < \dot{x} \end{cases} \tag{3.11}$$

with the corresponding solutions

$$x(t) = \pm \varepsilon + C \cos(t + \varphi),$$

where C and φ are the constants of integration that can be determined from the initial conditions. Therefore, the trajectories in the domain where $v > \dot{x}$ will be driven by concentric circles centred at the point $C_1(\varepsilon, 0)$. Similarly, the trajectories in the domain where $v < \dot{x}$ will be driven by concentric circles centred at the point $C_2(-\varepsilon, 0)$.

Let $I_0(a_0, b_0)$ be an initial point. Taking I_0 in the domain where $v > \dot{x}$, such that $(a_0 - \varepsilon)^2 + b_0^2 \leq v^2$, we have a set of smooth periodic solutions (circles). On the
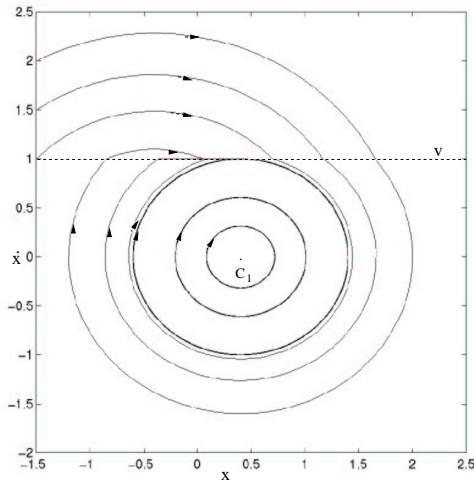
FIGURE 1. **The circles and the non-smooth solutions**.

other hand, taking I_0 in the domain where $v < \dot{x}$, we obtain a set of non-smooth solutions with the circle

$$(x - \varepsilon)^2 + \dot{x}^2 = v^2$$

as the limiting case. Figure 1 describes the phenomenon in the phase plane.

The occurrence of the smooth solutions (circles) arises as the solutions do not approach Σ_1, given by $\dot{x} = v$, whereas for the non-smooth ones Σ_1 is crossed or contained in the orbit. We certainly have a non-smoothness at the line $\dot{x} = v$. Moreover, we may have a sliding solution along the line, starting from the left before it slips into the limiting circle.

A similar example as Example 2 is considered in the monograph of Klotter [**29**] and in Popp and Stelter [**42**]. The authors gave a clear interpretation of the system in mechanical engineering. Unfortunately, they did not give a quite correct description of the phase portrait to illustrate the phenomenon as given in Figure 1 above. They conjectured that the limit of the set of non-smooth solutions is a periodic solution with a sliding segment along the discontinuity line which is symmetric with respect to the tangent point, instead of a circle which is tangent to the line. This is impossible because the line to the right of the tangent point is simply a crossing segment, which will not allow a solution to stay on or slide along the line. Therefore, the solution must cross the discontinuity line whenever it arrives at the line to the right of the tangent point.

From Figure 1 we see that there is a possibility of having a non-smooth solution with sliding. Again we have that the solution for $\varepsilon = 0$ approximates the solution for ε small to $\mathcal{O}(\varepsilon)$ on the time-scale 1. However, as in the previous example, a similar difficulty arises when we want to approximate the non-smooth solution with sliding.

It is possible to consider the equation (3.9) as the limit of a smooth equation, using a suitable order function $\delta(\varepsilon) \to 0$ as $\varepsilon \to 0$.

3.2.3. A remark on smoothing. In a number of cases it is possible to consider non-smooth systems as the limit of a smooth system. Consider the smooth equation

$$\ddot{x} + x = \varepsilon \frac{2}{\pi} \arctan(\frac{v - \dot{x}}{\delta(\varepsilon)}). \qquad (3.12)$$

The order function $\delta(\varepsilon)$ is positive if $\varepsilon > 0$ and has the properties that $\delta(\varepsilon) \to 0$ if $\varepsilon \to 0$ and $\delta(\varepsilon) = o(\varepsilon^n), n = 1, 2, \cdots$.

If $\varepsilon \to 0$, equation (3.12) tends to equation (3.10). A difference between the two equations is that, except if $\dot{x} = v$, the smooth equation (3.12) is slightly dissipative. We can correct this locally by introducing exponentially small terms. For instance near the critical point $(x, \dot{x}) = (\varepsilon \frac{2}{\pi} \arctan(\frac{v}{\delta(\varepsilon)}), 0)$ we can add to the equation the term

$$\varepsilon \frac{2}{\pi} \frac{\delta(\varepsilon)}{v^2 + \delta(\varepsilon)^2} \dot{x}.$$

The resulting equation is still not conservative like (3.10) but locally it will look conservative, especially as $\delta(\varepsilon)$ is exponentially small and can even be chosen smaller. We note that this inconsistency does not arise when discussing more realistic equations as in section 3.4.

Equations like (3.12) are studied in singular perturbation theory using slow manifolds; for an introduction see Jones [**27**]. In this case it would be natural to introduce the variable y by

$$\delta(\varepsilon)y = v - \dot{x},$$

which exhibits very fast motion except in and near the slow manifold given by $\dot{x} = v$. The transition between fast and slow motion is described by boundary layers, the size of which are proportional to $\delta(\varepsilon)$. So here the boundary layer contribution is smaller than any power of ε. In this way the solutions of (3.12) are expected to mimic the behaviour of the solutions of the non-smooth equation (3.10) very accurately.

The slow manifold is not (normally) hyperbolic so we cannot apply Fenichel theory. This is typical for equations resulting from smoothing. In general we have an n-dimensional problem with Σ_1 a single k-dimensional surface of discontinuity $(k < n)$. We assume that we can introduce local coordinates to describe Σ_1 after which we propose smoothing as in equation(3.12). Again Σ_1 will correspond with a slow manifold which is not (normally) hyperbolic.

It is easy to obtain approximations of the solutions of equation (3.12). Take for instance initial conditions $(x(0), \dot{x}(0)) = (x_0, 0)$. Away from the slow manifold i.e. at $O(1)$ distance, and if $\dot{x}(t) < v$, $x(t)$ is approximated by $\varepsilon + (x_0 - \varepsilon)\cos t$ plus exponentially small terms. If $\dot{x}(t)$ is ε-close to the slow manifold this approximation is still valid, if $\dot{x}(t)$ gets still nearer it helps to formulate the equivalent integral equation:

$$x(t) = x_0 \cos t + \varepsilon \frac{2}{\pi} \int_0^t \arctan(\frac{v - \dot{x}(\tau)}{\delta(\varepsilon)}) \sin(t - \tau) d\tau.$$

Partial integration of the integral expression produces local approximations near the slow manifold. A number of solutions of equation (3.12) are illustrated in Figure
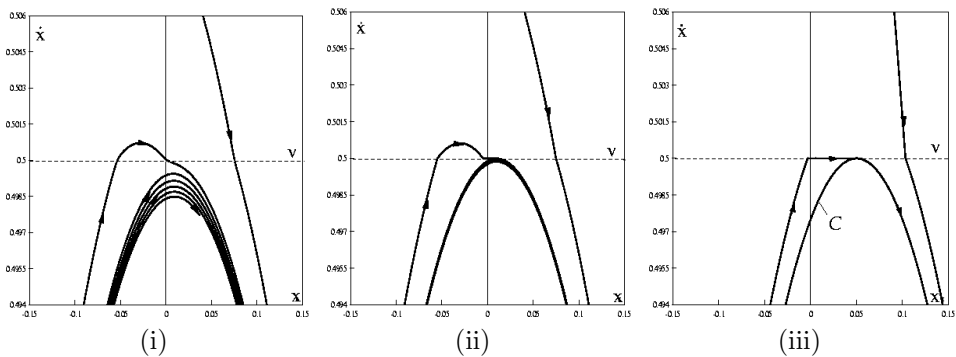
FIGURE 2. **Some solutions of equation (3.12)**. (i) for $\delta(\varepsilon) = \varepsilon^2$ with $\varepsilon = 0.07$, (ii) for $\delta(\varepsilon) = \varepsilon^3$ with $\varepsilon = 0.07$, (iii) for $\delta(\varepsilon) = e^{-\frac{1}{\varepsilon}}$ with $\varepsilon = 0.07$. $\mathcal{C}$ is the limiting circle and $\dot{x} = v = 0.5$ is the discontinuity boundary.

2. Considering equation (3.10) as a limiting case of equation (3.12) we note that smoothing confirms the analysis of the non-smooth system.

In Figure 2 we observe the phase portrait of the solution near the discontinuity boundary $\dot{x} = v = 0.5$; $\{(x, \dot{x}); -0.15 \leq x \leq 0.15, 0.494 \leq \dot{x} \leq 0.506\}$. Taking different functions for $\delta(\varepsilon)$, we can compare the closeness of the approximation of the solution of (3.12). For $\delta(\varepsilon) = \varepsilon^2$ with $\varepsilon = 0.07$ we obtain a smooth approximate solution of (3.12) which is, clearly, dissipative (Figure 2 (i)). However, by taking $\delta(\varepsilon) = \varepsilon^3$ with the same value of ε, we obtain a similar smooth solution but with small dissipation. This can be seen in Figure 2(ii) shown by a thick curve describing that by taking a longer time integration, the solution will collapse to the equilibrium of the equation. Furthermore, taking $\delta(\varepsilon) = e^{-\frac{1}{\varepsilon}}$, the approximate solution mimics the solution of equation (3.10) very nicely. This is described by Figure 2(iii) where we find a limiting circle $\mathcal{C}$, which corresponds with the limiting circle of equation (3.10) as shown in Figure 1.

We note that a comparison study for obtaining the periodic non-smooth solution numerically by smoothing and by implementing the shooting method to a switch model of the system can be found in [**37**].

3.2.4. The averaging method. To obtain asymptotic solutions of a differential equation, the classical averaging method requires at least Lipschitz continuity of the right-hand side of the differential equation. However, with some modifications in the theorems, we may still apply averaging to a system containing a discontinuity.

In [**40, 41**], Plotnikov considered a perturbation problem which is in the following standard form

$$\dot{\mathbf{y}} = \varepsilon \tilde{\mathbf{f}}(t, \mathbf{y}), \ \mathbf{y}(0) = y_0 \tag{3.13}$$

with $\mathbf{y}(t) \in \mathbf{D} \subset \mathbb{R}^n$, ε is a small positive parameter, and $\tilde{\mathbf{f}}$ is a vector function containing a discontinuity with respect to $\mathbf{y}$.

To approximate the solution of the initial value problem (3.13), it is sufficient to approximate the solution of its corresponding differential inclusion, which is of the following form

$$\dot{\mathbf{y}} \in \varepsilon \widetilde{\mathbf{F}}(t, \mathbf{y}), \ \mathbf{y}(0) = y_0, \tag{3.14}$$

with the same definitions of $\mathbf{y}$ and ε as before. $\tilde{\mathbf{F}}$ is assumed to be compact, T-periodic, continuous and uniformly bounded and satisfies the Lipschitz condition with respect to $\mathbf{y}$. In correspondence with the inclusion (3.14), one can consider the averaged inclusion

$$\dot{\xi} \in \varepsilon \widetilde{\mathbf{F}}^0(\xi), \ \ \xi(0) = y_0, \tag{3.15}$$

where

$$\widetilde{\mathbf{F}}^0(\xi) = \lim_{T \to \infty} \frac{1}{T} \int_0^T \widetilde{\mathbf{F}}(t, \xi) dt, \tag{3.16}$$

which is assumed to exist as well. Using the Hausdorff distance between two sets, P and Q:

$$\mathfrak{d}(P, Q) = \min \{ d \mid P \subset \mathcal{N}_d(Q), \ Q \subset \mathcal{N}_d(P) \},$$

where $\mathcal{N}_d(A)$ is the d-neighbourhood of the set $A \subset \mathbb{R}^n$, the author generalised the averaging theorem in the sense of differential inclusions. He showed the asymptotic relation between the solutions of (3.14) and (3.15) with the following estimate

$$\mathfrak{d}(\hat{\varrho}(t), \overline{\varrho}(t)) \le k\varepsilon, \ k \text{ constant}, \tag{3.17}$$

where $\hat{\varrho}(t)$ is a section of the family of solutions of the inclusion (3.15) and $\overline{\varrho}(t)$ is the closure of the section $\varrho(t)$ of the family of solutions of the inclusion (3.14).

Independently, Matveev et al. [38] constructed a similar result as above to show the applicability of the averaging method to approximate solutions of differential inclusions.

On the other hand, in [19] Fidlin treated a discontinuous system of the following form:

$$\dot{x} = \varepsilon X(x, t) + Z(z, t)[E(g(t) + \varepsilon f(x, t)) - E(g(t))], \ x(0) = x_0, \tag{3.18}$$

where E is a one-step function, and all the functions are continuous and T-periodic. By first showing that the right-hand side of the differential equation in (3.18) fulfils the Lipschitz condition in the integral sense, then applying Gronwall's lemma, averaging theorems are formulated and proven for such a system.

In [45], Samoilenko and Pere'styuk considered a differential equation system with impulsive action of the following form:

$$\begin{aligned}
\frac{dx}{dt} &= \varepsilon X(t, x), \text{ for } t \ne t_i \\
Dx|_{t=t_0} &= x(t_i + 0) - x(t_i - 0) = \varepsilon I_i(x),
\end{aligned} \tag{3.19}$$

where ε is a small parameter. By assuming that

$$\lim_{T \to \infty} \frac{1}{T} \int_t^{t+T} X(\tau, x) d\tau = X_0(x), \ \lim_{T \to \infty} \frac{1}{T} \sum_{t < t_i < t+T} I_i(x) = I^0(x)$$

exist and are finite uniformly with respect to $t \in (-\infty, \infty)$, $x \in \mathcal{D} \subset \mathbb{R}^n$, equation (3.19) has the corresponding averaged system

$$\frac{dx}{dt} = \varepsilon[X_0(x) + I^0(x)]. \tag{3.20}$$

Using a special transformation of the original variables and making use of the asymptotic method of Krylov-Bogoliubov-Mitropolsky, they proved a theorem that the equilibrium point of (3.20), for small ε, corresponds with a periodic solution of (3.19). In [**44**] the authors considered a more general system which is subjected to an impulse every time it passes a particular position, e.g. $x = x_0$, with a nonnegative velocity. By first transforming the system into a system with impulsive action for specific times t_i as formulated by (3.19), the averaging method again applies and a similar asymptotic validity theorem was constructed.

The applicability of the averaging method for systems with discontinuities is surprising, as the method requires at least Lipschitz continuity of the function in the considered systems. Some important assumptions have been made in [**19, 38, 40, 41, 45, 44**], in order to guarantee the applicability of the averaging method. That is, one should know a priori when the discontinuity jumps occur and one should assume that the size of the jump is small. These kind of assumptions are all we need to tackle the difficulties arise when applying the concept of differential inclusion and the variation of constants explained earlier. However, to obtain the standard forms to be analysed, one still needs to construct the generalised Green's function to invert the operator.

We are now ending up with the question on how to treat systems with discontinuities, for which we do not know a priori when the jumps occur and for which the size of the jump is not necessarily small. In the sequel we consider such a system which is also of practical importance.

3.3. Solutions of systems with dry friction

To start with, we consider first a planar system of the Filippov type which has two subspaces of continuity $\mathcal{V}_i$, $i = 1, 2$, i.e.

$$\dot{x} = \begin{cases} f_1(x), & x \in \mathcal{V}_1 \\ f_2(x), & x \in \mathcal{V}_2 \end{cases} \tag{3.1}$$

where f_i are smooth and C^1 on $\mathcal{V}_i \cup \Sigma$, and Σ is a discontinuity boundary, separating the two subspaces;

$$\Sigma = \{x \in \mathbb{R}^2 \mid h(x) = 0\}$$

where h is a smooth scalar function with $\nabla(h(x)) \neq 0$ on Σ. Therefore, the subspaces $\mathcal{V}_i$ can be formulated as follows:

$$\mathcal{V}_1 = \{x \in \mathbb{R}^2 \mid h(x) > 0\} \text{ and } \mathcal{V}_2 = \{x \in \mathbb{R}^2 \mid h(x) < 0\}.$$

Due to the presence of the discontinuity boundary between the two subspaces, the solution of system (3.1) does not really follow the usual analysis of solutions of systems with a continuous right-hand side.

Solutions that are initially started from one of the domains $\mathcal{V}_i$ are obtained by solving one-sided differential equations in (3.1), depending on where they are. However, as soon as solutions reach the discontinuity boundary Σ, there is a lack of information on how solutions may be continued.

For simplicity reasons, we assume that Σ is a smooth curve in the phase plane, dividing $\mathbb{R}^2$ into the subsets $\mathcal{V}_1$ and $\mathcal{V}_2$. For the point x^* approaching the point $x \in \Sigma$, let

$$\lim_{x^* \to x, x^* \in \mathcal{V}_1} f_1(x^*) = f_+(x), \ \lim_{x^* \to x, x^* \in \mathcal{V}_2} f_2(x^*) = f_-(x).$$

Then, either of the following conditions can take place.

    A. $n^T f_+(x).n^T f_-(x) > 0$, or
    B. $n^T f_+(x).n_T{}^f_-(x) < 0$, or
    C. $n^T f_+(x).n^T f_-(x) = 0$,

where n is the normal vector of the curve Σ. $n^T f_+(x)$ and $n^T f_-(x)$ are the projections of $f_+(x)$ and $f_-(x)$, respectively, on the normal vector of the curve Σ at the point x.

Now, we are ready for the construction of solutions of the system (3.1). Taking $x(0) \in \mathcal{V}_1$, the solution $x(t)$ can be determined by solving the corresponding equation $\dot{x} = f_1(x)$. As the solution reaches the line Σ at $t = t_1$, either of the three conditions above must hold and a concatenation of the solution is undertaken.

Condition A implies that the vector fields in the limit approaching Σ have the same sign. The condition assigns the solution undergoes crossing off the curve Σ at $x(t_1)$. Then, we switch to the equation $\dot{x} = f_2(x)$ in $\mathcal{V}_2$ and solve it to obtain the continuation of the solution for $t \geq t_1$. This is usually called the *slip phase* or *crossing solution*.

Condition B implies two possible cases. The first case is the case of $n^T f_+(x(t_1)) > 0$, $n^T f_-(x(t_1)) < 0$, which assigns the condition that the solution cannot leave the curve Σ as t increases. By using the Filippov convex method (see [20]), the continuation of the solution so obtained is a part of Σ described by

$$g(x) = \beta f_+(x) + (1 - \beta) f_-(x), \ \beta = \frac{n^T f_-(x)}{n^T (f_-(x) - f_+(x))}, \quad (3.2)$$

where $x \in \Sigma$. Thus, we are in the so-called *stick phase* or *attracting sliding solution*. Then we have the case of $n^T f_+(x(t_1)) < 0$, $n^T f_-(x(t_1)) > 0$, which assigns the condition that the solution may go off the line Σ at any moment. The solution is not unique in forward time. Therefore, the curve Σ is unstable and it is called a *repulsing sliding solution*. We will not look at this kind of solution.

Condition C assigns the condition when either at least one of the vectors f_i is tangent to Σ at $x(t_1)$, or one of the vectors f_i is equal to zero at $x(t_1)$. With regard to the system considered later in this paper, we restrict ourselves to only considering the case that f_i are non-zero vectors and only one of them is tangent to Σ. This point is called a *singular point* or a *tangent point*.

3.3.1. Periodic solutions. There are some methods for the construction of a periodic solution of system (3.1). A discussion on the topic can be found in [20], or in [36] for a more recent one. However, regarding the system considered in this paper,
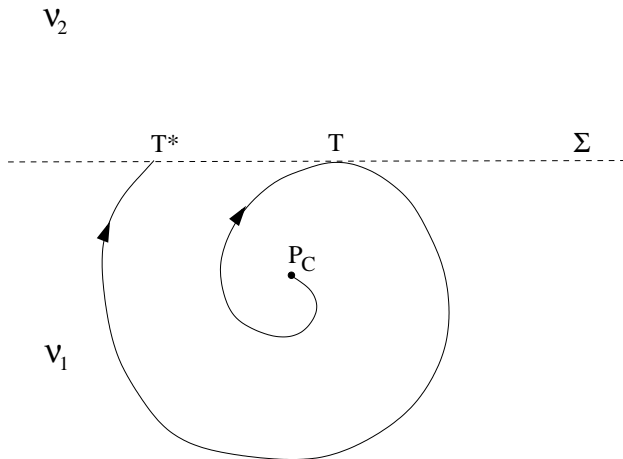
ν_2

T*   T Σ

P_C

ν_1

FIGURE 3. **The unstable focus**.

we only present the following general setting for the construction of the periodic solution.

Consider the planar system $\dot{x} = f_1(x)$ in $\mathcal{V}_1$. Assume that the discontinuity boundary Σ is a horizontal line in the phase plane and the system has a hyperbolic equilibrium of focus type. Let the focus be unstable, then a periodic solution can be constructed by the mechanism described in Figure 3.

The trajectory which lies in $\mathcal{V}_1$ may result in the construction of a closed orbit, corresponding to a periodic solution of system (3.1). However, it depends solely upon the behaviour of the vector field in $\mathcal{V}_2$. This brings us to the question on how the trajectory in $\mathcal{V}_1$ will be continued, after it crosses Σ to enter $\mathcal{V}_2$. That is, we shall determine which one of the three conditions mentioned earlier holds for the continuation.

We are going to continue the solution from T^*. Since P_c is an unstable focus, right after the solution is tangent to the discontinuity line at point T, where condition C holds, the next hit of the solution to the discontinuity line, at point T^*, cannot be a tangent point in $\mathcal{V}_1$ again. Thus, we cannot have a closed orbit which entirely lies in $\mathcal{V}_1$. Since point $T^* \in \Sigma$, either condition A or condition B must hold.

Suppose that at point T^* condition A holds. As a result, we have a slip phase at point T^*. Then, in order to obtain a closed orbit, the following additional condition must be satisfied. That is, the next hit of the orbit to the discontinuity line Σ, for instance at point TS, is such that it does not exceed to the right of point T (Otherwise, there will not be any periodic solution obtained). Again, since point $TS \in \Sigma$, either condition A or condition B must hold, depending on where it is. Condition A holds at point TS, if point TS coincides with point T. Then, the solution immediately slips and comes into $\mathcal{V}_1$. Thus, a non-smooth closed orbit without sliding, i.e. *crossing cycle*, is constructed. Condition B holds at point TS, if point TS is between point T^* and point T. Thus, a stick phase or sliding solution takes place and the solution is given by equation (3.2). Eventually, the sliding

solution tends to point T where the solution slips and comes into $\mathcal{V}_1$ again. Thus, a closed orbit with sliding, i.e. *sliding cycle*, is obtained.
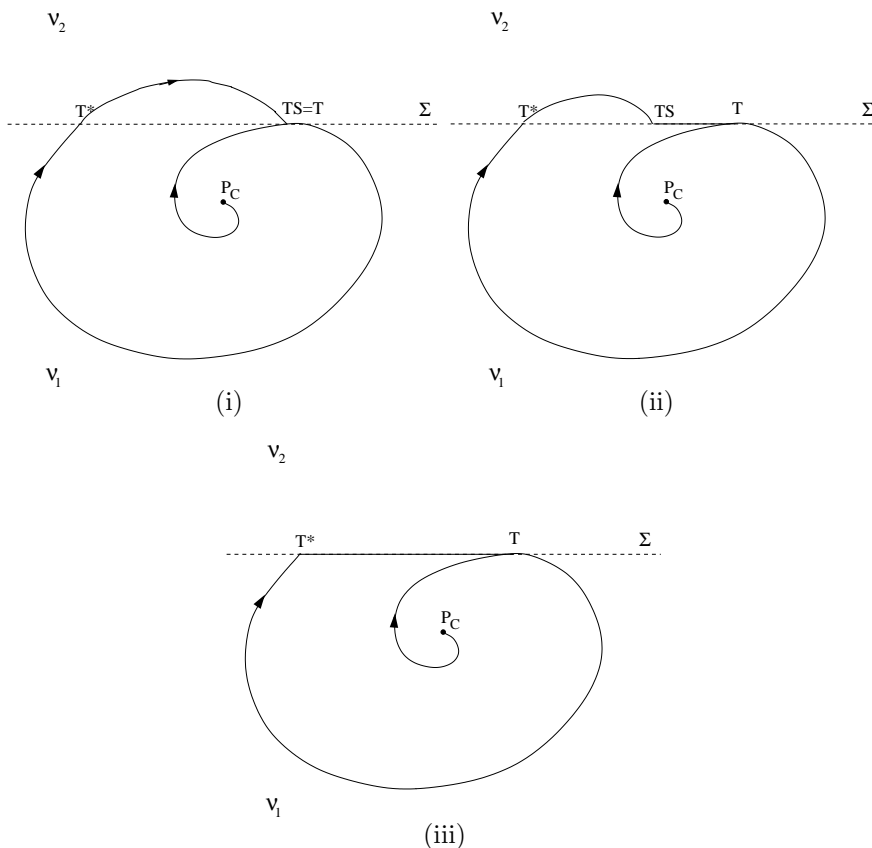

FIGURE 4. **The non-smooth periodic solution**. (i) and (ii) when condition A holds at point T^*. (iii) when condition B holds at point T^*.

If at point T^* condition B holds, the solution immediately experiences a stick phase or sliding solution that is derived from equation (3.2). Thus, there is a concatenation of the orbit approaching point T^* from $\mathcal{V}_1$ with the sliding segment. Then, along the sliding segment the orbit tends to point T, and then immediately slips and backs to point T^*. Thus, another type of sliding cycle is constructed. Figure 4 clearly illustrates the closed orbits so obtained, which are, in fact, non-smooth with or without sliding due to the concatenation of the solution at the line of discontinuity.

The presence of the sliding segment as a part of the periodic solution of the system prevents us to apply any of the asymptotic methods explained in section 3.2. A special study is still needed to apply the concept of differential inclusion or
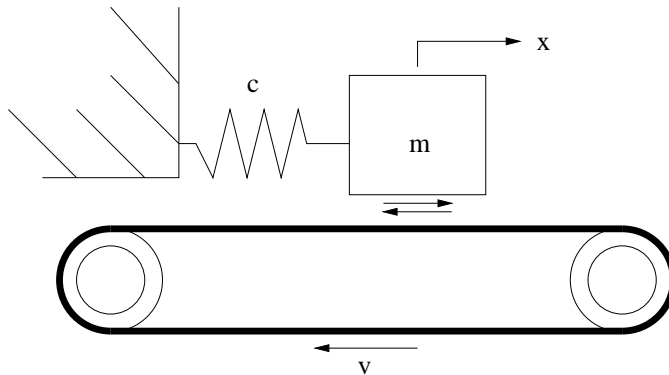
FIGURE 5. **The model of oscillator with dry friction**.

Lagrange's variation of constants, in order to approximate such a solution. (a similar situation happened when treating Example 1 of section 3.2). Also, we cannot apply the averaging method as in [**38, 40, 41, 45, 44, 19**], since we do not know explicitly when the jumps due to the discontinuity in the system occur.

In the following section, where the main application of this paper is discussed, we show that to study the solutions of the problem we shall follow the analysis of non-smooth solutions explained above. Moreover, a bifurcation analysis of the solution obtained will be carried out numerically.

3.4. The self-excited autoparametric system

Having some insight into the periodic solutions of systems with dry friction, we are now ready to consider our autoparametric system. We begin with a well-known prototype of an oscillator with self-excited oscillations induced by relative dry friction: Consider a mass m resting on a continuous conveyor belt moving at constant speed v, the mass being held near the equilibrium position by a linear spring with stiffness c. Let the mass be acted upon by an absolute dry friction damper. See Figure 5 for an illustration.

When the belt moves, the equilibrium position is unstable. When the static friction force, which is a function of the spring force cx, reaches its maximum value, the mass oscillates on the belt. Then, self-excited vibrations of the mass arise when the absolute magnitude of the 'kinetic' friction force is a decreasing function of the relative velocity $v - \dot{x}$, where $\dot{x}$ is the velocity of the mass.

Such a motion described above will act as an oscillator in the self-excited autoparametric system considered in this paper. To this purpose, we suppose the oscillator (x mode) on the belt is nonlinearly coupled to a damped oscillator (y mode). The system is represented by the following differential equations, after transforming the equations into dimensionless form,

$$\begin{aligned}
x'' + x &= F(v - x') - \gamma_1 y^2 \\
y'' + \frac{1}{4}y &= -(\kappa y' + \sigma y + \gamma_2 xy),
\end{aligned} \tag{3.1}$$

where $F(v - x')$ has a discontinuity when $v = x'$. The simplest case is by considering $F(v - x')$ as a function of the following form.

$$F(v - x') = \alpha_0 \operatorname{sgn}(v - x') - \alpha_1(v - x'), \ \alpha_0, \ \alpha_1 > 0,$$

where sgn is the signum function.

Assuming that the parameters are small, we rescale all the parameters of the system: $\alpha_0 = \varepsilon\bar{\alpha}_0$, $\alpha_1 = \mu\bar{\alpha}_1$, $\kappa = \delta\bar{\kappa}$, $\sigma = \delta\bar{\sigma}$, $\gamma_1 = \delta\bar{\gamma}_1$, $\gamma_2 = \delta\bar{\gamma}_2$, where ε, μ, and δ are small positive parameters which may be different in order. Substituting these into (3.1), then, after dropping the bars, we obtain the following:

$$\begin{aligned}
x'' + x &= \varepsilon\alpha_0 \operatorname{sgn}(v - x') - \mu\alpha_1(v - x') - \delta\gamma_1 y^2 \\
y'' + \frac{1}{4}y &= -\delta(\kappa y' + \sigma y + \gamma_2 xy).
\end{aligned} \tag{3.2}$$

3.4.1. The semitrivial solution. The analysis in this section is related to some results in Galvanetto and Bishop [**21**]. The semitrivial solution of system (3.2) is defined by putting $y = 0$. Thus, we analyse the equation:

$$x'' + x = \varepsilon\alpha_0 \operatorname{sgn}(v - x') - \mu\alpha_1(v - x'). \tag{3.3}$$

Writing (3.3) in vector form by putting $x = x_1$, $x' = x_2$, we find the planar linear system

$$\mathbf{x}' = \begin{pmatrix} x_1' \\ x_2' \end{pmatrix} = \begin{cases} f_1(\mathbf{x}), \ v > x_2 \\ f_2(\mathbf{x}), \ v < x_2, \end{cases} \tag{3.4}$$

where

$$f_1(\mathbf{x}) = \begin{pmatrix} x_2 \\ -x_1 + \varepsilon\alpha_0 + \mu f_0 \end{pmatrix}, \ f_2(\mathbf{x}) = \begin{pmatrix} x_2 \\ -x_1 - \varepsilon\alpha_0 + \mu f_0 \end{pmatrix},$$

with $f_0 = -\alpha_1(v - x_2)$.

Since we are interested in solutions that can undergo self-excitation, we investigate the existence of periodic solutions of the system. Thus, we need to analyse the vector fields in both domains $\mathcal{V}_1$ and $\mathcal{V}_2$ where $v > x_2$ and $v < x_2$, respectively.

Assume first that $v > x_2$ holds. So, we are dealing with the system

$$\begin{aligned}
x_1' &= x_2 \\
x_2' &= -x_1 + \varepsilon\alpha_0 - \mu\alpha_1(v - x_2).
\end{aligned} \tag{3.5}$$

A straightforward calculation gives the result that system (3.5) has a critical point $P_1 = (\varepsilon\alpha_0 - \mu\alpha_1 v, 0)$. Linearisation in a neighbourhood of point P_1 leads to eigenvalues of the following form

$$\lambda_{1,2} = \frac{\mu\alpha_1 \pm \sqrt{\mu^2\alpha_1^2 - 4}}{2}. \tag{3.6}$$

From (3.6) we conclude that P_1 is an unstable focus. Moreover, by taking $x'_2 = 0$, we have the line l_1 passing points P_1 and $T_1(\varepsilon\alpha_0, v)$, where trajectories in $\mathcal{V}_1$ have zero derivatives. (See Figure 6.)

Similarly, assuming that $v < x_2$ holds, we obtain the corresponding critical point $P_2 = (-\varepsilon\alpha_0 - \mu\alpha_1 v, 0)$, having the same stability characteristic as point P_1. Also, we have the line l_2 passing points P_2 and $T_0(-\varepsilon\alpha_0, v)$, where trajectories in $\mathcal{V}_2$ have zero derivatives. Note that by assuming $\alpha_0 > 0$, $\alpha_1 > 0$, $v > 0$, the positions of point P_2 and line l_2 are to the left of point P_1 and line l_1, respectively. (See Figure 6.)

The calculation above provides the information that trajectories in domain $\mathcal{V}_1$ are influenced by the presence of point P_1, which is unstable, and hence line l_1 in the domain, provided that the mechanism described in Figure 3 might follow. The trajectory started from point P_1 is winding away from the point until it arrives at its tangent point T_1 with the discontinuity line $\Sigma \equiv v - x_2 = 0$ and at its next hit T_1^* to the line. On the other hand, in domain $\mathcal{V}_2$ the presence of point P_2 and line l_2 play a role to the flow in the domain, and hence to the continuation of the solution from point T_1^* entering $\mathcal{V}_2$.

The continuation of the solution starting from point T_1^* depends upon the position of the point with respect to the lines l_1 and l_2. If point T_1^* is to the left of line l_2, there are three possibilities to have a continuation of the solution to be concatenated at point T_1^*. Due to the property of point P_2 and the presence of line l_2, a trajectory starting from point T_1^* sooner or later will hit line Σ, whether exactly at point T_1, at a point between points T_0 and T_1, the intersection between Σ and, respectively, l_2 and l_1, or at a point to the right of point T_1. To the first case, a crossing cycle of Figure 4 (i) type is obtained. In the second case, right after the trajectory hits line Σ, for instance at point T_2, the continuation of the solution will experience a sliding solution. Thus, we obtain a sliding cycle of Figure 4 (ii) type. While the last case implies no periodic solution can be obtained.

If point T_1^* coincides with point T_0, we have a sliding cycle of Figure 4 (iii) type consisting of sliding segment T_0T_1. Similarly, the same type of sliding cycle so obtained, If point T_1^* is between points T_0 and T_1 (or between lines l_2 and l_1). Figure 6 illustrates the construction of all possible periodic solutions described above.

The constructions of non-smooth periodic solutions described in Figure 6 leads us to the bifurcation analysis of the periodic solution of system 3.4. One can notice that the cases described in Figure 6(i) and Figure 6(iii) are critical cases where the periodic solution bifurcate. Thus, we are studying so-called *sliding bifurcations*.

3.4.2. The boundary case of the sliding periodic solution. The boundary case of equation 3.4 for certainly having a sliding periodic solution is described by Figure 6(i). In the following, we derive such a boundary by calculating the critical value of parameters from which we are able to conclude the existence of the periodic solution consisting of a sliding segment.
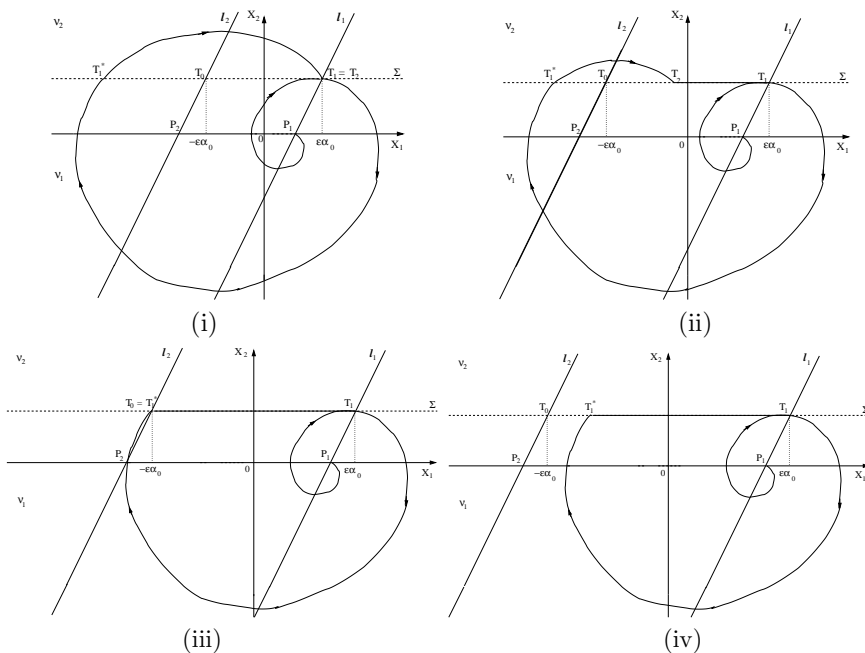
(i)   (ii)

(iii)   (iv)

FIGURE 6. **The possible construction of periodic solutions** .
(i) The case when T_2 coincides with T_1. (ii) The case when T_2 is
between T_0 and T_1. (iii) The case when T_1^* coincides with T_0. (iv)
The case when T_1^* is between T_0 and T_1. l_1 and l_2 are the lines
where the trajectories in $\mathcal{V}_1$ and $\mathcal{V}_2$, respectively, have zero deriva-
tives.

Solving $\mathbf{x}' = f_1(\mathbf{x})$ with point $T_1(\varepsilon\alpha_0, v)$ as the initial condition, we obtain

$$
x_1(t) = \mu\alpha_1 v e^{\frac{1}{2}\mu\alpha_1 t} \cos(\frac{1}{2}\sqrt{4 - \mu^2\alpha_1^2}t) + \frac{(2 - \mu^2\alpha_1^2)v}{\sqrt{4 - \mu^2\alpha_1^2}} e^{\frac{1}{2}\mu\alpha_1 t} \times \\
\sin(\frac{1}{2}\sqrt{4 - \mu^2\alpha_1^2}t) + \varepsilon\alpha_0 - \mu\alpha_1 v. \tag{3.7}
$$

We know that $x_1'(t) = v$, for some $t = t_1^*$; i.e.

$$
v e^{\frac{1}{2}\mu\alpha_1 t_1^*} \cos(\frac{1}{2}\sqrt{4 - \mu^2\alpha_1^2}t_1^*) - \frac{\mu\alpha_1 v}{\sqrt{4 - \mu^2\alpha_1^2}} e^{\frac{1}{2}\mu\alpha_1 t_1^*} \sin(\frac{1}{2}\sqrt{4 - \mu^2\alpha_1^2}t_1^*) = v. \tag{3.8}
$$

Suppose that $t_1^* = 2\pi - \triangle t$, then Taylor expand (3.8) with respect to μ and $\triangle t$, we
have (neglecting the higher order terms)

$$
-\frac{1}{2}(1 + \mu\alpha_1\pi + \frac{3}{8}\mu^2\alpha_1^2)\triangle t^2 + \frac{1}{8}\mu^2\alpha_1^2(2\pi - 1)\triangle t + \mu\alpha_1\pi + \frac{1}{4}\mu^2\alpha_1^2\pi = 0.
$$

Solving the last equation for $\triangle t$, we obtain:

$$\triangle t = \frac{1}{8}\mu^2\alpha_1^2(2\pi - 1) \pm \sqrt{2\mu\alpha_1\pi + \frac{5}{2}\alpha_1^2\pi^2\mu^2 + \mathcal{O}(\mu^3)}. \qquad (3.9)$$

By taking the positive sign in (3.9) and plugging $t_1^* = 2\pi - \triangle t$ into (3.7), Taylor expansion of the equation with respect to μ and $\triangle t$, results in:

$$x_1(t_1^*) = -v\sqrt{2\mu\alpha_1\pi} + \varepsilon\alpha_0 - \mu\alpha_1 v\pi\sqrt{2\mu\alpha_1\pi} - \frac{5}{4}\mu^2\alpha_1^2 v\pi + \text{ h.o.t.} \qquad (3.10)$$

Having the coordinate of point T_1^*, we continue by concatenating the obtained solution with the solution in the other domain. Thus, we switch to domain $\mathcal{V}_2$ and solve $\mathbf{x}' = f_2(\mathbf{x})$ with point $T_1^*(x_1(t_1^*), v)$ as the initial condition. Therefore, we proceed the calculation to obtain:

$$\begin{aligned} x_2(t) &= C_1 e^{\frac{1}{2}\mu\alpha_1 t}\cos(\frac{1}{2}\sqrt{4 - \mu^2\alpha_1^2}t) + C_2 e^{\frac{1}{2}\mu\alpha_1 t}\sin(\frac{1}{2}\sqrt{4 - \mu^2\alpha_1^2}t) \\ &\quad - \varepsilon\alpha_0 - \mu\alpha_1 v, \end{aligned} \qquad (3.11)$$

where $C_1 = x_1(t_1^*) + \varepsilon\alpha_0 + \mu\alpha_1 v$, and $C_2 = \frac{2v - \mu\alpha_1 C_1}{\sqrt{4 - \mu^2\alpha_1^2}}$.

Similarly as before, we are looking for some $t = t_1$ such that $x_2'(t_1) = v$. Thus, after Taylor expansion with respect to μ, we have

$$\begin{aligned} &(-\frac{1}{2}v - \varepsilon\mu\alpha_0\alpha_1 + \frac{1}{2}\mu\alpha_1 v\sqrt{2\mu\alpha_1\pi} - \frac{1}{2}\mu^2\alpha_1^2 v)t_1^2 \\ &\quad + (v\sqrt{2\mu\alpha_1\pi} - 2\varepsilon\alpha_0 + \mu\alpha_1 v\pi\sqrt{2\mu\alpha_1\pi} + \frac{5}{4}\mu^2\alpha_1^2 v\pi)t_1 + \text{h.o.t} = 0. \quad (3.12) \end{aligned}$$

Neglecting the higher order terms, we solve (3.12) for t_1; $t_1 = 0$ or

$$t_1 = \frac{2\varepsilon\alpha_0 - v\sqrt{2\mu\alpha_1\pi} - \mu\alpha_1 v\pi\sqrt{2\mu\alpha_1\pi} - \frac{5}{4}\mu^2\alpha_1^2 v\pi}{-\frac{1}{2}v - \varepsilon\mu\alpha_0\alpha_1 + \frac{1}{2}\mu\alpha_1 v\sqrt{2\mu\alpha_1\pi} - \frac{1}{2}\mu^2\alpha_1^2 v}. \qquad (3.13)$$

Since we are interested in periodic solutions of system (3.3), the condition that

$$x_2(t) \leq \varepsilon\alpha_0, \ t_1^* < t < t_1 \qquad (3.14)$$

must hold. Substituting the latter value of t_1 in (3.13) into (3.11) and apply the inequality (3.14), we have the following relation:

$$\mu \leq \mu_0, \qquad (3.15)$$

where $\mu_0 \approx \frac{-v + \sqrt{v^2 + 64\alpha_0^2\varepsilon^2}}{4\alpha_1 v\pi}$ which gives the boundary value for parameter μ where a periodic solution consisting of a sliding segment of system (3.4) may take place.

3.4.3. Bifurcation analysis using SLIDECONT**.** To perform bifurcation analysis for the solutions of system of the form (3.3), which consists of discontinuities, we apply SLIDECONT, a recent software package by Dercole and Kuznetsov [10]. SLIDE-CONT is a suite of routines accompanying AUTO97 (see [11]) for sliding bifurcation analysis of discontinuous piecewise-smooth autonomous systems.

We start the computation using SLIDECONT by providing data files which specify numerically the starting solution. We take the non-smooth periodic solution of Figure 6(ii) type, as our starting solution, by fixing the parameter values: $\varepsilon =$

0.1, $\mu = 0.07$, $\alpha_0 = 4$, $\alpha_1 = 4, v = 0.5$, with the initial point $T_1(0.4, 0.5)$. At these particular values, in fact, the periodic solution is coexisted with an exponentially unstable crossing cycle which will be continued separately. After providing the suitable constants file required by SLIDECONT for such a problem, we continue our starting periodic solution for increasing values of μ (PAR(2)). We get the following output

```
BR   PT  TY LAB   PAR(2)        PAR(11)       PAR(12)       PAR(25)       PAR(26)
1    40       2 7.577569E-02 5.093463E+00  9.284519E-01 -5.375930E-01  2.624070E-01
1    80       3 8.477924E-02 5.047204E+00  1.308431E+00 -3.868472E-01  4.131528E-01
1   120       4 9.479559E-02 5.002518E+00  1.673162E+00 -1.834290E-01  6.165710E-01
1   148  UZ  5 1.023117E-01 4.973173E+00  1.903980E+00 -2.747659E-10  8.000000E-01
1   160       6 1.057707E-01 4.960783E+00  1.998549E+00  9.477795E-02  8.947780E-01
1   200  EP  7 1.175286E-01 4.923548E+00  2.272102E+00  4.743172E-01  1.274317E+00
```

We provide another data files for the starting solution of the unstable crossing cycle. Taking the same parameter values as above and after providing the suitable constants file required by SLIDECONT for such a problem, the continuation of the cycle for increasing values of μ (PAR(2)) gives the following output.

```
BR   PT  TY LAB   PAR(2)        PAR(11)       PAR(12)       PAR(21)       PAR(22)
1    40       2 7.650734E-02 3.886142E+00  2.508395E+00  9.353822E-01  1.735382E+00
1    80       3 8.721882E-02 4.060236E+00  2.392258E+00  6.606936E-01  1.460694E+00
1   120       4 9.729280E-02 4.292873E+00  2.252847E+00  4.142413E-01  1.214241E+00
1   160       5 1.035993E-01 4.577489E+00  2.100710E+00  2.079071E-01  1.007907E+00
1   180  LP  6 1.044549E-01 4.730361E+00  2.024133E+00  1.205938E-01  9.205938E-01
1   200       7 1.035279E-01 4.890144E+00  1.945318E+00  3.947016E-02  8.394702E-01
1   211  UZ  8 1.023117E-01 4.973173E+00  1.903980E+00 -1.028633E-11  8.000000E-01
1   240       9 9.613130E-02 5.206056E+00  1.781395E+00 -1.060742E-01  6.939258E-01
1   250  EP 10 9.307145E-02 5.284681E+00  1.735776E+00 -1.416944E-01  6.583056E-01
```

Note that UZ and EP indicate, respectively, a bifurcation point and an endpoint, LP indicates a saddle-node bifurcation point. PAR(11) and PAR(12) are the time length needed for the passage through, respectively, domains $\mathcal{V}_1$ and $\mathcal{V}_2$, PAR(20+k) assigns the test function k. (See [**10**] for all details about SLIDECONT).

Label **5** (in accordance with label **8**) indicates a *crossing* bifurcation [**36**], i.e. a crossing orbit of vector fields in $\mathcal{V}_1$ and $\mathcal{V}_2$ connecting two tangent points of the same vector field in $\mathcal{V}_1$. (zero of test function 5 (PAR(25))).
Label **6** indicates a saddle-node bifurcation of the cycles; two cycles collide and a new cycle with different stability property takes place.
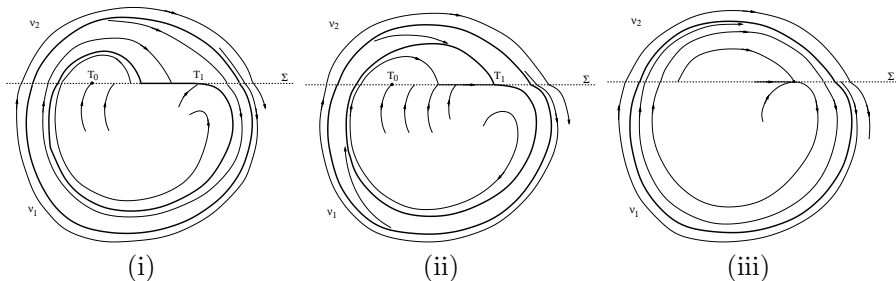

FIGURE 7. **The crossing bifurcation**.

One can notice that the value of μ (PAR(2)) at label **5** corresponds with the boundary value $\mu = \mu_0$ obtained previously, when the critical case described by

Figure 6(i) occurs. Note also that due to some truncations in calculation presented in subsection 3.4.2, the value of μ_0 obtained earlier is quite different from that obtained numerically.

Figure 7 clearly illustrates the phenomenon of the existence of the periodic solution and its bifurcation. Taking $\mu < \mu_0$ there exists a stable sliding cycle coexisting with an exponentially unstable crossing cycle (Figure 7 (i)). Figure 7(ii) is the boundary case $\mu = \mu_0$, when the sliding cycle becomes a stable crossing cycle, while the unstable crossing cycle still coexists. Taking $\mu_0 < \mu < 0.104455\cdots$, the two cycles comes closer to each other, until they collide when $\mu = 0.104455\cdots$, where the saddle-node bifurcation occur; a new crossing cycle which is stable from inside but unstable from outside takes place (Figure 7(iii)).

Note that taking $\mu > 0.1044055\cdots$ there is no more attractor.

Continuing the same starting periodic solution for decreasing value of μ (`PAR(2)`) and taking the same values of the other parameters as before, we get the following output

```
BR   PT  TY LAB    PAR(2)     ...     PAR(11)       PAR(23)         PAR(24)
1    20       2  6.408450E-02 ... 5.163572E+00 -8.967644E-01 -9.676436E-02
1    28  UZ   3  5.573552E-02 ... 5.221891E+00 -8.000000E-01  2.504543E-10
1    40       4  4.394584E-02 ... 5.319004E+00 -6.674277E-01  1.325723E-01
1    60       5  2.759741E-02 ... 5.494567E+00 -4.850706E-01  3.149294E-01
1    80       6  1.540296E-02 ... 5.679865E+00 -3.394173E-01  4.605827E-01
1   100  EP   7  6.992006E-03 ... 5.869885E+00 -2.183029E-01  5.816971E-01
```

and the corresponding output of the continuation of the unstable crossing cycle is as follows

```
BR  PT  TY LAB    PAR(2)       PAR(11)       PAR(12)       PAR(21)       PAR(22)
1   40       2  6.410177E-02  3.725900E+00  2.625593E+00  1.323278E+00  2.123278E+00
1   80       3  5.673113E-02  3.643200E+00  2.690173E+00  1.616141E+00  2.416141E+00
1  120       4  5.071809E-02  3.580562E+00  2.740972E+00  1.909066E+00  2.709066E+00
1  160       5  4.577884E-02  3.531709E+00  2.781720E+00  2.201174E+00  3.001174E+00
1  200       6  4.167504E-02  3.492618E+00  2.815033E+00  2.492262E+00  3.292262E+00
1  240       7  3.822340E-02  3.460656E+00  2.842735E+00  2.782363E+00  3.582363E+00
1  250  EP   8  3.744541E-02  3.453557E+00  2.848944E+00  2.854746E+00  3.654746E+00
```

Label 3 indicates a *switching (buckling)* bifurcation [36], i.e. the presence of an orbit of vector field in $\mathcal{V}_1$ connecting a tangent point of $\mathcal{V}_1$ with a tangent point of $\mathcal{V}_2$. (zero of test function 4 (`PAR(24)`)). This corresponds to the critical case described by Figure 6(iii).
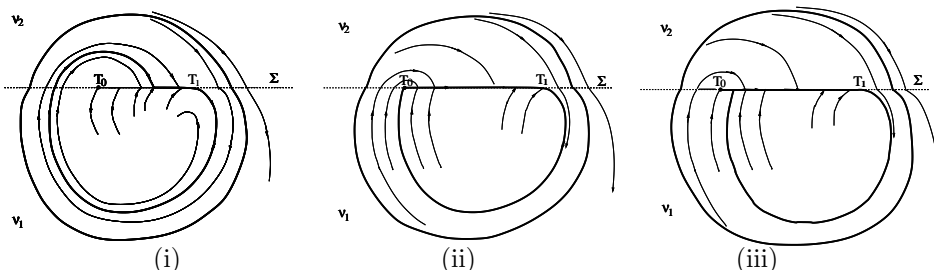

(i)   (ii)   (iii)

FIGURE 8. **The switching (buckling) bifurcation**.

On the other hand, continuation of the unstable crossing cycle for decreasing values of μ only shows the persistence of the unstable cycle coexisting with the sliding cycle due to the switching bifurcation explained previously. The cycle grows bigger as μ decreases.

Figure 8 illustrates the bifurcation of the sliding cycle and the persistence of the unstable crossing cycle.

For the analysis of co-dimension 1 sliding bifurcations of planar systems, see [**36**].

3.4.4. The nontrivial solution. As in the semitrivial case, we cannot apply the standard techniques of Poincarè expansion or averaging explained in section 3.2. And unfortunately, neither can we apply SLIDECONT to perform bifurcation analysis for the nontrivial case. This is because of the difficulty in providing the starting solution that is required by SLIDECONT; we could do this in the semitrivial case. However, it is still possible to perform a qualitative analysis regarding the solutions of the full system. In addition, a numerical integration consisting of a routine which allows an automatic switch between the two domains might also be performed to provide us a confirmation for the analytical calculation.

From the previous calculation, for having a solution with a sliding segment, we may take $\mu = \varepsilon^2 < \mu_0$. Thus, system (3.2) becomes:

$$
\begin{aligned}
x'' + x &= \varepsilon\alpha_0 \,\mathrm{sgn}\,(v - x') - \varepsilon^2\alpha_1(v - x') - \delta\gamma_1 y^2 \\
y'' + \frac{1}{4}y &= -\delta(\kappa y' + \sigma y + \gamma_2 xy).
\end{aligned}
\tag{3.16}
$$

Since we do not know the order of δ, to study (3.16) we consider two cases; the case of $\delta = \varepsilon^2$ and the case of $\delta = \varepsilon$.

3.4.4.1. **The case of $\delta = \varepsilon^2$.** Taking $\delta = \varepsilon^2$, we have:

$$
\begin{aligned}
x'' + x &= \varepsilon\alpha_0 \,\mathrm{sgn}\,(v - x') - \varepsilon^2(\alpha_1(v - x') + \gamma_1 y^2) \\
y'' + \frac{1}{4}y &= -\varepsilon^2(\kappa y' + \sigma y + \gamma_2 xy).
\end{aligned}
\tag{3.17}
$$

Assuming that we are in the domain where $v > x'$, then we can approximate the solution of the system in the domain. First, let $x = \varepsilon\alpha_0 - \varepsilon^2\alpha_1 v + r_1\cos(\tau + \psi_1)$, $x' = -r_1\sin(\tau + \psi_1)$, $y = r_2\cos(\frac{1}{2}\tau + \psi_2)$, $y' = -\frac{1}{2}r_2\sin(\frac{1}{2}\tau + \psi_2)$. Then, applying averaging over τ to second order in ε, we obtain the following averaged system (after introducing the phase-difference $\phi = \psi_1 - 2\psi_2$)

$$
\begin{aligned}
r_1' &= \varepsilon^2(\frac{1}{2}\alpha_1 r_1 + \frac{1}{4}\gamma_1 r_2^2 \sin\phi) \\
r_2' &= \varepsilon^2(-\frac{1}{2}\kappa r_2 - \frac{1}{2}\gamma_2 r_1 r_2 \sin\phi) \\
\phi' &= \varepsilon^2((\frac{1}{4}\gamma_1 \frac{r_2^2}{r_1} - \gamma_2 r_1)\cos\phi - 2\sigma),
\end{aligned}
\tag{3.18}
$$

which shows that only higher order terms play a part for nontrivial solutions of the system to occur.

For the construction of nontrivial solutions of the system, we need to determine whether or not we have an "unstable focus" in the domain, as described in Figure 3, to guarantee that, after some time, the solution will intersect the discontinuity curve (or surface in the full system). Thus, a non-smooth solution can be obtained. Hence, in the analysis which follows, we study the behaviour of the amplitudes r_1 and r_2 in (3.18) and their role in the construction of the nontrivial solution of the system.

The simplest case is by taking $\sigma = 0$, meaning that we are dealing with the exact resonance case. Then, we look for phase-locked solutions in the manifold where $\cos \phi = 0$. This implies that $\sin \phi = \pm 1$. Thus, taking $\sin \phi = 1$ and after absorbing the rescaling factor ε^2, we have:

$$
\begin{aligned}
r_1' &= \frac{1}{2}\alpha_1 r_1 + \frac{1}{4}\gamma_1 r_2^2 \\
r_2' &= -\frac{1}{2}\kappa r_2 - \frac{1}{2}\gamma_2 r_1 r_2.
\end{aligned}
\tag{3.19}
$$

A phase plane study for equation (3.19) gives the information about the behaviour of r_1 and r_2, as shown in Figure 9 (taking $\alpha_1 = 4$ and $\kappa = 1$).

In the domain where $v < x'$, similar phase portraits as shown in Figure 9 are obtained. As in the planar case, a non-smooth solution in the full system can be obtained, if a solution in one of the domains crosses the discontinuity surface and then passes through the other domain. Or else, the solution slides along the discontinuity surface and then goes back into the same domain where it comes from. Due to the assumption that $\mu = \varepsilon^2$, the latter case of solution (which is periodic) is under consideration.

To read Figure 9, one should associate each of the phase portraits with the corresponding phase portraits (which are, in fact, identical) of the other domain. Hence, as in the planar case, the non-smooth periodic solution with a sliding segment that is constructed is mainly subject to the influence of the flows in both domains to a solution, especially when the solution hits the discontinuity surface.

In the case of Figure 9(i) (associated with that of the other domain), r_1 grows at any time, but $r_2 = 0$ (corresponding with $y = 0$) is a stable manifold. Thus, after some time the non-smooth nontrivial solution so constructed will collapse to the semitrivial solution. Figure 9(ii) demonstrates a similar situation as Figure 9(i) does, if we take an initial point to the right of the curve where $r_1 = -\frac{1}{2}\frac{\gamma_1}{\alpha_1}r_2^2$. In Figure 9(iii) both r_1 and r_2 grow to infinity as time increases, while in Figure 9(iv) both amplitudes may also grow, depending on where their initial points are in the phase plane. One should pay attention to the presence of the unstable focus in the domain, when taking an initial point for having the non-smooth nontrivial solution.

The last two cases imply the possibility of the existence of a non-smooth nontrivial solution which will *not* tend to the semitrivial solution at any time.

By performing a numerical simulation, we obtain an attracting non-smooth nontrivial solution of the full system. Figure 10 describes the solution projected in the
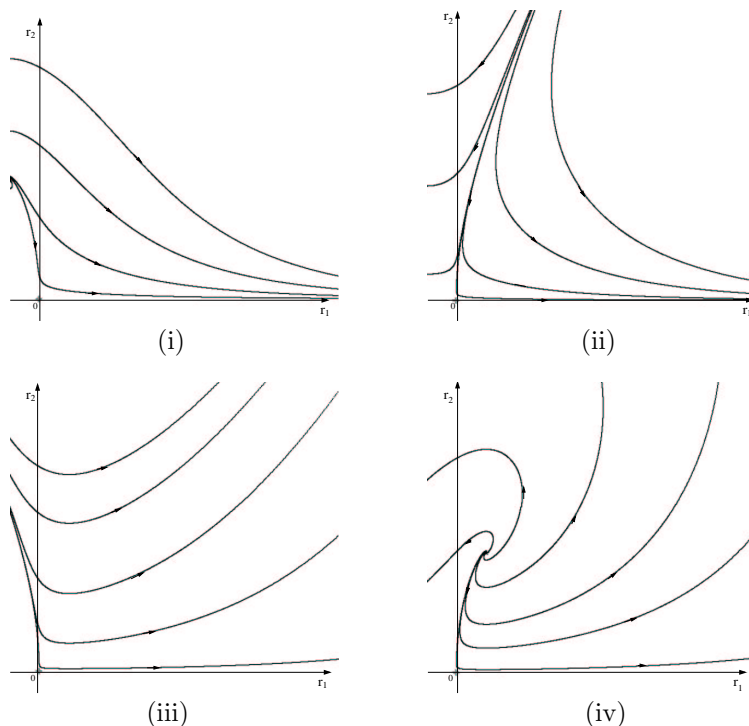
FIGURE 9. **The phase plane in the domain where** $v > x'$. (i) the case of $\gamma_1 > 0, \ \gamma_2 > 0$, (ii) the case of $\gamma_1 < 0, \ \gamma_2 > 0$, (iii) the case of $\gamma_1 > 0, \ \gamma_2 < 0$, (iv) the case of $\gamma_1 < 0, \ \gamma_2 < 0$.

$x - x' - y$ phase space for the case of Figure 9(iii), which represents a non-smooth cylinder.

More information about the solutions of the full system can be drawn if we proceed as follows. Consider again for $v > x'$ the averaged system (3.18). We may define the following transformation in order to remove the singularity of the system:

$$u = r_1 \cos \phi, \ w = r_1 \sin \phi, \ \rho = r_2^2. \tag{3.20}$$

And, after absorbing the rescaling factor, we obtain:

$$
\begin{aligned}
u' &= \frac{1}{2}\alpha_1 u + \gamma_2 u w + 2\sigma w \\
w' &= \frac{1}{2}\alpha_1 w + \frac{1}{4}\gamma_1 \rho - \gamma_2 u^2 - 2\sigma u \\
\rho' &= -\kappa\rho - \gamma_2 \rho w.
\end{aligned}
\tag{3.21}
$$

Taking $\sigma = 0$, we immediately see that $u = 0$ and $\rho = 0$ are invariant manifolds of the system. Considering $r_1 \neq 0$ (otherwise we end up with the trivial solution of the system), the manifold $u = 0$ simply corresponds with the solutions where
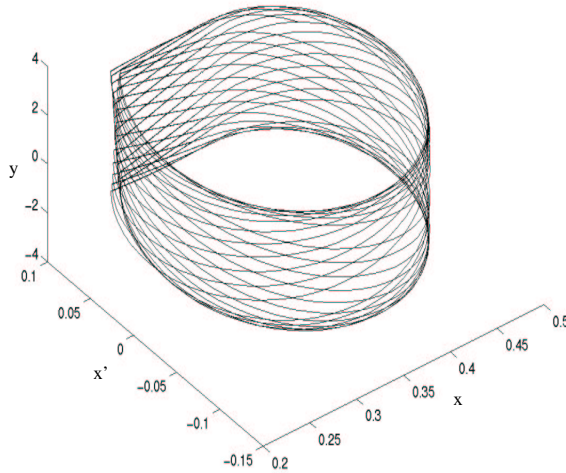
FIGURE 10. **The non-smooth cylinder**. Taking $\gamma_1 = 1$, $\gamma_2 = -3$, and $v = 0.1$

$\cos\phi = 0$ which we have analysed previously. The manifold $\rho = 0$ corresponds with the semitrivial solution of the system. By taking certain values of the parameters, we may conclude that the manifolds are attracting. For example, taking $\alpha_1 = 4$, $\kappa = 1, \gamma_1 = 1$, $\gamma_2 = 3$, and $\sigma = 0$ (the case of Figure 9(i)), the solution starting from outside the manifolds, will be expanding and attracted to plane $u = 0$ and plane $\rho = 0$ alternately, before it finally collapses into plane $\rho = 0$. The observations of the other cases follow similarly, and we omit them for brevity.

3.4.4.2. **The case of** $\delta = \varepsilon$. In the case of $\delta = \varepsilon$, we obtain the following averaged system:

$$
\begin{aligned}
r_1' &= \varepsilon \frac{1}{4}\gamma_1 r_2^2 \sin\phi + \varepsilon^2 \xi_1(r_1, r_2, \phi) \\
r_2' &= \varepsilon(-\frac{1}{2}\kappa r_2 - \frac{1}{2}\gamma_2 r_1 r_2 \sin\phi) + \varepsilon^2 \xi_2(r_1, r_2, \phi) \\
\phi' &= \varepsilon((\frac{1}{4}\frac{r_2^2}{r_1}\gamma_1 - \gamma_2 r_1)\cos\phi - 2\sigma) + \varepsilon^2 \xi_3(r_1, r_2, \phi),
\end{aligned}
\tag{3.22}
$$

where

$$\xi_1 = \frac{1}{2}\alpha_1 r_1 - \frac{1}{2}\gamma_1\sigma r_2^2 \sin\phi + \frac{1}{4}\gamma_1\kappa r_2^2 \cos\phi$$

$$\xi_2 = \gamma_2\sigma r_1 r_2 \sin\phi - \frac{1}{2}\gamma_2\kappa r_1 r_2 \cos\phi$$

$$\xi_3 = \gamma_1\gamma_2 r_2^2 - \frac{1}{4}\gamma_1\kappa\frac{r_2^2}{r_1}\sin\phi - \frac{1}{2}\gamma_1\sigma\frac{r_2^2}{r_1}\cos\phi + \frac{1}{4}\gamma_2^2 r_1^2 + 2\gamma_2\sigma r_1 \cos\phi$$

$$+ \gamma_2\kappa r_1 \sin\phi + \frac{1}{2}\kappa^2 + 2\sigma^2 - 2\gamma_2\alpha_0.$$

As in the previous case, we take $\sigma = 0$ and look for special solutions where $\sin\phi = 1$. Thus, we have:

$$
\begin{array}{rcl}
r_1' & = & \varepsilon(\frac{1}{4}\gamma_1 r_2^2) + \varepsilon^2\frac{1}{2}\alpha_1 r_1 \\
r_2' & = & \varepsilon(-\frac{1}{2}\kappa r_2 - \frac{1}{2}\gamma_2 r_1 r_2).
\end{array}
\tag{3.23}
$$

A similar reasoning as in the previous case can be applied to equations (3.22) and (3.23). We involve the higher order terms in the analysis, due to the degeneracy of the fixed point of the first approximation. Then, from the analysis we conclude that qualitatively similar results as the previous case are obtained, except that the attraction of the manifold $r_2 = 0$ is now stronger. So, in this case, the nontrivial solution so constructed, which follows from similar descriptions given by Figure 9(i) and 9(ii), will collapse to the semitrivial solution faster than that in the case of $\delta = \varepsilon^2$. This can be seen immediately if we compare equations (3.19) and (3.23). The other two cases follows similarly as the previous corresponding cases. Therefore, we have a similar conclusion with regard to the possibility for having an attracting non-smooth manifold in the phase space, as a nontrivial solution of the system.

3.5. Concluding remarks

The implementation of the dry friction oscillator to the autoparametric system features some interesting phenomena in the analysis. The periodic solution, which is typical in self-excited autoparametric systems, is non-smooth. The solution is constructed in such a way that stick-slip conditions as explained in section 3.3 are met.

The study of the semitrivial solutions of the system is very interesting. The boundary value μ_0 is important in the application. Especially if we expect a periodic solution arises in systems containing a self excitation. Moreover, the bifurcation analysis of the non-smooth periodic solution using SLIDECONT gives more insight in the behaviour of the solution to be expected when we vary the value of one of the parameters of the system. One may undertake a continuation by varying the value of another parameter and similar bifurcation results as presented in subsection 3.4.3 might follow.

The study of the nontrivial solutions of the system is far from complete. There are many complications in the analysis due to the lack of analytical and numerical

techniques to analyse such a system. However, by doing a qualitative analysis and performing numerical simulations, even in the manifold $\cos\phi = 0$ we obtain some interesting results already. That is, an attracting non-smooth nontrivial solution may exist, depending on the assumption on the parameter values. A further study may be carried out to find out the boundary value for the existence of the non-smooth nontrivial solution, related to the boundary value for the existence of the non-smooth periodic solution in the semitrivial case. Moreover, the study of the case when $\sigma \neq 0$ (the near resonance case) is also interesting from the application point of view.

We note finally that a different 4-dimensional non-smooth system was studied by Galvanetto, Bishop, and Briseghella [22]. In this paper two masses can be separately or simultaneously in a stick-slip phase. The dynamics is again complex but of a different nature.

Autoparametric Resonance of Relaxation Oscillations

A joint work with Ferdinand Verhulst.

Has been submitted to journal.

4.1. Introduction

Autoparametric resonance plays an important part in nonlinear engineering while posing interesting mathematical challenges. The linear dynamics is already nontrivial whereas the nonlinear dynamics of such systems is extremely rich and largely unexplored. A general characterisation of autoparametric systems is given in Tondl, Ruijgrok, Verhulst and Nabergoj [**59**]. In studying autoparametric systems, the determination of stability and instability conditions of the semi-trivial solution or normal mode is always the first step. After this it is of interest to look for other periodic solutions, bifurcations and classical or chaotic limit sets.

In actual engineering problems, the loss of stability of the normal mode response depends on frequency tuning of the various components of the system, and on the interaction (the coupling) between the components. Autoparametric vibrations occur only in a limited region of the tuning parameters.

In a self-excited autoparametric system with a relaxation oscillator, to have autoparametric resonance, destabilisation of the relaxation oscillation of the system is needed. It turns out that to destabilize relaxation oscillations one needs in addition rather strong interactions of a special form. This is tied in with the necessity to perturb the slow manifold which characterises to a large extent the relaxation oscillation. The results in this paper are an extension of Verhulst [**61**].

The monograph by Tondl et al. [**59**] contains a survey of the literature on self-excited autoparametric systems, in particular for weak self-excitation and weak interactions; see also Schmidt and Tondl [**47**] and Cartmell [**9**].

4.2. Formulation of the problem

A typical formulation for autonomous systems runs as follows. Consider the one-degree-of-freedom i.e. two-dimensional system

$$\dot{x} = f(x)$$

where $f(x)$ is a smooth 2-dimensional vector field and assume that the equation has a stable periodic solution. Suppose that this corresponds with undesirable behaviour, as is for instance the case of flow-induced vibrations. Can we introduce a kind of energy absorber, mathematically speaking can we couple the equation to another system such that this periodic solution arises as an unstable normal mode in the full system? This entails the introduction of the system

$$\begin{array}{rcl}
\dot{x} & = & f(x) + g(x, y), \\
\dot{y} & = & h(x, y),
\end{array} \tag{4.1}$$

in which y is n-dimensional, g and h are smooth vector fields, with $h(x, 0) = 0$. In most cases we assume $g(x, 0) = 0$, so that the original periodic solution corresponds with a normal mode of the coupled system. Sometimes $g(x, y)$ includes a perturbation resulting in a normal mode close to the unperturbed one. The important questions are 'what are the requirements for the coupling terms g and h to achieve effective destabilisation of the normal mode' and 'how do we choose the system parameters'.

Suppose $\phi(t) : \mathbb{R} \to \mathbb{R}^2$ is a stable T-periodic solution of the equation

$$\dot{x} = f(x) + g(x, 0).$$

We shall study the stability of this normal mode in system (4.1).

4.3. Linearisation and decoupling

We put $x = \phi(t) + u$, $y = y$ and expand to obtain the linearised system

$$\begin{array}{rcl}
\dot{u} & = & \dfrac{\partial f}{\partial x}(\phi(t))u + \dfrac{\partial g}{\partial x}(\phi(t), 0)u + \dfrac{\partial g}{\partial y}(\phi(t), 0)y, \\
\dot{y} & = & h(\phi(t), 0).
\end{array} \tag{4.2}$$

With a slight abuse of notation we kept u and y for the solutions of the linear system. It is clear that the linear system is *decoupled* in the following sense. The equation for y can be studied independently with the requirement to produce instability. Subsequently in the equation for u the behaviour of y can be introduced to study the behaviour of u.

If $y = 0$ is unstable for the second equation, the normal mode is unstable. The instability becomes however effective for our purpose if also the solution u of the first equation is unstable.

The homogeneous part of the first equation of (4.2) reads

$$\dot{v} = \frac{\partial f}{\partial x}(\phi(t))v + \frac{\partial g}{\partial x}(\phi(t), 0)v,$$

which is a linear equation with T-periodic coefficients. One of the solutions is $\dot{\phi}(t)$ and we can easily construct a second independent solution by d'Alembert's method. What interests us, however, are the characteristic (or Flocquet- or Lyapunov-) exponents. The exponent corresponding with $\dot{\phi}(t)$ is of course zero, as this solution is

periodic. The second exponent, λ, is negative by assumption and reads

$$\lambda = \frac{1}{T}\int_0^T Tr(\frac{\partial f}{\partial x}(\phi(t)) + \frac{\partial g}{\partial x}(\phi(t),0))dt. \qquad (4.3)$$

For a proof of these classical statements see for instance Verhulst [**60**]. This result can now be used to study the stability of the trivial solution of the equation for u where the inhomogeneous part $u_i(t)$ may destabilize $u = 0$.
It follows from Flocquet-theory that the second independent solution is of the form $e^{-\lambda t}\psi(t)$, where $\psi(t)$ is T-periodic. With fundamental matrix $\Theta(t) = (\dot{\phi}(t), e^{-\lambda t}\psi(t))$, the inhomogeneous part of the solution for u becomes

$$u_i(t) = \Theta(t)\int_0^t \Theta^{-1}(s)\frac{\partial g}{\partial y}(\phi(s),0)y(s)ds.$$

It is clear from this expression that the growth of $y(t)$ - the instability of $y = 0$ - is a necessary condition for the instability of $u = 0$. Whether this condition is sufficient depends on the actual autoparametric system as we shall see in the applications.

Often the first equation of (4.2) is a scalar second order equation of the form

$$\ddot{u} + p(t)\dot{u} + q(t)u = F(t)y \qquad (4.4)$$

with scalar independent (homogeneous) solutions $\dot{\phi}(t)$ and $e^{-\lambda t}\psi(t)$ and Wronskian $e^{-\lambda t}\chi(t)$, $\chi(t)$ a T-periodic function. In this case the inhomogeneous solution of equation (4.4) reads

$$u_i(t) = \dot{\phi}(t)\int_0^t \frac{\psi(s)}{\chi(s)}F(s)y(s)ds - e^{-\lambda t}\psi(t)\int_0^t \frac{e^{\lambda s}}{\chi(s)}\dot{\phi}(s)F(s)y(s)ds.$$

Note that $\chi(t)$ has no zeros.

4.4. Weak coupling of self-excited oscillations

For reasons of comparison with the results in the sequel we make some observations about weak self-excitation and weak interaction. We shall express these by using the small, positive parameter ε.

Consider the case of flow-induced vibrations represented by the Rayleigh oscillator embedded in the autoparametric system (different from the example in the figure)

$$\begin{aligned}
\ddot{x} + x &= \varepsilon(1 - \dot{x}^2)\dot{x} + \varepsilon(c_1 x^2 + c_2 xy + c_3 y^2) \\
\ddot{y} + \varepsilon\kappa\dot{y} + q^2 y &= \varepsilon y(d_1 x + d_2 y).
\end{aligned} \qquad (4.5)$$

The damping coefficient κ is positive, the frequency q and the coefficients c_i, d_i will be chosen suitably, i.e. to provide optimal instability of the normal mode $\phi(t)$ obtained by putting $y = 0$. The T-periodic solution $\phi(t)$ corresponds with self-excited vibrations and we linearise around this normal mode, putting $x = \phi(t) + u$, $y = y$, to find:
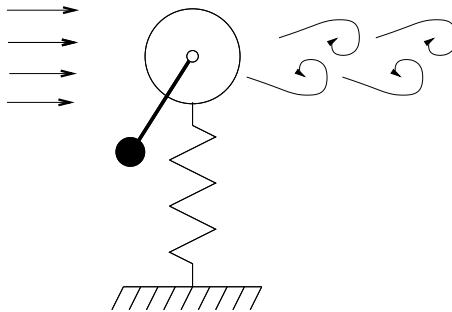
FIGURE 1. **Example of an autoparametric system with flow-induced vibrations**. The system consists of a single mass on a spring to which a pendulum is attached as an energy absorber. The flow excites the mass and the spring but not the pendulum.

$$\begin{aligned} \ddot{u} + u &= \varepsilon(1 - 3\dot{\phi}(t)^2)\dot{u} + \varepsilon(2c_1\phi(t)u + c_2\phi(t)y), \\ \ddot{y} + \varepsilon\kappa\dot{y} + q^2 y &= \varepsilon d_1\phi(t)y. \end{aligned} \tag{4.6}$$

The equation for y is Hill's equation with damping added which can be reduced to Mathieu's equation by using that ε is small.

It is well known that we have for the periodic solution of the modified Rayleigh oscillator

$$\ddot{x} + x = \varepsilon(1 - \dot{x}^2)\dot{x} + \varepsilon c_1 x^2$$

the approximation

$$\phi(t) = 2\cos(t) + O(\varepsilon).$$

The estimate for amplitude and period is valid for all time. Inserting this into the equation for y yields

$$\ddot{y} + \varepsilon\kappa\dot{y} + (q^2 - 2\varepsilon d_1 \cos(t))y = 0.$$

In parameter space a relatively large instability domain arises on choosing $q = \frac{1}{2}$. The usual analysis (Poincaré-Lindstedt, averaging or harmonic balance) leads to the (known) requirement $|d_1| > \frac{1}{2}\kappa$ for instability of $y = 0$.

Returning to the equation for u we note that we have from equation (4.3) and the first equation of (4.6)

$$\lambda = -\varepsilon\frac{1}{2\pi}\int_0^{2\pi}(1 - 3\dot{\phi}(s)^2)ds = -5\varepsilon + O(\varepsilon^2).$$

Independent solutions of the homogeneous part of the first equation of (4.6) are according to Flocquet theory $\dot{\phi}(t)$ and $e^{-5\varepsilon t}\psi(t) + O(\varepsilon)$ with $\psi(t)$ a T-periodic solution which can be obtained by d'Alembert's construction. The Wronskian to $\mathcal{O}(\varepsilon)$

becomes $e^{-5\varepsilon t}\chi(t)$ with again $\chi(t)$ a T-periodic function without zeros. The inhomogeneous solution of the equation for u takes the form

$$u_i(t) = \varepsilon c_2 \dot{\phi}(t) \int_0^t \frac{\psi(s)\phi(s)}{\chi(s)} y(s) ds - \varepsilon c_2 e^{-5\varepsilon t} \psi(t) \int_0^t e^{5\varepsilon s} \frac{\dot{\phi}(s)\phi(s)}{\chi(s)} y(s) ds. \quad (4.7)$$

We conclude that on choosing $q = \frac{1}{2}, d_1 > \frac{1}{2}\kappa$ the solution $y = 0$ becomes unstable which destabilises the normal mode in the y-direction. On choosing $c_2 \neq 0$ the solution $u = 0$ also becomes unstable which enforces the instability of the normal mode. The parameters c_1, c_3, d_2 play no part at this level of approximation.
Note that Abadi [1] studied this autoparametric system in the case $c_1 = c_2 = d_2 = 0$ with emphasis on the bifurcation phenomena in the case of an unstable normal mode.

We mention that in the case of weak interaction the analysis does not change much when we replace the Rayleigh oscillator by van der Pol self-excitation. The Lyapunov exponents of the normal mode in this case are 0 and $\lambda = -\varepsilon + O(\varepsilon^2)$.

4.5. Interaction with relaxation oscillations

A different problem arises when we wish to quench a relaxation oscillation. We take as an example the van der Pol relaxation oscillator embedded in an autoparametric system of the form

$$\begin{aligned}
\ddot{x} + x &= \mu(1 - x^2)\dot{x} + F(x, \dot{x}, y, \dot{y}), \\
\ddot{y} + \kappa\dot{y} + q^2 y &= yG(x, \dot{x}, y, \dot{y}),
\end{aligned} \quad (4.8)$$

where κ is again a positive damping coefficient. We assume that if the $(y, \dot{y})$-vibration is absent, F vanishes to produce a pure van der Pol relaxation oscillation: $F(x, \dot{x}, 0, 0) = 0$. The functions F and G, and the remaining parameters have to be chosen to produce instability of the (periodic relaxation) normal mode, obtained by putting $y = 0$ in the case $\mu \gg 1$. We will use results on this relaxation oscillator which were summarised and extended by Grasman [23]. We will also use results on slow manifolds in geometric singular perturbations; for an introduction see Kaper [28] and the original papers by Fenichel [15, 16, 17, 18].

Introducing $\phi(t)$ for the T_μ-periodic relaxation normal mode, putting $x = \phi(t) + u$, $y = y$ produces

$$\begin{aligned}
\ddot{u} + u &= \mu(1 - \phi(t)^2)\dot{u} - 2\mu\phi(t)\dot{\phi}(t)u + \cdots, \\
\ddot{y} + \kappa\dot{y} + (q^2 - d_1\phi(t))y &= \cdots,
\end{aligned} \quad (4.9)$$

where the nonlinear terms are indicated by dots. The linearised equations suffice for the stability analysis.

4.6. The Lyapunov exponent of relaxation

The normal mode is T_μ-periodic with the estimate (see Grasman [23])

$$T_\mu = (3 - 2\log 2)\mu + O(\frac{1}{\mu^{\frac{1}{3}}}) \text{ as } \mu \to \infty.$$
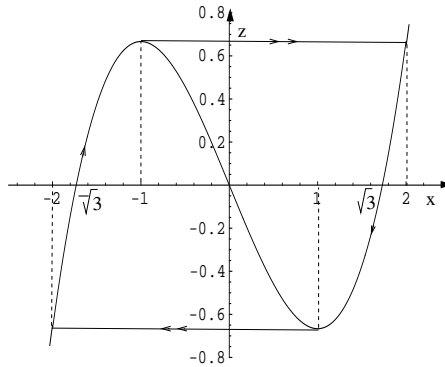
FIGURE 2. **The phase plane of the van der Pol relaxation oscillation**. The slow manifold is approximated by the cubic curve, fast motion is indicated by double arrows.

To compute the rate of attraction from the integral in (4.3) we use the slow-fast motion in the Liénard plane by replacing the van der Pol equation by

$$\dot{x} = \mu(z + x - \frac{1}{3}x^3), \ \mu\dot{z} = -x.$$

In the $x - z$ Liénard plane we have

$$(z + x - \frac{1}{3}x^3)\frac{dz}{dx} = -\frac{x}{\mu^2},$$

which illustrates that as μ is large dz/dx is very small except if $z = -x + \frac{1}{3}x^3$. This cubic curve in the Liénard plane corresponds with the slow manifold of the system. See Figure (2).

With this knowledge it is not difficult to obtain a first order approximation of the characteristic exponent. From equation (4.3) and the first equation of (4.9), we have

$$\lambda = \mu\frac{1}{T_\mu}\int_0^{T_\mu}(1 - \phi(t)^2)dt.$$

Integration of van der Pol's equation for the periodic solution yields

$$\int_0^{T_\mu}(\ddot{\phi}(t) + \phi(t))dt = \mu\int_0^{T_\mu}(1 - \phi^2(t))\dot{\phi}(t)dt$$

or, using the periodicity,

$$\int_0^{T_\mu}\phi(t)dt = \mu\oint(1 - x^2)dx = 0,$$

where the contour integral is taken over the limit cycle in the phase plane. With this result, using partial integration and the equation for z we have

$$\int_0^{T_\mu}\phi(t)^2dt = -\int_0^{T_\mu}(\int\phi(t)dt)\dot{\phi}(t)dt = \mu\oint z(x)dx.$$

Integration in the Liénard plane yields the approximation

$$\lambda = \mu(1 - \frac{9}{2}\frac{\mu}{T_\mu}) + o(1) \approx -1.79\mu$$

which, as $\mu \gg 1$, corresponds with strong attraction.

4.7. Instability of $y = \dot{y} = 0$

The periodic coefficient $\phi(t)$ in the equation for y has a period proportional to $\mu \gg 1$, so it is natural to rescale $t = \frac{T_\mu}{2\pi}\tau$ which, after linearisation, produces

$$\frac{d^2y}{d\tau^2} + \frac{\kappa T_\mu}{2\pi}\frac{dy}{d\tau} + (\frac{q^2 T_\mu{}^2}{4\pi^2} - \frac{d_1 T_\mu^2}{4\pi^2}\phi_r(\tau))y = 0 \qquad (4.10)$$

with $\phi_r(\tau) = \phi(\frac{T_\mu}{2\pi}\tau)$, 2π-periodic in τ. We observe that the instability behaviour of the solutions of the Flocquet equation (4.10) is qualitatively the same as for the damped Mathieu-equation. A consequence is that to obtain prominent instability of $y = 0$ and so destabilisation of the relaxation oscillation we have to couple to a low-frequency oscillator (y) with, using the first-order estimate for the period,

$$\kappa = O(\frac{1}{\mu}), \ q = \frac{\pi}{(3 - 2\log 2)\mu}, \ d_1 = O(\frac{1}{\mu^2}) \text{ as } \mu \to \infty.$$

The actual choice of κ and d_1 depends on the amount of quenching one wants to achieve. We explore the small parameter case

$$\frac{\kappa T_\mu}{2\pi} = \frac{\kappa_0}{\mu}, \ \frac{q^2 T_\mu^2}{\pi^2} = 1, \ \frac{d_1 T_\mu^2}{4\pi^2} = \frac{d}{\mu}$$

with κ_0 and d independent of μ. We have from equation (4.10)

$$\frac{d^2y}{d\tau^2} + \frac{\kappa_0}{\mu}\frac{dy}{d\tau} + (\frac{1}{4} - \frac{d}{\mu}\phi_r(\tau))y = 0. \qquad (4.11)$$

To obtain the boundaries of the Flocquet-tongue we impose the periodicity conditions

$$\int_0^{2\pi}(-\kappa_0\frac{dy(\tau)}{d\tau} + d\phi_r(\tau))y(\tau)\sin\frac{\tau}{2} = 0,$$
$$\int_0^{2\pi}(-\kappa_0\frac{dy(\tau)}{d\tau} + d\phi_r(\tau))y(\tau)\cos\frac{\tau}{2} = 0. \qquad (4.12)$$

With the Poincaré expansion $y(\tau) = a_0\cos\frac{\tau}{2} + b_0\sin\frac{\tau}{2} + \frac{1}{\mu}\cdots$, we have

$$\frac{1}{2}\kappa_0 a_0 - dI b_0 = 0, \ dI a_0 - \frac{1}{2}\kappa_0 b_0 = 0,$$

where we used the symmetry of $\phi_r(\tau)$; I is a positive number given by

$$I = \int_0^{2\pi}\phi_r(\tau)\cos\tau d\tau.$$

Nontrivial solutions arise if the determinant vanishes or

$$\frac{1}{2}\kappa_0 = \pm dI.$$

We have instability of $y = 0$ if $|d| > \frac{\kappa_0}{2I}$.

4.8. Deformation of the slow manifold

To analyse the relaxation oscillation in the 4-dimensional problem of system (4.8) we assume that the interaction term F contains quadratic and cubic terms and is of the form

$$F(x, \dot{x}, y, \dot{y}) = \mu(c_1 \dot{x}y + c_2 x\dot{x}y + c_3 \dot{x}y^2).$$

An easy way to see that these are the leading terms of F runs as follows. Transform the time in the first equation of (4.8) $t \to \mu\tau$ and indicate differentiation with respect to τ with a prime:

$$\frac{1}{\mu^2}x'' + x = (1 - x^2)x' + F(x, \frac{1}{\mu}x', y, \frac{1}{\mu}y')$$

or

$$x' = v, \quad \frac{1}{\mu^2}v' = (1 - x^2)v + F(x, \frac{1}{\mu}v, y, \frac{1}{\mu}y').$$

The slow manifold is obtained by putting the right-hand side of the equation for v to zero. For F to induce a significant deformation its terms have to depend on v but this produces a factor $\frac{1}{\mu}$; terms containing v^2 or vy' produce terms of order $\frac{1}{\mu^2}$ and can be omitted.

As an illustration we choose for the attached (y) oscillator $G = dx$.

We generalise the Liénard transformation $(x, \dot{x}) \to (x, z)$ to

$$
\begin{aligned}
\frac{1}{\mu}\dot{x} &= z + x - \frac{1}{3}x^3 + c_1 xy + \frac{1}{2}c_2 x^2 y + c_3 xy^2, \\
\dot{z} &= -\frac{1}{\mu}x - c_1 x\dot{y} - \frac{1}{2}c_2 x^2 \dot{y} - 2c_3 xy\dot{y}.
\end{aligned}
\tag{4.13}
$$

The slow manifold is given by

$$z = -x + \frac{1}{3}x^3 - c_1 xy - \frac{1}{2}c_2 x^2 y - c_3 xy^2.$$

It is unstable if

$$1 - x^2 + c_1 y + c_2 xy + c_3 y^2 > 0.$$

The c_3-term is semidefinite, which is important, as far as stability is concerned. So, we choose this term for our model of destabilisation of the relaxation oscillation. Replacing c_3 by c we have the system

$$
\begin{aligned}
\ddot{x} + x &= \mu(1 - x^2)\dot{x} + \mu c\dot{x}y^2, \\
\ddot{y} + \kappa\dot{y} + q^2 y &= dxy.
\end{aligned}
\tag{4.14}
$$

In generalised Liénard variables this becomes

$$
\begin{aligned}
\frac{1}{\mu}\dot{x} &= z + x - \frac{1}{3}x^3 + cxy^2, \\
\dot{z} &= -\frac{1}{\mu}x - 2cxy\dot{y}
\end{aligned}
\tag{4.15}
$$

with the equation for y added. The slow manifold is given by

$$z = -(1 + cy^2)x + \frac{1}{3}x^3,$$

which is unstable if $1 + cy^2 - x^2 > 0$. The slow manifold corresponds with a 3-dimensional cubic cylinder parallel to the $\dot{y}$-axis.

We are now able to illustrate the behaviour of this autoparametric system.

4.9. Numerical experiments

At present the dynamics of system (4.14) in the case of an unstable normal mode is far from clear. In anticipation of a more theoretical analysis in the near future we perform a number of numerical experiments to illustrate interesting phenomena. We choose $\mu = 10$ throughout.

The stability of the slow manifold is determined by the sign of $1 + cy^2 - x^2$. We shall take c negative, $c = -2.2$, to illustrate the effect of a growing y-oscillation. In this case $1 + cy^2 = 0$ if $y = 0.67 \cdots$. Figure 3 describes the slow manifold and the corresponding unstable domain.
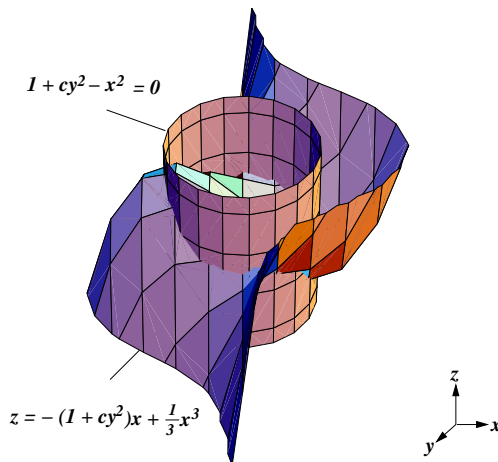
FIGURE 3. **The slow manifold and its unstable domain** for $c = -2.2$.

- Choose $c = -2.2$, $d = 0.03$, $\kappa = 0.075$.
  Starting the y-oscillation near the normal mode plane $y = \dot{y} = 0$, the 3-dimensional projection of the solution is rather messy but a projection on the $x - \dot{x}$ plane produces an orbit which seems to fill up a large part of the space taken by the unperturbed orbit; see Figure 4. Calculation of the Lyapunov exponents of the solution gives the result
  $\lambda_1 = 0.05205 \cdots$, $\lambda_2 \approx 0$, $\lambda_3 = -0.13449 \cdots$, $\lambda_4 = -13.14938 \cdots$.
  This leads us to a conclusion that we have a *chaotic attractor*, with the corresponding Kaplan-Yorke dimension near 2.3. Figure 5 shows the projection of the 3-dimensional Poincaré section of the orbit in $\dot{x} - y$ plane,

taking $x = 0.5$ as the section (the vertical line in Figure 4). The projection fits with the previous calculation that the attractor has a dimension larger than 2.
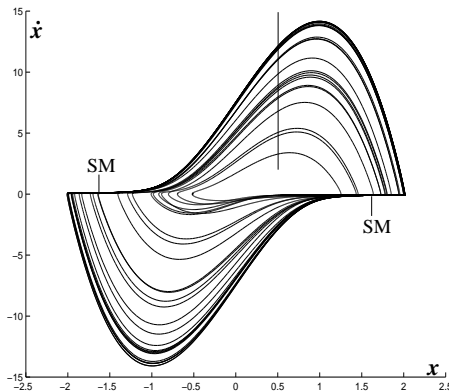

FIGURE 4. **A limit set of system (4.14)** for $\mu = 10$, $c = -2.2$, $d = 0.03$, $\kappa = 0.075$ with small starting values of the y-oscillation, projected on the $x - \dot{x}$ plane. SM is the stable part of the slow manifold. The vertical line corresponds with the Poincaré section of Figure 5
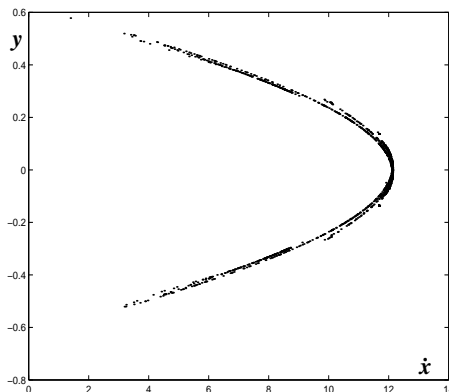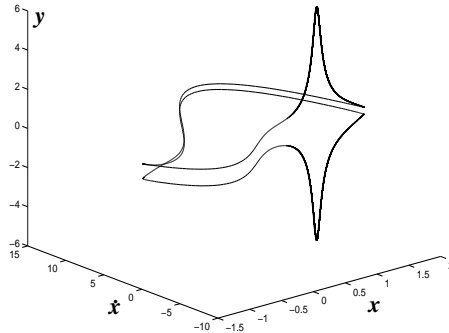

FIGURE 5. **The Poincaré section** of the limit set of Figure 4, projected on the $\dot{x} - y$ plane.

- Consider the same dynamics, $c = -2.2$, $d = 0.03$, $\kappa = 0.075$, but starting at $y(0) = 3$, $\dot{y}(0) = 0.1$ we have oscillations so that $y(t)$ takes alternating values above and below $0.67\cdots$. Leaving out the transient we find a periodic limit set illustrated in Figure 6; this is a projection in 3-dimensional

FIGURE 6. **A periodic limit set of system (4.14)** for $\mu = 10$, $c = -2.2$, $d = 0.03$, $\kappa = 0.075$ with high starting values of the y-oscillation. Transient orbits are left out. The stable part of the slow manifold is present near the extreme values of y.
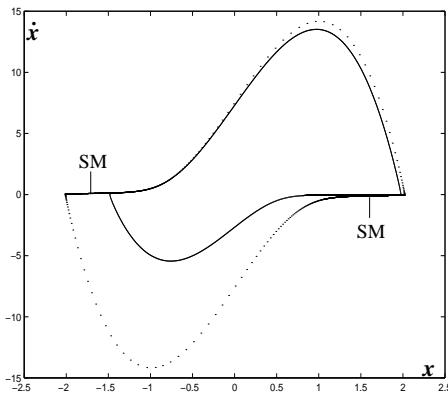
FIGURE 7. **A periodic limit set of system (4.14)** for $\mu = 10$, $c = -2.2$, $d = 0.03$, $\kappa = 0.075$ with high starting values of the y-oscillation, projected on the $x - \dot{x}$ plane. The dotted orbit corresponds with the unperturbed relaxation oscillation. In the perturbed state the slow manifolds are reduced and the limit cycle becomes asymmetric. SM is the stable part of the slow manifold.

space. Projecting the limit set on the $x, \dot{x}$-plane we find a strongly perturbed relaxation oscillation, see Figure 7. For comparison the unperturbed relaxation oscillation (coupling $c = 0$) is indicated by dots.

Thus, we have at least two attractors.

- For certain parameter values we find unbounded solutions. We discard these cases as they correspond with a break-down of the model.
- Another possibility to clarify the dynamics is to replace system (4.14) by the equation

$$\ddot{x} + x = \mu(1 - x^2)\dot{x} + \mu c \dot{x} \cos^2 qt. \qquad (4.16)$$

This equation might be illustrative for the behaviour of the relaxation oscillation in the special case when the solutions for y are $2\pi/q$-periodic. At the same time it is a model of the van der Pol relaxation oscillator with parametric excitation added.
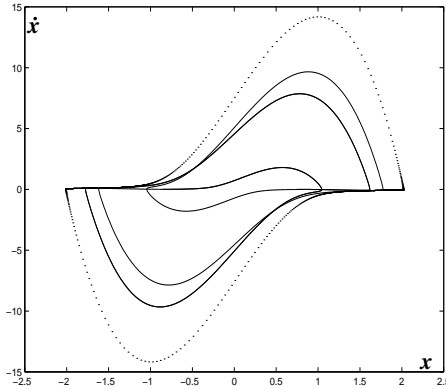
FIGURE 8. **A limit set of system (4.16)** for $\mu = 10$, $c = -16$. The limit set contains one periodic orbit. The relaxation oscillation corresponding with $c = 0$ is dotted.
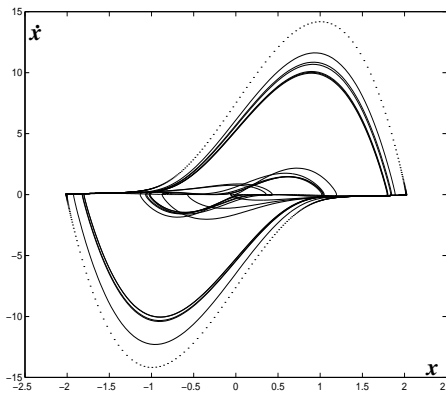
FIGURE 9. **A limit set of system (4.16)** for $\mu = 10$, $c = -18.1$. The limit set is long-periodic or aperiodic. The relaxation oscillation corresponding with $c = 0$ is dotted.
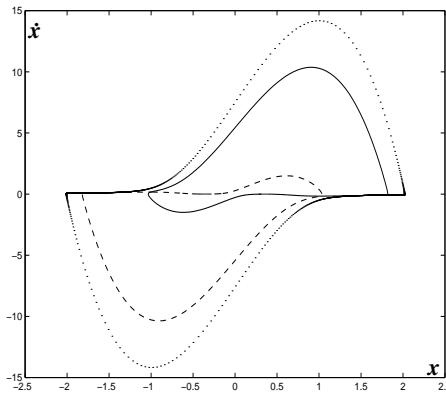
FIGURE 10. **A limit set of system (4.16)** for $\mu = 10$, $c = -19$.
The limit set contains of two periodic orbits, both attracting (one is
indicated by a full line, one by dashes). The relaxation oscillation
corresponding with $c = 0$ is dotted.

Interesting phenomena arise when varying c, see Figures (8-10). Choosing
$c = -16$ we have periodic limiting behaviour; near $c = -18$ it is not clear
whether the attractor is (long-)periodic or not periodic. This behaviour
corresponds with a small window in parameter space as for $c = -19$ we
have again periodic behaviour with two periodic attractors; see Figure 10.
In all cases we observe quenching of the van der Pol relaxation oscillation.
If we increase c above -16 or if we decrease c below -19 the quenching is
diminished.

4.10. Discussion

The most important conclusion is that to quench relaxation oscillations, apart
from the usual tuning conditions, we have to choose the interaction such that strong
deformation of the slow manifolds is possible.
In the case that the normal mode relaxation oscillation is destabilised, a number of
different limit sets are possible.

Numerical experiments have been done show some interesting results. We obtain
a chaotic attractor coexisted with a stable periodic solution. The results also show
the effectiveness of the coupling to deform the relaxation oscillation of the system.
In the near future further study of this result will be carried out.

CHAPTER 5

Interaction Between Self-excitation and Parametric Excitation

5.1. Introduction

Some high tower-like building constructions, such as masts and chimneys are often self-excited by wind flow. The self-excited vibration can be an undesirable phenomenon leading to dangerous oscillations of the constructions. There are many other systems where self-excited vibration must be studied. The sources of the excitation that may cause different types of vibration modes can vary. Systems with flow-induced vibrations and system with dry friction provide important examples.

Much effort has been devoted to study systems which are self-excited. Most of the efforts are concerned with eliminating all dangerous oscillations from the system. In [51, 52], Tondl studied systems consisting of self-excitations that can be represented by the van der Pol, the Rayleigh, or dry friction oscillators. Various means are used to quench self-excited vibration of the systems, such as absorbers and resilient foundations (see [51]).

Further and more specific results are due to Tondl and Ecker [56, 12], Tondl [50] and Tondl and Nabergoj [55]. The authors introduced systems that consist of a self-excited oscillator in one mode and absorber(s) with parametric excitation in the other mode(s). These models show the possibility of using parametric excitation to suppress self-excitation. It was proved that for systems with parametric excitation due to periodic stiffness variation, when the combination parametric resonance occurs in the neighbourhood of

$$\eta = \Omega_j + \Omega_k, \ j \neq k,$$

then conditions for suppression of the self-excited vibration can be achieved, i.e. when the parametric excitation frequency is in the neighbourhood of

$$\eta = |\Omega_j - \Omega_k|, \ j \neq k,$$

where η is the parametric resonance frequency and $\Omega_{j,k}$ are the natural frequencies of the linearised system without damping. This is called *parametric combination anti-resonance.*

Starting with the model in [12], Fatimah and Verhulst [14] applied averaging (see [60]) to the system. After obtaining the same results as in [12], they studied the bifurcations of the solutions. Moreover, even in the case of a small absorber mass, they concluded that partly suppression of the self-excitation is still possible.

Other studies on systems with self-excitation are by Abadi [**1, 2**]. He considered autoparametric systems (see [**58**]) with different sources of self-excitation, i.e. by using Rayleigh and dry friction oscillators, and he studied the effect of the use of a pendulum with viscous damping as an absorber of the systems. The results show that there is a possibility of suppression of the self-excitation as shown by a bifurcation diagram. Moreover, sliding bifurcation analysis was also performed in [**2**], showing a new phenomenon in bifurcation analysis regarding mechanical systems consisting of a dry friction oscillator.

In this paper, we deal with the problem of suppressing self-excited vibration using parametric excitation. We will use simplified models of a massless rod or slender structure with concentrated masses. Assuming one (main) mass is self-excited, parametric excitations due to periodic stiffness variation subjected to elastic mounting of the ends of the rod, are implemented. We divide the problem into two cases; the case of a two-mass system and the case of a three-mass system.

We leave out the possibility of self-excited relaxation oscillations; these are studied in a separate chapter.

5.2. The two-mass system

We start with analysing a two-mass system. Let us denote the masses as m_1 and m_2 with their corresponding deflections y_1 and y_2, respectively. The mass m_1 is attached to a spring, stiffness k_1, on one side, and is connected to the mass m_2 on the other side, by a linear spring having also stiffness k_1. The mass m_2 is attached to a spring having periodically variable stiffness $k_2(1 + \varepsilon \cos \omega t)$. The mass m_1 is self-excited by flow having a constant velocity U. This will be expressed by a negative damping of Rayleigh type $\beta_0 U^2 (1 - \gamma_0 \dot{y}_1^2) \dot{y}_1$, $\beta_0, \gamma_0 > 0$. (In [**50**] Tondl studied a similar system, but using van der Pol type of damping). This system is a simplified model of a structure (e.g. a rod). Figure 1 illustrates the description above. The system is governed by the following differential equations of motion:

$$
\begin{aligned}
m_1 \ddot{y}_1 - \beta_0 U^2 (1 - \gamma_0 \dot{y}_1^2) \dot{y}_1 + 2k_1 y_1 - k_1 y_2 &= 0 \\
m_2 \ddot{y}_2 + b \dot{y}_2 + k_2 (1 + \varepsilon \cos \omega t) y_2 - k_1 (y_1 - y_2) &= 0,
\end{aligned}
\tag{5.1}
$$

where ε is the parametric excitation amplitude and it is supposed to be small. Using the time transformation $\omega_1 t \to \tau$, where $\omega_1 = \sqrt{\frac{2k_1}{m_1}}$ is the natural frequency of the mass m_1, we have the equations in the dimensionless form:

$$
\begin{aligned}
y_1'' - \beta V^2 (1 - \gamma y_1'^2) y_1' + y_1 - \frac{1}{2} y_2 &= 0 \\
y_2'' + \kappa y_2' + q^2 (1 + \varepsilon \cos \eta t) y_2 - \frac{1}{2} M (y_1 - y_2) &= 0,
\end{aligned}
\tag{5.2}
$$

where $V = \frac{U}{U_0}$, $\beta = \frac{\beta_0 U_0^2}{m_1 \omega_1}$, $\gamma = \gamma_0 \omega_1^2$ for U_0 is a chosen reference value for the flow velocity, and $\eta = \frac{\omega}{\omega_1}$, $\kappa = \frac{b}{m_2 \omega_1}$, $q^2 = \frac{k_2}{m_2 \omega_1^2}$, $M = \frac{m_1}{m_2}$.

We use the small parameter ε by rescaling $\beta = \varepsilon \bar{\beta}$, $\kappa = \varepsilon \bar{\kappa}$ and considering the case that $M = \mathcal{O}(1)$, after dropping the bars:
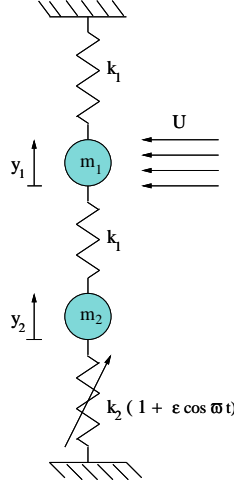
FIGURE 1. **The two-mass model**. y_1 and y_2 are the deflections of the masses m_1 and m_2, respectively.

$$
\begin{aligned}
y_1'' + y_1 - \frac{1}{2}y_2 - \varepsilon\beta V^2(1 - \gamma {y_1'}^2)y_1' &= 0 \\
y_2'' - \frac{1}{2}M(y_1 - y_2) + q^2(1 + \varepsilon\cos\eta t)y_2 + \varepsilon\kappa y_2' &= 0.
\end{aligned}
\tag{5.3}
$$

We transform (5.3) into quasi-normal form using the following linear transformation:

$$
\begin{aligned}
y_1 &= x_1 + x_2 \\
y_2 &= a_1 x_1 + a_2 x_2,
\end{aligned}
\tag{5.4}
$$

to find

$$
\begin{aligned}
x_1'' + \Omega_1^2 x_1 &= -\varepsilon\mathcal{F}_1(x_1, x_1', x_2, x_2') \\
x_2'' + \Omega_2^2 x_2 &= -\varepsilon\mathcal{F}_2(x_1, x_1', x_2, x_2').
\end{aligned}
\tag{5.5}
$$

where

$$
\mathcal{F}_1(x_1, x_1', x_2, x_2') = \theta_{11}x_1' + \theta_{12}x_2' + (Q_{11}x_1 + Q_{12}x_2)\cos\eta\tau - B_1(x_1' + x_2')^3
$$

$$
\mathcal{F}_2(x_1, x_1', x_2, x_2') = \theta_{21}x_1' + \theta_{22}x_2' + (Q_{21}x_1 + Q_{22}x_2)\cos\eta\tau + B_2(x_1' + x_2')^3,
$$

with

$$
\theta_{11} = \frac{a_1\kappa + a_2\beta V^2}{a_1 - a_2}, \theta_{12} = \frac{a_2(\kappa + \beta V^2)}{a_1 - a_2},\ \theta_{21} = -\frac{a_1(\kappa + \beta V^2)}{a_1 - a_2},
$$

$$
\theta_{22} = -\frac{a_2\kappa + a_1\beta V^2}{a_1 - a_2},\ Q_{11} = \frac{q^2 a_1}{a_1 - a_2},\ Q_{12} = \frac{q^2 a_2}{a_1 - a_2},
$$

$$Q_{21} = -\frac{q^2 a_1}{a_1 - a_2}, \; Q_{22} = -\frac{q^2 a_2}{a_1 - a_2}, \; B_1 = \frac{a_2 \beta V^2 \gamma}{a_1 - a_2}, \; B_2 = \frac{a_1 \beta V^2 \gamma}{a_1 - a_2}.$$

5.2.1. Conditions for suppression of self-excited vibration. A parametric combination anti-resonance with detuning arises when taking $\eta = \eta_0 + \varepsilon\sigma$, where $\eta_0 = \Omega_2 - \Omega_1$. Using the time transformation $\eta\tau \to t$, (5.5) becomes:

$$
\begin{aligned}
\bar{x}_1'' + \varpi_1^2 \bar{x}_1 &= -\frac{\varepsilon}{\eta_0^2} \bar{\mathcal{F}}_1(\bar{x}_1, \bar{x}_1', \bar{x}_2, \bar{x}_2') \\
\bar{x}_2'' + \varpi_2^2 \bar{x}_2 &= -\frac{\varepsilon}{\eta_0^2} \bar{\mathcal{F}}_2(\bar{x}_1, \bar{x}_1', \bar{x}_2, \bar{x}_2').
\end{aligned}
\tag{5.6}
$$

where $\varpi_i = \frac{\Omega_i}{\eta_0}, \; i = 1, 2$, and

$$\bar{\mathcal{F}}_1 = -2\varpi_1 \Omega_1 \sigma \bar{x}_1 + \eta_0(\theta_{11}\bar{x}_1' + \theta_{12}\bar{x}_2') + (Q_{11}\bar{x}_1 + Q_{12}\bar{x}_2)\cos t - \eta_0^3 B_1(\bar{x}_1' + \bar{x}_2')^3$$

$$\bar{\mathcal{F}}_2 = -2\varpi_2 \Omega_2 \sigma \bar{x}_2 + \eta_0(\theta_{21}\bar{x}_1' + \theta_{22}\bar{x}_2') + (Q_{21}\bar{x}_1 + Q_{22}\bar{x}_2)\cos t + \eta_0^3 B_2(\bar{x}_1' + \bar{x}_2')^3.$$

Using the transformation:

$$
\begin{aligned}
\bar{x}_1 &= u_1 \cos \varpi_1 t + v_1 \sin \varpi_1 t, & \bar{x}_1' &= -u_1 \varpi_1 \sin \varpi_1 t + v_1 \varpi_1 \cos \varpi_1 t \\
\bar{x}_2 &= u_2 \cos \varpi_2 t + v_2 \sin \varpi_2 t, & \bar{x}_2' &= -u_2 \varpi_2 \sin \varpi_2 t + v_2 \varpi_2 \cos \varpi_2 t
\end{aligned}
\tag{5.7}
$$

averaging over t and rescaling the time through $\frac{\varepsilon}{\eta_0^2}$, we obtain:

$$
\begin{aligned}
u_1' &= -\Omega_1 \sigma v_1 - \frac{1}{2}\eta_0 \theta_{11} u_1 + \frac{1}{4}\frac{Q_{12}}{\varpi_1} v_2 + \mathcal{G}_1(u_1, v_1, u_2, v_2) \\
v_1' &= \Omega_1 \sigma u_1 - \frac{1}{2}\eta_0 \theta_{11} v_1 - \frac{1}{4}\frac{Q_{12}}{\varpi_1} u_2 + \mathcal{G}_2(u_1, v_1, u_2, v_2) \\
u_2' &= -\Omega_2 \sigma v_2 - \frac{1}{2}\eta_0 \theta_{22} u_2 + \frac{1}{4}\frac{Q_{21}}{\varpi_2} v_1 + \mathcal{G}_3(u_1, v_1, u_2, v_2) \\
v_2' &= \Omega_2 \sigma u_2 - \frac{1}{2}\eta_0 \theta_{22} v_2 - \frac{1}{4}\frac{Q_{21}}{\varpi_2} u_1 + \mathcal{G}_4(u_1, v_1, u_2, v_2)
\end{aligned}
\tag{5.8}
$$

where

$$
\begin{aligned}
\mathcal{G}_1(u_1, v_1, u_2, v_2) &= \frac{3}{4}\eta_0^3 B_1(\frac{1}{2}\varpi_1^2 u_1(u_1^2 + v_1^2) + \varpi_2^2 u_1(u_2^2 + v_2^2)) \\
\mathcal{G}_2(u_1, v_1, u_2, v_2) &= \frac{3}{4}\eta_0^3 B_1(\frac{1}{2}\varpi_1^2 v_1(u_1^2 + v_1^2) + \varpi_2^2 v_1(u_2^2 + v_2^2)) \\
\mathcal{G}_3(u_1, v_1, u_2, v_2) &= -\frac{3}{4}\eta_0^3 B_2(\varpi_1^2 u_2(u_1^2 + v_1^2) + \frac{1}{2}\varpi_2^2 u_2(u_2^2 + v_2^2)) \\
\mathcal{G}_4(u_1, v_1, u_2, v_2) &= -\frac{3}{4}\eta_0^3 B_2(\varpi_1^2 v_2(u_1^2 + v_1^2) + \frac{1}{2}\varpi_2^2 v_2(u_2^2 + v_2^2))
\end{aligned}
$$

Linearisation of (5.8) in the neighbourhood of the trivial solution, we have the coefficient matrix

$$\begin{pmatrix} -\frac{1}{2}\eta_0\theta_{11} & -\Omega_1\sigma & 0 & \frac{1}{4}\frac{Q_{12}}{\varpi_1} \\ \Omega_1\sigma & -\frac{1}{2}\eta_0\theta_{11} & -\frac{1}{4}\frac{Q_{12}}{\varpi_1} & 0 \\ 0 & \frac{1}{4}\frac{Q_{21}}{\varpi_2} & -\frac{1}{2}\eta_0\theta_{22} & -\Omega_2\sigma \\ -\frac{1}{4}\frac{Q_{21}}{\varpi_2} & 0 & \Omega_2\sigma & -\frac{1}{2}\eta_0\theta_{22} \end{pmatrix}$$

with the corresponding characteristic equation:

$$c_0\lambda^4 + c_1\lambda^3 + c_2\lambda^2 + c_3\lambda + c_4 = 0,$$

where $c_i,\ i = 0..4$, depend on the parameters.

To determine the stability interval of the trivial solution, to the characteristic equation we apply the Routh-Hurwitz criterion, from which it follows that

rh-A. $\theta_{11} + \theta_{22} > 0$,
rh-B. $\mathcal{K}_0\sigma^4 + \mathcal{K}_1\sigma^2 + \mathcal{K}_2 > 0$,

where $\mathcal{K}_i,\ i = 0, 1, 2$ depend on the parameters. Figure 2 shows the boundaries of θ_{11} and θ_{22} in the $M - q$ plane when fixing the other parameter values.
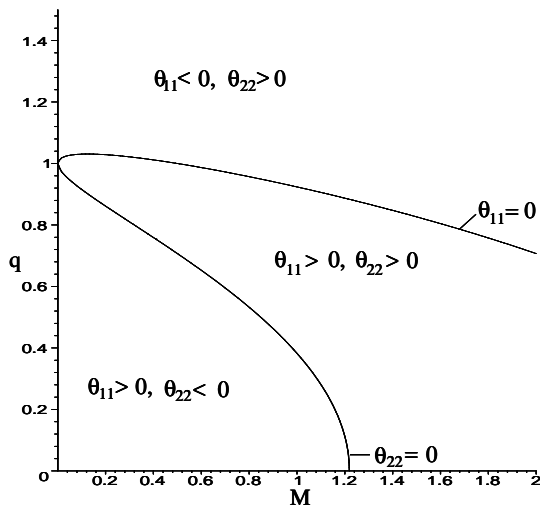
FIGURE 2. **The Boundaries of θ_{11} and θ_{22}** for $\kappa = 0.18,\ \beta = 0.1$

For the initiation of self-excitation of the system, either θ_{11} or θ_{22} (or both) must be negative. Thus, when both $\theta_{11} > 0$ and $\theta_{22} > 0$, self-excitation of the system is not possible. Therefore, in this case the application of parametric excitation is not necessary; the trivial solution is stable. From rh-1 it follows that only one of θ_{11} or θ_{22} can be negative and its absolute value must be smaller than that of the other positive coefficient (see Figure 2, there is no case that both θ_{11} and θ_{22} are negative).
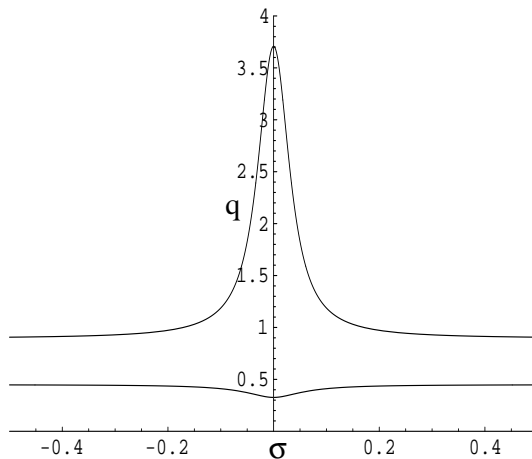
FIGURE 3. **The stability region of the trivial solution**. Fixing $\kappa = 0.18$, $\beta = 0.1$, and $M = 1$.

Solving rh-B for the boundary, we obtain

$$\sigma_{1,2} = \mp(\theta_{11} + \theta_{22})\sqrt{\frac{-(\Omega_1\Omega_2\theta_{11}\theta_{22} + Q_{12}Q_{21})}{4\Omega_1\Omega_2\theta_{11}\theta_{22}}}, \tag{5.9}$$

while σ_3 and σ_4 are always imaginary. From equation (5.9), to have real values we must take $\theta_{11}\theta_{22} < 0$ and $4\Omega_1\Omega_2\theta_{11}\theta_{22} + Q_{12}Q_{21} > 0$, since $\Omega_1\Omega_2$ is always positive and since the case $\theta_{11} > 0$ and $\theta_{22} > 0$ has been left out of discussion. Thus, the value of the detuning parameter σ is in the following interval

$$\sigma_1 \leq \sigma \leq \sigma_2. \tag{5.10}$$

Therefore, the interval of stability of the trivial solution in the neighbourhood of parametric combination anti-resonance is given by

$$\eta_0 + \varepsilon\sigma_1 < \eta < \eta_0 + \varepsilon\sigma_2 \tag{5.11}$$

5.2.2. The stability region of the trivial solution. Considering M is $\mathcal{O}(1)$, we fix $M = 1$. Then, the stability region of the trivial solution in the $\sigma - q$ plane is shown in Figure 3, σ satisfying (5.10).

In the area between the curves the self-excitation of the system is fully suppressed. Note that the width of the horizontal stretch with respect to the frequency ratio q corresponds to that of Figure 2 for $M = 1$.

By fixing parameter values of M, κ, and β, equation (5.11) also gives a stability region of the trivial solution in the $\eta - q$ plane. Figure 4 shows the region.

Similarly, the width of the horizontal stretch of the region corresponds with that of Figure 2 for $M = 1$. While the stretch along the parametric combination anti-resonance $\eta = \Omega_2 - \Omega_1$ is due to the parametric excitation amplitude being chosen. And the trivial solution is stable (or the self-excitation is fully suppressed) in the region between the curves. Note that the stability regions shown by Figure 3 and 4
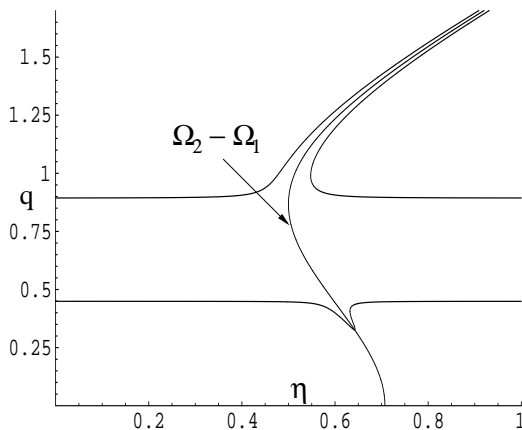
FIGURE 4. **The stability region of the trivial solution.** Fixing
$\kappa = 0.18, \ \beta = 0.1, \ M = 1$.

are less "symmetric" compared to those in [**14**] (or in [**12**]). The region along the parametric combination anti-resonance $\eta = \Omega_2 - \Omega_1$ stretches to infinity.

It is possible to enlarge the region of stability by taking a larger value of the mass ratio M to enlarge the width of the horizontal stretch, or by taking a larger value of the parametric excitation amplitude ε to enlarge the width of the stretch along the parametric combination anti-resonance curve. These possibilities are summarised in [**12**].

5.2.3. Nontrivial solutions. For the analysis of the nontrivial solutions of the system, it is more convenient to use the amplitude-phase transformation

$$
\begin{aligned}
\bar{x}_1 &= R_1 \cos(\varpi_1 t + \psi_1), & \bar{x}'_1 &= -R_1 \varpi_1 \sin(\varpi_1 t + \psi_1) \\
\bar{x}_2 &= R_2 \cos(\varpi_2 t + \psi_2), & \bar{x}'_2 &= -R_2 \varpi_2 \sin(\varpi_2 t + \psi_2)
\end{aligned} \tag{5.12}
$$

to equation (5.6), and average to have:

$$
\begin{aligned}
R'_1 &= -\frac{1}{2}\theta_{11}R_1 - \frac{1}{4}\frac{Q_{12}}{\Omega_1}R_2 \sin\phi + \frac{3}{8}B_1(\Omega_1^2 R_1^2 + 2\Omega_2^2 R_2^2) \\
R'_2 &= -\frac{1}{2}\theta_{22}R_2 + \frac{1}{4}\frac{Q_{21}}{\Omega_2}R_1 \sin\phi - \frac{3}{8}B_2(2\Omega_1^2 R_1^2 + \Omega_2^2 R_2^2) \\
\phi' &= \sigma + \frac{1}{4}\left(\frac{Q_{21}R_1}{\Omega_2 R_2} - \frac{Q_{12}R_2}{\Omega_1 R_1}\right)\cos\phi
\end{aligned} \tag{5.13}
$$

where $\phi = \psi_2 - \psi_1$. Note that any hyperbolic fixed point of the averaged system (5.13) corresponds with a periodic solution of system (5.8).

The analysis of (5.13) can be divided into two cases: exact resonance case ($\sigma = 0$) and near resonance case ($\sigma \neq 0$).

5.2.3.1. *The case of exact resonance $\sigma = 0$.* By performing numerical analysis using CONTENT, a continuation and bifurcation analysis software package [**35**], the

occurrence of nontrivial solutions can be detected outside the stability region of the trivial solution.

We refer to Figure 3 to check that at $\sigma = 0$ (the q axis), full suppression of the self-excitation of the system is carried out within the interval

$$0.326 \cdots \leq q \leq 3.707 \cdots .$$

This is illustrated by Figure 5 (i) and (ii), where outside the interval, nontrivial solutions arise. From Figure 5 (i) and (ii) one can study the behaviour of the amplitudes of the nontrivial solutions. For $0 < q < 0.326 \cdots$, R_1 (corresponding with the amplitude of x_1) is much smaller compared to R_2 (corresponding with the amplitude of x_2). On the other hand, for $q > 3.707 \cdots$, the opposite situation occurs.
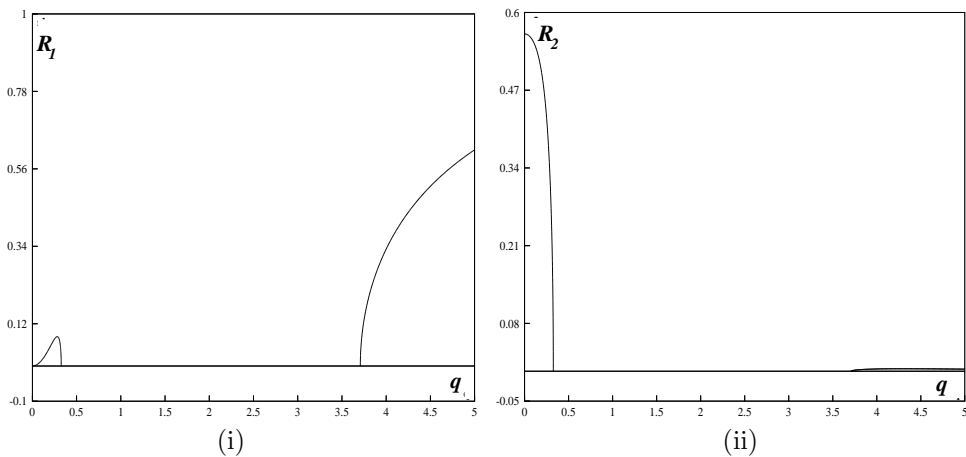
FIGURE 5. **The nontrivial solution for varying q (the frequency ratio)**. Fixing $\sigma = 0$, $M = 1$.

In the regions, where simultaneously nontrivial solutions arise and where θ_{11} and θ_{22} have different signs , condition for suppression of the self-excited vibration of the system can still be fulfilled, depending on the sign of their sum. (Recall condition rh-1 in subsection 2.1).

5.2.3.2. *The case of near resonance $\sigma \neq 0$.* Similar phenomena as in the case of exact resonance also appear in this case. Fixing $\sigma = 0.4$, $M = 1$ the stability region of the trivial solution is in the interval

$$0.445 \cdots \leq q \leq 0.913 \cdots ,$$

which is narrower than that of the exact resonance case. Again, this agrees with the width of the horizontal stretch for $\sigma = 0.4$ as shown in Figure 3, and nontrivial solutions appear outside the interval. Figure 6(i) and (ii) illustrate those solutions.
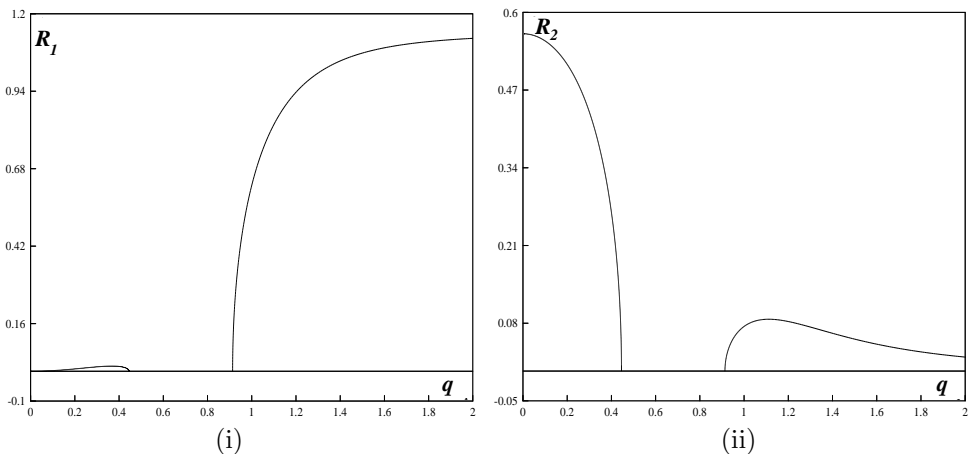
FIGURE 6. **The nontrivial solution for varying** q **(the frequency ratio) varies.** Fixing $\sigma = 0.4,\ M = 1$.

5.3. The three-mass system

We consider a three-mass system as an extension of the two-mass system considered in the previous section. We replace the attached spring of the mass which is self-excited with another mass. The third mass is attached to a spring having the same periodically variable stiffness as in the two-mass model. Figure 7 clearly illustrates the setting.

The system is governed by the following differential equations of motion:

$$
\begin{array}{rcl}
m_1\ddot{y}_1 + b\dot{y}_1 + k_0(1 + \varepsilon\cos\omega t)y_1 - k_1(y_2 - y_1) & = & 0 \\
m_2\ddot{y}_2 - \beta_0 U^2(1 - \gamma_0\dot{y}_2^2)\dot{y}_2 + 2k_1y_2 - k_1(y_1 + y_3) & = & 0 \\
m_3\ddot{y}_3 + b\dot{y}_3 + k_0(1 + \varepsilon\cos\omega t)y_3 - k_1(y_2 - y_3) & = & 0,
\end{array}
\tag{5.1}
$$

where ε represents the small amplitude of the parametric excitations.

The study of the system will be divided into two cases: symmetric case $(m_1 = m_3)$ and non-symmetric case $(m_1 \neq m_3)$.

5.3.1. The symmetric case $(m_1 = m_3)$. We take $m_1 = m_3 = m$ and use time transformation $\omega_0 t \to \tau$. Thus, we obtain the corresponding dimensionless equations:

$$
\begin{array}{rcl}
y_1'' + \kappa y_1' + q^2(1 + \varepsilon\cos\eta\tau)y_1 - \dfrac{1}{2}M(y_2 - y_1) & = & 0 \\[2mm]
y_2'' - \beta V^2(1 - \gamma y_2'^{\,2})y_2' + y_2 - \dfrac{1}{2}(y_1 + y_3) & = & 0 \\[2mm]
y_3'' + \kappa y_3' + q^2(1 + \varepsilon\cos\eta\tau)y_3 - \dfrac{1}{2}M(y_2 - y_3) & = & 0,
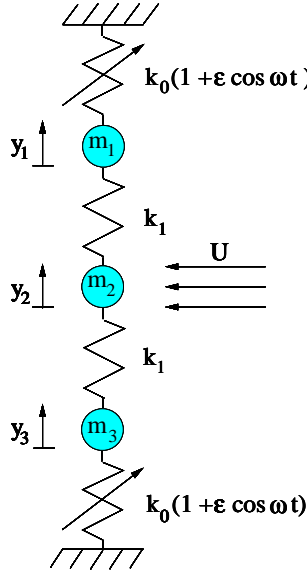\end{array}
\tag{5.2}
$$

73

FIGURE 7. **The three-mass system.** y_1, y_2, and y_3 are the deflection of the masses m_1, m_2, and m_3, respectively.

where $M = \frac{m_2}{m}$, $\kappa = \frac{b}{m\omega_0}$, $q^2 = \frac{k_0}{m\omega_0^2}$, $\gamma = \gamma_0\omega_0^2$, $V = \frac{U}{U_0}$, $\beta = \frac{\beta_0 U_0^2}{m_2\omega_0}$ and $\eta = \frac{\omega}{\omega_0}$, where U_0 is a chosen reference value for the flow velocity.

Rescale $\bar{\kappa} = \varepsilon\kappa$ $\bar{\beta} = \varepsilon\beta$, and transform (5.2) into quasi-normal form by using the following relations:

$$
\begin{aligned}
y_1 &= a_1 x_1 + a_2 x_2 + a_3 x_3 \\
y_2 &= x_1 + x_2 \\
y_3 &= a_1 x_1 + a_2 x_2 - a_3 x_3,
\end{aligned}
\tag{5.3}
$$

we obtain the following standard form (after applying time transformation $\eta\tau \to t$ and dropping the bars):

$$
\begin{aligned}
x_1'' + \varpi_1^2 x_1 &= \frac{\varepsilon}{\eta_0^2}[2\Omega_1\omega_1\sigma x_1 + \eta_0(\theta_{11}x_1' + \theta_{12}x_2') + \\
&\quad (Q_{11}x_1 + Q_{12}x_2)\cos t + B_1\eta_0^3(x_1' + x_2')^3] \\
x_2'' + \varpi_2^2 x_2 &= \frac{\varepsilon}{\eta_0^2}[2\Omega_2\omega_2\sigma x_2 + \eta_0(\theta_{21}x_1' + \theta_{22}x_2') + \\
&\quad (Q_{21}x_1 + Q_{22}x_2)\cos t + B_2\eta_0^3(x_1' + x_2')^3] \\
x_3'' + \varpi_3^2 x_3 &= \frac{\varepsilon}{\eta_0^2}[2\Omega_3\omega_3\sigma x_3 - q^2\cos t x_3 - \eta_0\kappa x_3'].
\end{aligned}
\tag{5.4}
$$

The third equation of (5.4), which is a Mathieu equation with damping, is decoupled from the first two equations. As the solutions of the third equation of (5.4) are

already well-known, we can analyse the first two equations of (5.4) separately. Thus, it will follow similar lines as the previous analysis of the two-mass system.

5.3.2. The non-symmetric case $(m_1 \neq m_3)$. Without loss of generality (with some rescalings) for system (5.1) we may take $k_0 = 1$, and take $m_1 = 1$, $m_2 = \frac{1}{\lambda}$, $m_3 = \frac{1}{\mu}$, where λ and μ are nonzero and $\mu \neq 1$, to guarantee asymmetry. In this analysis we also assume that $k_1 = 1$. With a slight abuse of the notations, taking $\beta_0 \rightarrow \beta$, $\gamma_0 \rightarrow \gamma$, and then rescaling $b = \varepsilon \bar{b}, \beta = \varepsilon \bar{\beta}$, after dropping the bars, the system becomes:

$$
\begin{aligned}
y_1'' + 2y_1 - y_2 &= \varepsilon(-by_1' - \cos \omega t \ y_1) \\
y_2'' - \lambda y_1 + 2\lambda y_2 - \lambda y_3 &= \varepsilon(\lambda \beta U^2(1 - \gamma {y_2'}^2)y_2') \\
y_3'' - \mu y_2 + 2\mu y_3 &= \varepsilon(-\mu b y_3' - \mu \cos \omega t \ y_3).
\end{aligned}
\tag{5.5}
$$

To obtain a quasi-normal form for (5.5) we diagonalise the coefficient matrix of the left-hand side of (5.5). We find a 3×3 transformation matrix P such that $Y = PX$, where $Y = (y_1, y_2, y_3)^T$ and $X = (x_1, x_2, x_3)^T$.

There are several main resonances for such a three-mass system. In this discussion we choose the easiest case of $1 : 2 : 3$-resonance in the new variables. In principal we can always choose the values of λ and μ for having the right resonance. After some numerical work, we find $\lambda = 0.361$ and $\mu = 0.39$ to have $1 : 2 : 3$-resonance in the new variables. Thus, we have:

$$
X'' + JX = \varepsilon G(X, X')
\tag{5.6}
$$

where J is a 3×3 diagonal matrix, with $j_{11} : j_{22} : j_{33} = 1 : 2 : 3$.

After time transformation, we average (5.6) to obtain the normal form. Using the transformation

$$
\begin{aligned}
x_i &= u_i \cos \omega_i \tau + v_i \sin \omega_i \tau \\
\dot{x}_i &= -u_i \omega_i \sin \omega_i \tau + v_i \omega_i \cos \omega_i \tau, \ i = 1, 2, 3
\end{aligned}
$$

for $\omega_1 : \omega_2 : \omega_3 = 1 : 2 : 3$. The averaged system is of the following form

$$
\dot{\nu} = A\nu + \xi(\nu),
\tag{5.7}
$$

where $\nu = (u_1, v_1, u_2, v_2, u_3, v_3)^T$, $\xi = (\xi_j, j = 1...6)^T$ are nonlinear functions of ν. $\xi_{1,2}$ contain cubic terms in u_1 and v_1, $\xi_{3,4}$ contain cubic terms in u_2 and v_2, $\xi_{5,6}$ contain cubic terms in u_3 and v_3. Matrix A is a 6×6 matrix of the following from:

$$
A = \begin{pmatrix} A_{11} & A_{12} & \varnothing \\ A_{21} & A_{22} & \varnothing \\ \varnothing & \varnothing & A_{33} \end{pmatrix}
$$

where $A_{ij}, i, j = 1, 2, A_{33}$ and $\varnothing$'s are 2×2 matrices.

As before, to analyse nontrivial solutions of system (5.7), it is more convenient to use the amplitude-phase transformation,

$$
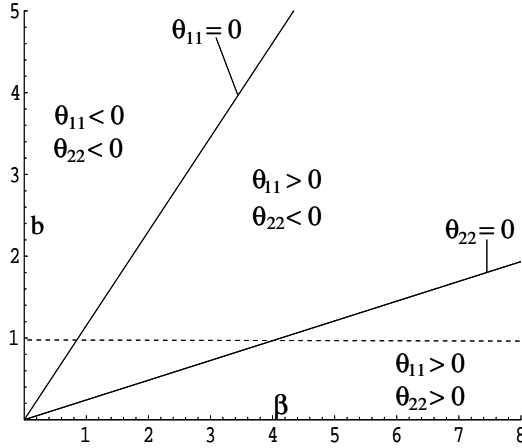x_i = R_i \cos(\omega_i \tau + \psi_i), \ i = 1, 2, 3 \text{ and } \omega_1 : \omega_2 : \omega_3 = 1 : 2 : 3,
$$

FIGURE 8. **The boundaries of θ_{11} and θ_{22}.** Fixing $\gamma = 1, U = 1$.

to have a reduced averaged system:

$$
\begin{array}{rcl}
R_1' & = & \eta_0(-\dfrac{1}{4}\dfrac{Q_{12}R_2}{\Omega_1}\sin\Psi + \dfrac{1}{2}\theta_{11}R_1 + \dfrac{3}{8}\gamma_{11}\Omega_1^2R_1^3) \\[2mm]
R_2' & = & \eta_0(\dfrac{1}{4}\dfrac{Q_{21}R_1}{\Omega_2}\sin\Psi + \dfrac{1}{2}\theta_{22}R_2 + \dfrac{3}{8}\gamma_{22}\Omega_2^2R_2^3) \\[2mm]
\Psi' & = & \eta_0(\sigma + \dfrac{1}{4}(\dfrac{Q_{21}R_1}{\Omega_2R_2} - \dfrac{Q_{12}R_2}{\Omega_1R_1})\cos\Psi) \\[2mm]
R_3' & = & \eta_0(\dfrac{1}{2}\theta_{33}R_3 + \dfrac{3}{8}\gamma_{33}\Omega_3^2R_3^3) \\[2mm]
\psi_3' & = & -\Omega_3\sigma,
\end{array}
\tag{5.8}
$$

where $\Psi = \psi_1 - \psi_2$.

Note that any hyperbolic fixed point of system (5.8) corresponds with a periodic solution of system (5.7).

The normal form (5.8) contains a surprise. We see that the last two equations of (5.8), which correspond with variable x_3, is decoupled from the others. Therefore, the stability of the trivial solution can be analysed from the first three equations of (5.8), which correspond with variable x_1 and x_2. The analysis is in the following subsections.

5.3.3. Condition for suppression of self-excited vibration.

As has been done previously, the condition for quenching (or suppressing) the self-excited vibration of the system can be derived from the Routh-Hurwitz criterion, which gives the boundaries for θ_{11} and θ_{22}. The expressions for θ_{11} and θ_{22}, which are contained in equation (5.6), can be plotted in the $\beta - b$ plane, after fixing the other parameter values. Figure 8 shows the boundaries.
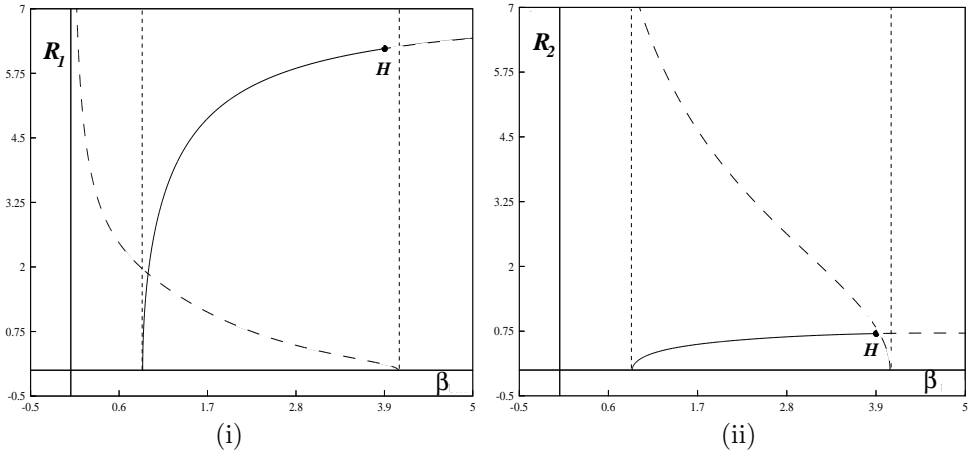
FIGURE 9. **The nontrivial solution for β varies.** Fixing $\sigma = 0.4$, $b = 1$, $\gamma = 1, U = 1$.

A numerical analysis has been performed by fixing $b = 1$, for $\sigma = 0.4$. From Figure (8), along the line $b = 1$, condition for full suppression of the self-excitation because there is no self-excitation of the system can happen at $\beta > 4.073 \cdots$ ($\beta = 4.073 \cdots$ is the intersection between $b = 1$ and $\theta_{22} = 0$). In the interval $0.893 \cdots < \beta < 4.073 \cdots$ ($\beta = 0.893 \cdots$ is the intersection between $b = 1$ and $\theta_{11} = 0$), full suppression of the self-excitation can be achieved by applying the Routh-Hurwitz criterion, as has been done previously. While at $0 < \beta < 0.893 \cdots$ there is no way to quench self-excitation of the system, as both θ_{11} and θ_{22} are negative. (See [**52, 56, 12**] for more details).

Figure (9) (i) and (ii) show the occurrence of the nontrivial solutions of the system in x_1 and x_2 modes, respectively. The two vertical dashed lines correspond with $\beta = 0.893 \cdots$ (the left line) and $\beta = 4.703 \cdots$ (the right line).

To the right of the right vertical dashed line, the self-excitation is fully suppressed because both θ_{11} and θ_{22} are positive (no self-excitation occurs).
Between the two dashed lines there are two nontrivial solutions, one is stable and the other is unstable. These will lead to a quenching possibility for certain values of β satisfying the Routh-Hurwitz criterion. Moreover, there is a subcritical Hopf bifurcation (denote by point H) through the stable nontrivial solution; a family of unstable periodic solutions persists within the region between the two dashed lines. Note that this bifurcation corresponds with a torus (Neimark-Sacker) bifurcation in system (5.7).
Whereas to the left of the left vertical dashed line, it is not possible to suppress (even partly) the self-excitation of the system, as the unstable nontrivial solution grows to infinity.

5.4. Conclusions

The use of parametric excitation for suppressing undesirable self-excitation of vibrating systems can be very effective. With the knowledge of the so-called parametric combination anti-resonance, conditions for suppression of self-excited vibration can be determined.

The study of the two-mass system, one self-excited and the other parametrically excited, adds some new aspects to the results of the previous work, i.e. [**12**] and [**14**]. The stability regions of the trivial solution of the system along the parametric combination anti-resonance stretch to infinity. The phenomenon of the occurrence of the nontrivial solutions gives information to why such a suppression of self-excitation can be achieved, despite the presence of the nontrivial solutions.

In the three-mass system, the surprising presence of the invariant subset governed by a two degree-of-freedom system is typical, when we introduce the transformation to obtain the corresponding quasi-normal form. The two degree-of-freedom system which is obtained depends on the choice of external resonance (in our case we chose $\eta_0 = \Omega_2 - \Omega_1$). This two degree-of freedom system makes the analysis easier, especially when considering nontrivial solutions. The detection of the subcritical Hopf bifurcation of the nontrivial solution is crucial, especially when we are talking about suppression of the self-excited vibration. The results show that full suppression or quenching (partly suppression) of the self-excited vibration is possible in the three-mass system under consideration.

It is important to look into the possibility of partial decoupling in the case of other resonances than $1 : 2 : 3$.

Bibliography

[1] Abadi. On Self-excited Autoparametric System. *Nonlinear Dynamics*, 24:147–166, 2001.

[2] Abadi. A Self-excited Autoparametric System with Dry Friction. *submitted*, 2003.

[3] M. A. Aizerman and F. R. Gantmakher. Stability in Linear Approximation of the Periodic Solution of System of Differential Equations with Discontinuous Right Hand Sides. *Prikl. Mat. Mekh*, 21, 5:658–669, 1957.

[4] A. A. Andronow and C. E. Chaikin. *Theory of Oscillations*. Princeton University Press, Princeton, 1949.

[5] J. P. Aubin and A. Cellina. *Differential Inclusions*. Springer-Verlag, Berlin, 1984.

[6] V. I. Babitsky and V. L. Krupenin. *Vibration of Strongly Nonlinear Discontinuous Systems*. Springer-Verlag, Berlin, 2001.

[7] D. Bothe. Periodic Solutions of Non-smooth Friction Oscillators. *Z. Angew. Math. Phys*, 50:779–808, 1999.

[8] J. Carr. *Applications of Centre Manifold Theory*. Appl.Math.Sciences 35, Springer-Verlag, New York, 1981.

[9] M. Cartmell. *Introduction to Linear, Parametric and Nonlinear Vibrations*. Chapman & Hall, London, 1990.

[10] F. Dercole and Yu A. Kuznetsov. SLIDECONT: An AUTO97 Driver for Sliding Bifurcation Analysis. *Universiteit Utrecht, preprint*, 2002.

[11] E. Doedel, A. Champneys, T. Fairgrieve, Yu A. Kuznetsov, B. Sanstede, and X. Wang. *AUTO97: Continuation and Bifurcation Software for Ordinary Differential Equations (with* HOMCONT*), User's Guide*. Concordia University, Canada, 1997.

[12] H. Ecker and A. Tondl. Suppression of Flow-induced Vibrations by a Dynamic Absorber with Parametric Excitation. In *Proc. 7th International Conference on Flow-Induced Vibrations - FIV 2000*, page 757. Luzern, 2000.

[13] S. Fatimah. *Bifurcations in Dynamical Systems with Parametric Excitation*. PhD thesis, Utrecht University, 3584 CD, Utrecht, 2002.

[14] S. Fatimah and M. Ruijgrok. Bifurcation in an Autoparametric System in 1:1 Resonance with Parametric Excitation. *Int. J. Nonlinear Mechanics*, 37:297–308, 2002.

[15] N. Fenichel. Persistence and Smoothness of Invariant Manifolds for Flows. *Ind. Univ. Math. J.*, 21:193–225, 1971.

[16] N. Fenichel. Asymptotic Stability with Rate Conditions. *Ind. Univ. Math. J.*, 23:1109–1137, 1974.

[17] N. Fenichel. Asymptotic Stability with Rate Conditions, II. *Ind. Univ. Math. J.*, 26:81–93, 1977.

[18] N. Fenichel. Geometric Singular Perturbations Theory for Ordinary Differential Equations. *J. Diff. Eq.*, 31:53–98, 1979.

[19] A. Fidlin. On the Asymptotic Analysis of Discontinuous Systems. *Z. Angew. Math. Mech*, 82, 2:75–88, 2002.

[20] A. F. Filippov. *Differential Equations with Discontinuous Right-hand Side*. Nauka, Moscow, 1970.

[21] U. Galvanetto and S. R. Bishop. Dynamics a Simple Damped Oscillator Undergoing Stick-slip Vibrations. *Meccanica*, 34:337–347, 1999.

[22] U. Galvanetto, S. R. Bishop, and L. Briseghella. Mechanical Stick-slip Vibrations. *International Journal of Bifurcation and Chaos*, 5, 3:637–651, 1995.

[23] J. Grasman. *Asymptotic Methods for Relaxation Oscillations and Applications*. Springer-Verlag, New York, 1987.

[24] R. Grimshaw. *Nonlinear Ordinary Differential Equations*. Blackwell Scientific Publications, Oxford, 1990.

[25] J. Guckenheimer and P. Holmes. *Nonlinear Oscillations, Dynamical Systems, and Bifurcations of Vector Fields*. Appl.Math.Sciences 42, Springer-Verlag, New York, 1997.

[26] J. Guckenheimer, M. R. Myers, F. J. Wicklin, and P. A. Worfolk. DsTool: *Dynamical System Toolkits with an Interactive Graphical Interface, User's Manual*, 1995.

[27] C. K. R. T. Jones. Geometric Singular Perturbation Theory. In R. Johnson, editor, *Dynamical Systems*, Lecture Notes in Mathematics 1609, pages 44–118. Springer, Berlin, montecatini terme 1994 edition, 1995.

[28] T. J. Kaper. An introduction to Geometric Methods and Dynamical Systems Theory for Singular Perturbation Problems. In J. Cronin and R. E. O'Malley Jr., editors, *Analyzing Multiscale Phenomena Using Singular Perturbation Methods*, Proc. Symposia Appl. Math, AMS 56, pages 85–131. Springer(revisi), Berlin(revisi), 1999.

[29] K. Klotter. *Technische Schwingungslehre*. Springer, Berlin, 1978.

[30] M. Krupa. Robust Heteroclinic Cycles. *J. Nonlinear Sci.*, 7:129–176, 1997.

[31] M. Krupa and I. Melbourne. Asymptotic Stability of Heteroclinic Cycles in Systems with Symmetry. *Ergod. Th. & Dynam. Sys.*, 15:121–147, 1995.

[32] M. Kunze. *Non-smooth Dynamical Systems*. Springer, Berlin, 2000.

[33] M. Kunze and T. Küpper. Qualitative Bifurcation Analysis of a Non-smooth Friction-oscillator Model. *Z. Angew. Math. Phys*, 48:87–101, 1997.

[34] Yu A. Kuznetsov. *Elements of Applied Bifurcation Theory*. Appl.Math.Sciences 112, Springer-Verlag, New York, 1998.

[35] Yu A. Kuznetsov and V. Levitin. CONTENT: *Integrated Environment for the Analysis of Dymanical Systems*, 1997. ftp://ftp.cwi.nl/pub/CONTENT.

[36] Yu A. Kuznetsov, S. Rinaldi, and A. Gragnani. One-parameter Bifurcations in Planar Filippov Systems. *Int. J. Bifurcation and Chaos*, to appear, 2002.

[37] R. I. Leine, D. H. van Campen, A. de Kraker, and L. van den Steen. Stick-slip Vibrations Induced by Alternate Friction Models. *Nonlinear Dynamics*, 16, 1:41–54, 1998.

[38] N. M. Matveev, S. L. Nosov, and A. N. Pokrovskii. The Averaging-principle question. *Differential Equations*, 14:261–263, 1978.

[39] R. Nabergoj and A. Tondl. Autoparametric Resonance in Self-Excited Single Mass System. *Proc. EUROMECH-2nd European Nonlinear Oscillation Conference*, 2:151–156, 1996.

[40] V. A. Plotnikov. Averaging of Differential Inclusions. *Ukranian Math. J.*, 31:454–457, 1979.

[41] V. A. Plotnikov. The Averaging method for Differential Inclusions and Its Application to Optimal-control Problems. *Differential Equations*, 15:1013–1018, 1979.

[42] K. Popp and P. Stelter. Stick-slip Vibrations and Chaos. *Phil. Trans. Roy. Soc. Lond.*, A 332:89–105, 1990.

[43] M. Ruijgrok. *Studies in Parametric and Autoparametric Resonance*. PhD thesis, Utrecht University, 3584 CD, Utrecht, 1995.

[44] A. M. Samoilenko and N. A. Pere'styuk. N. N. Bogolyubov's Second Theorem for Differential Equation Systems with Impulse Action. *Differential Equations*, 10:1543–1550, 1974.

[45] A. M. Samoilenko and N. A. Pere'styuk. The Method of Averaging in Systems with an Impulsive Action. *Ukrainian Math. J.*, 26:342–347, 1974.

[46] J. A. Sanders and F. Verhulst. *Averaging Methods in Nonlinear Dynamical Systems*. Appl. Math. Sciences 59, Springer-Verlag, New York, 1985.

[47] G. Schmidt and A. Tondl. *Non-linear Vibrations*. Cambridge University Press, Cambridge, 1986.

[48] J. J. Stoker. *Nonlinear Vibrations*. Interscience Publishers, New York, 1950.

[49] J. W. Swift. Convection in a Rotating Fluid Layer. *Contemporary Mathematics, AMS*, 28:435–448, 1984.

[50] A. Tondl. *Self-excited Vibrations*. Monograph and Memoranda No. 9, National Research In-
stitute for Machine Design, Běchovice, 1970.

[51] A. Tondl. *On the Interaction between Self-excited and Forced Vibrations*. Monograph and
Memoranda No. 20, National Research Institute for Machine Design, Běchovice, 1976.

[52] A. Tondl. *On the Interaction between Self-excited and Parametric Vibrations*. Monograph and
Memoranda No. 25, National Research Institute for Machine Design, Běchovice, 1978.

[53] A. Tondl. *Quenching of Self-Excited Vibrations*. Elsevier, Amsterdam, 1991.

[54] A. Tondl. Nonlinearly coupled systems. *Engineering Mechanics*, 6(2):87–96, 1999. *In Czech.*

[55] A. Tondl. Suppressing Self-excited Vibration by Means of Parametric Excitation. In *Proc.
Colloquium Dynamics of Machines 2000, Institute of Thermomechanics ASCR*, page 225.
Prague, 2000.

[56] A. Tondl and H. Ecker. Cancelling of Self-excited Vibration by Means of Parametric Excita-
tion. In *Proc. 1999 ASME Design Engineering Technical Conferences, DETC/VIB-8071*. Las
Vegas, 1999.

[57] A. Tondl and R. Nabergoj. *Autoparametric Systems*. Report No. 16, Department of Naval
Architecture, Ocean and Environmental Engineering, Trieste, 1993.

[58] A. Tondl and R. Nabergoj. The Effect of Parametric Excitation on a Self-excited Three-mass
System. *Int. J. Non-Linear Mech, To appear*, 2003.

[59] A. Tondl, T. Ruijgrok, F. Verhulst, and R. Nabergoj. *Autoparametric Resonance in Mechanical
Systems*. Cambridge University Press, New York, 2000.

[60] F. Verhulst. *Nonlinear Differential Equations and Dynamical Systems*. Springer-Verlag, Berlin,
2000.

[61] F. Verhulst. Normal Mode Instability and Quenching. In *Proc. 6th Int. Conf. Vibration Prob-
lem*. Liberec, 2003.

[62] W. Walter. *Ordinary Differential Equations*. Springer-Verlag, New York, 1998.

[63] S. Wiggins. *Introduction to Applied Nonlinear Dynamical Systems and Chaos*. Springer-Verlag,
New York, 1990.

Samenvatting

Nietlineaire Dynamica van Zelf-excitatie
in Autoparametrische Systemen

Dit proefschrift is een verzameling van artikelen over zelf-geëxciteerde, voornamelijk autoparametrische oscillatoren. Wanneer we verschillende typen van zelf-excitatie bestuderen, vinden we uiteenlopende resultaten over oplossingen, stabiliteit en bifurcaties. Deze resultaten worden gepresenteerd in de hoofdstukken van dit proefschrift, die we hier kort samenvatten:

In hoofdstuk 1 herhalen we kort de achtergrondkennis die nodig is om dit proefschrift te begrijpen. We introduceren autoparametrische systemen en het begrip zelf-excitatie.

In hoofdstuk 2 beschouwen we een zelf-geëxciteerd autoparametrisch systeem dat een oscillator bevat van Rayleigh type. We bestuderen de semitriviale oplossing en haar stabiliteit. We zijn vooral geïnteresseerd in het bestaan en de stabiliteit van niettriviale oplossingen, die we bestuderen door parameters te variëren. We maken onderscheid tussen exacte resonantie en bijna-resonantie en gebruiken zowel normaalvorm technieken (middeling) als numerieke integratie. We vinden in dit systeem een rijk bifurcatiepatroon, een robuuste heterocliene cykel en instabiel gedrag.

In hoofdstuk 3 bekijken we een autoparametrisch systeem met een kleine parameter en een 'dry-friction' oscillator. Interessant aspect van de analyse van de semitriviale oplossing is de mogelijkheid om uit te rekenen bij welke parameterwaarden er niet-gladde periodieke oplossingen bestaan. Met het softwarepakket SLIDE-CONT vinden we dat deze periodieke oplossing een zogenaamde *sliding* bifurcatie ondergaat. We bestuderen het volledige vierdimensionale systeem kwalitatief met behulp van een asymptotische analyse en enkele numerieke simulaties.

Hoofdstuk 4 gaat over een autoparametrisch systeem met een relaxatie-oscillator van Van der Pol type. De koppelingsparameters in dit systeem moeten zo afgestemd worden dat ongewenste oscillaties worden onderdrukt. In dit geval is het nodig de gekoppelde oscillator een zeer lage frequentie te geven. Tevens moeten we de koppelingstermen en -parameters zo kiezen dat de langzame variëteit in het systeem vervormd wordt.

Hoofdstuk 5 tenslotte bestudeert trillende systemen waarin zowel zelf-excitatie als parametrische excitatie voorkomt. We willen meer te weten komen over de interactie tussen deze twee typen van excitatie. In het bijzonder vragen we ons af of het mogelijk is de parametrische excitatie te gebruiken om de zelf-excitatie (bijna)

helemaal te onderdrukken. We kijken eerst naar zogenaamde parametrische combi-natie anti-resonantie. In dit geval kan de zelf-excitatie volledig worden onderdrukt. We vinden bovendien het stabiliteitsgebied van de triviale oplossing. Buiten dit stabiliteitsgebied kunnen niettriviale oplossingen voorkomen, maar is het nog altijd mogelijk de zelf-excitatie te onderdrukken. In dit hoofdstuk beschouwen we syste-men van twee of drie massa's. Verrassend genoeg vindt er in het drie-massa-systeem in $1 : 2 : 3$ resonantie een gedeeltelijke ontkoppeling plaats.

We concluderen dat de nietlineaire dynamica van in hogere dimensies ingebedde zelf-geëxciteerde oscillatoren niet alleen van praktisch nut is, maar tegelijkertijd ook een bron is van wiskundig interessante fenomenen.

Translated by Bob Rink

Rangkuman

Dinamika Tak Linier dari Osilasi Bereksitasi Sendiri di Sistem-sistem Autoparametrik

Tesis ini merupakan kumpulan paper hasil penelitian tentang sistem-sistem mekanik yang memuat osilator bereksitasi sendiri (*self-excited oscillator*). Sebagian besar dari penelitian tersebut mengkhususkan pada sistem-sistem autoparametrik bereksitasi sendiri (*self-excited autoparametric systems*). Beberapa jenis osilator bereksitasi sendiri diterapkan ke dalam sistem, dan studi tentang solusi-solusi; kestabilan dan bifurkasinya, memberikan hasil-hasil yang sangat berbeda untuk setiap jenis osilator.

Hasil penelitian tersebut disajikan di tesis ini dalam bab-bab yang berbeda, dan dirangkum sebagai berikut:

Bab 1 merupakan pendahuluan yang berisi ringkasan dari latar belakang masalah dalam tesis ini; terutama tentang osilasi bereksitasi sendiri (*self-excited oscillation*) dan sistem autoparametrik (*autoparametric system*).

Bab 2 merupakan hasil penelitian tentang sistem autoparametrik bereksitasi sendiri dengan menerapkan osilator bereksitasi sendiri jenis Rayleigh ke dalam sistem. Penelitian tersebut mempelajari solusi 'semitrivial' serta domain ketakstabilan dari solusi semitrivial, di mana solusi tak trivial terjadi. Penelitian ini juga mempelajari keberadaan dan kestabilan solusi-solusi tak trivial dengan melakukan analisis bifurkasi, ketika nilai parameter-parameter dari sistem tersebut bervariasi. Diskusi tentang solusi tak trivial dibagi dalam dua kasus; resonansi eksak dan resonansi tak eksak.
Dalam melakukan analisis, digunakan metode 'averaging', didukung pula dengan metode kontinuasi secara numerik. Hasil studi tentang sistem tersebut menunjukkan keragaman bifurkasi solusi dari sistem, solusi heteroklinik dan perilaku ketakstabilan dari solusi.

Di bab 3 disajikan hasil penelitian tentang sistem autoparametrik bereksitasi sendiri dengan menerapkan osilator jenis gesekan kering (*dry friction oscillator*) ke dalam sistem. Seperti di dalam pembahasan di bab 2, penelitian ini mempelajari tentang solusi semitrivial dari sistem. Salah satu aspek yang menarik dari hasil analisis solusi semitrivial adalah kemungkinan untuk menghitung nilai batas keberadaan solusi periodik tak mulus dari sistem. Penggunaan paket software SLIDECONT menunjukkan terjadinya bifurkasi 'sliding' dari solusi periodik tak mulus dari sistem tersebut. Pembahasan tentang sistem 4-dimensi dilakukan secara kualitatif dengan menggunakan analisis asimtotik, yang didukung dengan simulasi numerik.

Bab 4 berisi hasil penelitian tentang sistem autoparametrik bereksitasi sendiri dengan menerapkan osilator relaksasi jenis van der Pol ke dalam sistem. Di bab ini dipelajari kemungkinan untuk membuat tak stabil getaran sistem yang disebabkan oleh getaran karakteristik yang stabil (*stable normal mode*) atau solusi semitrivial. Hal ini dapat dilakukan dengan melakukan pemilihan secara tepat nilai-nilai parameter pengatur frekuensi (*tuning parameter*) dan parameter perangkai (*coupling parameter*). Kondisi di mana getaran sistem akibat getaran karakteristik yang disebabkan oleh osilasi relaksasi dapat tercapai, apabila pada osilator yang dirangkai ke osilator relaksasi dikenakan frekuensi yang lemah. Hal lain yang perlu diketahui bahwa peredaman (*quenching*) getaran yang terjadi akan efektif apabila 'manifold pelan' (*slow manifold*) berubah bentuk. Hal ini mungkin dilakukan dengan pemilihan suku dan nilai parameter perangkai secara tepat ke dalam sistem persamaan.

Bab 5 menyajikan hasil penelitian yang agak berbeda dari hasil-hasil penelitian di bab-bab sebelumnya. Penelitian dilakukan terhadap sistem yang memuat osilator bereksitasi sendiri dan osilator bereksitasi secara parametrik (*parametrically excited oscillator*). Di bab ini dipelajari bagaimana eksitasi-eksitasi yang disebabkan oleh kedua jenis osilator tersebut berinteraksi di dalam sistem. Khususnya, dipelajari kondisi-kondisi untuk mengurangi atau menghilangkan sama sekali (*full suppression*) eksitasi yang disebabkan oleh osilator bereksitasi sendiri dengan menggunakan eksitasi parametrik yang dihasilkan oleh osilator bereksitasi secara parametrik.

Pertama-tama, ditentukan kondisi kombinasi parametrik anti resonansi (*parametric combination anti-resonance*), kondisi di mana penghilangan sama sekali eksitasi yang disebabkan oleh osilator bereksitasi sendiri dapat terjadi. Kemudian, ditentukan batas-batas dan daerah-daerah kestabilan dari solusi trivial. Dapat ditunjukkan bahwa di luar daerah kestabilan tersebut, di mana solusi tak trivial terjadi, kondisi untuk meredam eksitasi yang disebabkan oleh osilator bereksitasi sendiri masih mungkin berlaku. Pembahasan di bab ini dibagi dalam dua kasus; sistem dua massa dan sistem tiga massa. Satu hasil yang mengejutkan, bahwa bentuk normal (*normal form*) dari sistem tiga massa dalam resonansi 1 : 2 : 3 menunjukkan terjadinya pemisahan satu massa terhadap dua massa yang lain (*decoupling*).

Dapat disimpulkan bahwa dinamika tak linier yang diperoleh dengan menerapkan osilator bereksitasi sendiri ke dalam sistem berdimensi tinggi sangat menarik untuk dipelajari. Hasil-hasil di tesis ini menunjukkan bahwa dinamika tersebut dapat menjadi sumber terjadinya fenomena-fenomena yang menarik; perilaku kestabilan dan bifurkasi solusi dari sistem.

Acknowledgement

all the members of the family for the warmth and kindness they always offer. I will certainly miss the children.

I also want to thank Sri, Dwi, Diah, Hartono, Gede, Darma, Caswita, Budi, Happy, Ucup, Suyono, Gunarjo, Stanley and Ade. Thank you for the friendships we have threaded during which I managed to finish all the assignments.

So much fun and good times I have shared with my friends in the HMI Utrecht mail-list that I cannot mention them all by name in here. I am thankful to all of them and I wish them the best of luck.

I would like to thank PGSM Indonesia and CICAT TUDelft The Netherlands for the financial support. Many thanks especially to Durk Jellema and René Tamboer of CICAT TUDelft for their terrific job in the project.

My thanks should also go to Jurusan Matematika, Universitas Negeri Surabaya, Indonesia for giving me the opportunity to pursue my PhD study in The Netherlands.

All of my hard work abroad would have never been done properly without continuous support and encouragement especially from my dearest wife, Atik and our lovely sons, Levi and Dhani. They have struggled nicely in Indonesia during my absence in the last five years. I am really proud of them.

Finally, I would like to express my special gratitude to our parents, sisters and brothers who keep supporting my wife and sons while I was on leave.

Curriculum Vitae

Abadi was born on August 30th, 1965 in Surabaya, Indonesia. In 1990, he took his bachelor degree from Jurusan Pendidikan Matematika, IKIP Surabaya, Indonesia, at which he has been employed as a lecturer since 1991. The institute itself was recently restructured and has become Universitas Negeri Surabaya (or Surabaya State University).

He married Atik Wintarti on January 17th, 1993 and they have got two sons, Levi Aulia Batista and Trechsna Ali Ramadhani.

During the year of 1993, he spent time in Bandung, Indonesia to join The so-called Basic Sciences Bridging Programme, an AusAid programme of master candidates recruitment. The programme was held at Bandung Institute of Technology (ITB), and consisted of both mathematics and English courses.

In 1994, he started a master study at The Department of Mathematics, The University of Queensland, Brisbane, Australia. He got his Master of Science degree in mathematics from the university in 1997.

In the beginning of 1998, he attended an eight-week research workshop on differential equations which was held in ITB. The workshop was jointly financed by The Indonesian and The Netherlands governments, through PGSM in Jakarta and CICAT TUDelft in Delft. In that workshop he attended the lectures given by dr. Adriaan van der Burgh and Prof. dr. Ferdinand Verhulst, who later recommended him to pursue his PhD study in The Netherlands.

Since October 1998, he has been a PhD-student in the topic of dynamical systems at Mathematisch Instituut, Universiteit Utrecht, under the supervision of Prof. dr. Ferdinand Verhulst. October 6th, 2003 is the date when he defences his thesis, in which all of his research works in the last five years are collected.

During his PhD study, he also attended some conferences related to his work. In 2000, he attended the conference of Bifurcations: Numerical Methods, Software and Applications in Gent, Belgium. In 2002, he attended the conference of Symmetry and Perturbation Theory in Cala Gonone, Sardinia, Italy. In May 2003, he attended and presented his work at the SIAM conference in Snowbird, Salt Lake City, Utah, USA. Finally, in September 2003, he attended and presented a paper at the International Conference on Vibration Problems in Liberec, Czech Republic.